Journal
of
The Franklin Institute

EDITOR, HENRY BUTLER ALLEN, MET.E., D.SC.
ASSISTANT EDITOR, JOHN FRAZER, PH.D.

Associate Editors:

WILDER D. BANCROFT, PH.D. — A. S. EVE, F.R.S. — HENRY C. SHERMAN, SC.D
C. B. BAZZONI, PH.D. — PAUL D. FOOTE, PH.D. — W. F. G. SWANN, D.SC.
E. G. COKER, F.R.S. — W. J. HUMPHREYS, PH.D. — HUGH S. TAYLOR, D.SC.
ARTHUR L. DAY, SC.D. — C. E. K. MEES, D.SC. — A. F. ZAHM, PH.D.
R. EKSERGIAN, PH.D. — WILLIAM B. MELDRUM, PH.D. — JOHN ZELENY, PH.D.

Committee on Publications:

G. H. CLAMER, CHAIRMAN — LIONEL F. LEVY — HIRAM S. LUKENS
RICHARD HOWSON — MALCOLM LLOYD, JR. — RICHARD H. OPPERMANN
C. L. JORDAN — WINTHROP R. WRIGHT

Vol. 239 **APRIL, 1945** **No. 4**

CONTENTS

Theory of Bending, Torsion and Buckling of Thin-Walled Members of Open Cross Section ..... STEPHEN P. TIMOSHENKO 249

Studies in the Sensitivity of Photographic Materials ..... A. P. H. TRIVELLI 269

Microwave Radiation from the Sun ..... G. C. SOUTHWORTH 285

Eclipses of the Sun ..... ROY K. MARSHALL 299

Notes from the National Bureau of Standards 325

The Franklin Institute Notes 331

Notes from the Biochemical Research Foundation 334

A Chlorometric Method for the Determination of Some Organic Sulfides. A Preliminary Report ..... JAMES L. LEITCH

Book Reviews 339

Publications Received 340

Current Topics 296, 330, 341

Published by

THE FRANKLIN INSTITUTE OF THE STATE OF PENNSYLVANIA
Prince and Lemon Streets, Lancaster, Penna., and
Benjamin Franklin Parkway at Twentieth St., Philadelphia, Penna.

SIX DOLLARS PER YEAR (Foreign Postage Additional) **SINGLE NUMBERS, SIXTY CENTS**

Indexes to the semi-annual volumes of the JOURNAL are published with the June and December numbers. The contents are also indexed in *The Industrial Arts Index*.

ENGINEERING ACHIEVEMENTS THAT MADE

PHILCO

THE LEADER IN RADIO

Through 12 straight years of leadership, Philco research and engineering was the driving force for progress in the use and enjoyment of radio.

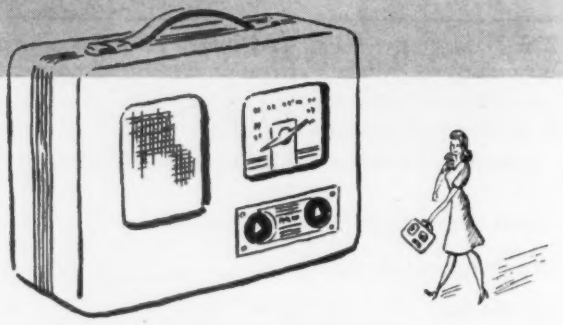

Portable Radios!

It was Philco who conceived and invented the idea of a radio that you could play anywhere outdoors . . . on the beach, at a picnic, in a boat . . . powered from a self-contained battery. *Another* example of Philco pioneering that will bring new radio joys for the future to all America.

PHILCO . . . Famous for Quality the World Over

Journal
of
The Franklin Institute
Devoted to Science and the Mechanic Arts

Vol. 239 APRIL, 1945 No. 4

THEORY OF BENDING, TORSION AND BUCKLING OF THIN-WALLED MEMBERS OF OPEN CROSS SECTION.

BY

STEPHEN P. TIMOSHENKO,

Professor of Theoretical and Applied Mechanics, Emeritus, Stanford University.

PART II.

4. **Non-uniform Torsion of Thin-Walled Bars.**—It was assumed in the previous discussion that torque is applied at the ends of the bar and that cross sections of the bar are free to warp. In such a case, warping is the same for all cross sections and is accomplished without any axial strain of longitudinal fibers. The problem becomes more complicated if cross sections are not free to warp or if the torque varies along the length of the bar. Warping in such cases varies along the bar and torsion is accompanied by tension or compression of longitudinal fibers. The rate of change of the angle of twist along the axis of the bar also varies, and we call this the case of *non-uniform torsion*.

We begin our discussion of this kind of problem with the simple case of torsion of an I-beam, the cross section of which has two axes of symmetry. We assume that one end of the beam is built-in and cannot warp. The torque T is applied at the other end, Fig. 18. It is evident that by building in the end of the beam and by eliminating warping, illustrated in Fig. 12, we increase the resistance of the beam to torsion. Torsion in this case is accompanied by bending of the flanges. The torque T will be balanced partially by shearing stresses of the kind discussed in the preceding article and partially by the resistance of the flanges to bending. The first part of the torque we denote by T_1. It is proportional to the rate of change of the angle of twist along the axis of the beam. Denoting this angle by φ, using eq. (19) and indicating by primes the derivatives of ζ with respect to z we obtain

$$T_1 = C\varphi'. \tag{29}$$

(Note—The Franklin Institute is not responsible for the statements and opinions advanced by contributors in the JOURNAL.)

The second part of the torque will be found from the consideration of bending of the flanges. It can be concluded from symmetry that in this case of torsion, cross sections of the beam rotate with respect to the centroidal axis and deflection of the upper flange of the beam is

$$u = \varphi \frac{h}{2}.$$

Using now eqs. (17) and (6), we conclude that the shearing force in the flange is

$$V_z = -\frac{dM_y}{dz} = -EI_y \frac{d^3u}{dz^3} = -\frac{EI_y h}{2} \varphi''',$$

where I_y is the moment of inertia of the cross section of one flange. The shearing force in the lower flange will be equal to that in the upper

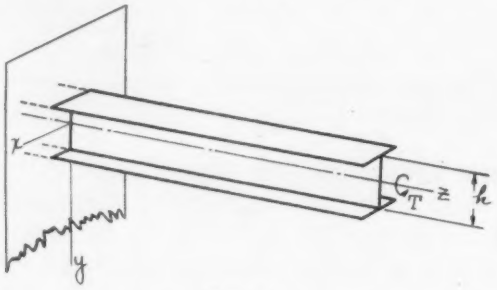

FIG. 18.

flange and opposite in direction. This couple of forces represents the second part of the torque:

$$T_2 = -\frac{EI_y h^2}{2} \varphi'''. \tag{30}$$

The equation for calculation of the angle of twist then becomes

$$T = T_1 + T_2 = C\varphi' - \frac{EI_y h^2}{2} \varphi'''. \tag{31}$$

The integration of this equation will be discussed later. We state only that when φ is found we can calculate both portions T_1 and T_2 of the torque and find the stresses produced in the beam by each of these portions.

We see that the above problem of non-uniform torsion was solved by assuming a variable twist along the axis of the bar and dividing the torque into two parts, one representing pure torsion which is defined by eq. (29) and the other depending on bending of flanges. Knowing the axis of rotation and angles of twist we obtained the deflection curves of the flanges. From these deflection curves, the shearing forces due to bending were found, which constitute the second part of the torque.

It should be noted that, in analysing bending of the flanges, we used eqs. (17), in which the curvature is taken proportional to bending moment. This means that only the effect of normal stresses σ_z on curvature was considered and the effect of shearing stresses was neglected, which is usual practice in analysing bending of beams.

The method of attack outlined above will now be applied to the analysis of non-uniform torsion of a thin-walled bar of any open cross section. Assume that Fig. 19 represents a bar, the end, $z = 0$, of which

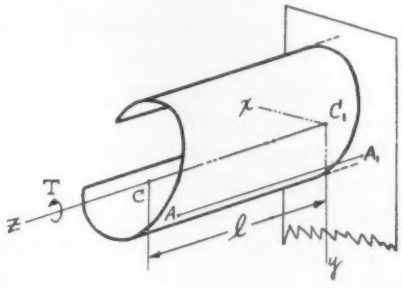

FIG. 19.

is built-in while to the other end, $z = l$, the torque T is applied. From the discussion of article 2, we know that a transverse force applied at the shear center A of the loaded end cross section produces only bending of the bar and no torsion. Thus, on the basis of the reciprocity theorem, we conclude that the torque T applied at the end will not produce any deflection of point A and the shear center axis AA_1 remains straight while cross sections of the bar rotate with respect to that axis during torsion. Denoting by φ the angle of rotation of any cross section, we find that the part T_1 of the torque, producing stresses of pure torsion, is given by eq. (29). In calculation of the second part T_2 of the torque, corresponding to bending of flanges in the case of an I-beam, we proceed as before and neglect the effect of shearing stresses on deformation of the middle surface of the wall. Then the axial displacements w, defining warping of cross sections, will be found in the same way as in the case of pure torsion (see eq. (28)). We observe only that the torsion is non-uniform now and replace the constant θ by the variable rate of change φ' of the angle of twist. Then

$$w = \varphi'(D - \omega_s). \tag{32}$$

Since φ' is varying along the length of the bar, adjacent cross sections will not be equally warped, which results in axial strain ϵ_z of longitudinal fibers of the bar. Observing that D and ω_s in eq. (32) are independent of z, we obtain

$$\epsilon_z = \frac{\partial w}{\partial z} = \varphi''(D - \omega_s).$$

Assuming now that the fibers do not press on each other laterally, we obtain normal stresses produced during non-uniform torsion as follows:

$$\sigma_z = E\varphi''(D - \omega_s). \tag{33}$$

We see that normal stresses at any cross section are proportional to corresponding axial displacements w. Hence the diagrams of the preceding article, illustrating warping of the cross sections, give also the picture of distribution of normal stresses σ_z produced during non-uniform torsion.

It can be shown that the resultant force and the moments M_x and M_y of stresses, distributed in accordance with eq. (33), vanish. To prove this we use the reciprocity theorem. Assume that normal stresses of magnitude p are uniformly distributed over the end cross section of the bar in Fig. 19. Such stresses evidently do not produce any rotation of the end and the acting torque T does not produce any work. Then in virtue of the reciprocity theorem the work done by the stresses p on the displacements w produced by torque must vanish and we obtain

$$\int_o^m wptds = p\varphi' \int_o^m (D - \omega_s)tds = 0.$$

Hence

$$\int_o^m (D - \omega_s)tds = 0 \tag{34}$$

and the resultant of stresses (33) vanishes. Let us apply now to the end of the bar bending stresses py, proportional to the distance from the x-axis.* Such stresses produce pure bending and no rotation of the end with respect to the z-axis. Torque does not produce work during this bending. Hence the work of bending stresses during torsion must vanish and we obtain

$$\int_o^m wpytds = p\varphi' \int_o^m (D - \omega_s)ytds = 0.$$

This shows that the moment with respect to the x-axis of stresses (33) vanishes. In the same manner, it can be proved that the moment M_y vanishes also.

Having eq. (33), for normal stresses, we can now calculate the corresponding shearing stresses which are of the same kind as those discussed in considering bending of the flanges of an I-beam, and which constitute the second portion T_2 of the torque. For this purpose we use equation of equilibrium (7). Substituting in this equation expression (33) for σ_z we obtain

$$\frac{\partial(\tau t)}{\partial s} = -Et\varphi'''(D - \omega_s).$$

* p denotes in this case the stress at the distance equal to unity from the x-axis.

Integrating it and observing that φ is independent of s and that τ vanishes for $s = 0$, we obtain

$$\tau t = - E\varphi''' \int_0^s (D - \omega_s)tds. \tag{35}$$

The portion T_2 of the torque is then obtained by a summation along the middle line of the moments of elemental shear forces $(\tau t)ds$ about the shear center, which gives

$$T_2 = \int_0^m (\tau t)rds = - E\varphi''' \int_0^m rds \int_0^s (D - \omega_s)tds. \tag{36}$$

This equation can be simplified if we observe that from notations (27) follows

$$rds = - \frac{d(D - \omega_s)}{ds} ds.$$

Hence

$$\int_0^m rds \int_0^s (D - \omega_s)tds = - \int_0^m \frac{d(D - \omega_s)}{ds} ds \int_0^s (D - \omega_s)tds.$$

Integrating on the right-hand side by parts and using eq. (34), we obtain

$$\int_0^m rds \int_0^s (D - \omega_s)tds = \int_0^m (D - \omega_s)^2 tds.$$

Substituting into eq. (36), the following expression for T_2 is obtained

$$T_2 = - E\varphi''' \int_0^m (D - \omega_s)^2 tds. \tag{37}$$

In the preceding article several examples of calculating the quantity $D - \omega_s$ along the middle line of the cross section were shown. Summing up the squares of this quantity along the middle line, we obtain the integral on the right-hand side of eq. (37). Examples of such calculations will be given later. Since D and ω_s have the dimension of length to the square, the integral will have the dimension of length to the sixth power. Introducing the notation

$$E \int_0^m (D - \omega_s)^2 tds = C_1, \tag{38}$$

we rewrite eq. (37) in the following form:

$$T_2 = - C_1\varphi'''. \tag{39}$$

This is the portion of the torque due to non-uniformity of torsion and to non-uniformity of warping. In further discussion it will be called the *warping torque* and the constant C_1, the *warping rigidity*. Combining eqs. (29) and (39), we obtain the differential equation for non-

uniform torsion of thin-walled bars of open cross section *

$$T = C\varphi' - C_1\varphi'''. \tag{40}$$

The previously obtained eq. (31) is only a particular case of eq. (40). When eq. (40) is solved and the expression for the angle of twist φ is found, we obtain T_1 and T_2 from eqs. (29) and (39), respectively. Stresses produced by T_1 are then calculated as for pure torsion. The normal and shearing stresses produced by T_2 are found from eqs. (33) and (35), respectively.

The calculation of warping rigidity requires, as we have seen, the evaluation of the integral on the left-hand side of eq. (38). Several examples of the derivation of expressions for $D - \omega_s$ have been shown in article 3. Using them, the expression for C_1 can be obtained without much difficulty. Take, for example, the cross-section in the form of the arc of a circle, Fig. 15. Then

$$D - \omega_s = a[a(\alpha - \psi) - e \sin(\alpha - \psi)].$$

Substituting into eq. (38) and integrating, we obtain for constant thickness

$$C_1 = Eta^3 \int_o^{2\alpha} [a(\alpha - \psi) - e \sin(\alpha - \psi)]^2 d\psi,$$

where, from eq. (11),

$$e = 2a \frac{\sin\alpha - \alpha\cos\alpha}{\alpha - \sin\alpha\cos\alpha}.$$

After integration, we obtain

$$C_1 = \tfrac{2}{3}Eta^5 \left[\alpha^3 - \frac{6(\sin\alpha - \alpha\cos\alpha)^2}{\alpha - \sin\alpha\cos\alpha}\right].$$

In the case of a channel, the values of $D - \omega_s$ are shown in Fig. 16. The value of the integral in eq. (38) is

$$2\frac{h^2}{4}t\int_o^b (b - d - s)^2 ds + d^2t\int_b^{b+h}\left(-\frac{h}{2} - b + s\right)^2 ds$$
$$= \frac{th^2}{12}[d^2h + 2b^3 - 6db(b - d)].$$

Substituting for d its value from eq. (10), we obtain

$$C_1 = E\frac{th^2b^3}{24}\left[1 + \frac{3h}{6b + h}\right].$$

* This equation was derived for the particular case of an I-section by the writer; see his paper in *Bull. Polyt. Inst. S. Petersburg*, 1905. Extension of the equation to sections with unequal flanges was made by C. Weber, *Ztschr. f. angew. Math. u. Mech.*, vol. 6, 1926, p. 85. Further extension of the equation to all thin-walled open sections is due to H. Wagner, Technische Hochschule, Danzig, the 25th Anniversary Publication, 1929.

In a similar manner, for the z-section shown in Fig. 17, we obtain

$$C_1 = E\frac{tb^3h^2}{12}\cdot\frac{4b^3 + 12b^2h + 9bh^2 + 2h^3}{8b^3 + 12b^2h + 6bh^2 + h^3}.$$

In the case of cross sections all flanges of which intersect along one axis, Fig. 11, the value of $D - \omega_s$ vanishes and the warping rigidity vanishes also.

5. **Calculation of the Angle of Twist.**—To obtain the angle of twist we have to integrate eq. (40). Introducing the notation

$$\frac{C}{C_1} = k^2,$$

eq. (40) becomes

$$\varphi''' - k^2\varphi' = -\frac{T}{C_1}.$$

The general solution of this equation is

$$\varphi = \frac{Tz}{k^2C_1} + A + A_1 \sinh kz + A_2 \cosh kz. \tag{41}$$

We find the constants of integration from conditions at the ends of the bar. In our case, Fig. 19, φ and φ' vanish at the built-in end, $z = 0$, since rotation of that cross section and its warping, given by eq. (32), are prevented. At the end $z = l$, we assume that there are no normal stresses. Then, as we see from eq. (33), φ'' vanishes for $z = l$. To satisfy all these conditions, we must take

$$A_1 = -\frac{T}{C_1k^2}; \qquad A = -A_2 = -\frac{T}{C_1k^3}\tanh kl.$$

Substituting into expression (41) for φ, we obtain

$$\varphi = \frac{T}{C_1k^3}[kz - \sinh kz + \tanh kl\,(\cosh kz - 1)]. \tag{42}$$

For the end of the bar, $z = l$, we obtain

$$\varphi_l = \frac{Tl}{C}\left(1 - \frac{1}{kl}\tanh kl\right).$$

The second term in parenthesis represents the effect on the angle of twist of warping rigidity of the bar. It is seen that this effect diminishes as the length of the bar increases.

The formula obtained for the angle of twist is in good agreement with experiments. To realize experimentally conditions, assumed for the built-in end, torsion was produced by a couple applied at the middle while the ends of the bar were restrained from rotation but were free

to warp, Fig. 20. From symmetry, it is evident that the middle cross section remains plane and each half of the bar is in the condition assumed in the derivation of the above formula for the angle of twist. Measuring the angle of twist at different distances from the middle the above developed theory can be checked.*

In the above analysis, it was assumed that the normal stresses σ_z vanish at the end $z = l$. If they do not vanish but are distributed as shown by eq. (33), the derivative φ'' at the end will be different from zero and there will be an additional twist produced by the stresses σ_z distributed at the end.† To establish the relation between φ'' and these normal stresses σ_z, we multiply both sides of eq. (33) by $(D - \omega_s)tds$

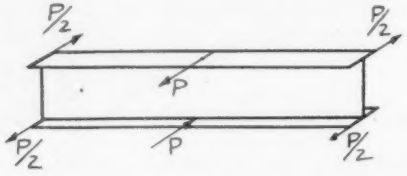

FIG. 20.

and integrate along the entire length m of the middle line of the cross section. In this way we obtain

$$\int_o^m \sigma_z(D - \omega_s)tds = E\varphi'' \int_o^m (D - \omega_s)^2 tds = C_1\varphi''$$

and

$$\varphi'' = \frac{1}{C_1}\int_o^m \sigma_z(D - \omega_s)tds. \tag{43}$$

Substituting for σ_z the values of normal stresses at the end, $z = l$, we find, from eq. (43), the value of ζ_l''. Using this value, instead of zero, in our previous analysis, we find that the angle of twist φ_l is obtained by adding to the previously found expression for φ_l the quantity

$$\frac{\varphi_l''}{k^2 \cosh kl}(\cosh kz - 1).$$

This quantity represents the angle of twist produced by normal stresses applied at the end of the bar. Substituting for φ_l'' its value (43) and substituting $k^2 = C/C_1$, we obtain for this angle the expression

$$\varphi = \frac{1}{C \cosh kl}(\cosh kz - 1)\int_o^m \sigma_z(D - \omega_s)tds. \tag{44}$$

* Such tests, using I-beams with various ratios of width of flanges to depth of the beam, were made by the writer. See *Bull. Polyt. Inst. S. Petersburg*, 1906.

† Such twist produced by longitudinal stresses was first discussed by V. Z. Vlasov; see his book "Thin Walled Elastic Bars," Moscow, 1940.

This solution assumes that the stresses σ_z are distributed along the cross section in accordance with eq. (33), which states that normal stresses are proportional to warping w as illustrated by Figs. 16 and 17. The resultant force and resultant moment of such stress distribution vanish, as was shown in article 4. On the basis of Saint Venant's principle, it can be concluded that such forces may produce only local effect, but in the case of thin-walled open sections this effect can become of practical importance and must be considered. For example, comparing a z-section the web of which is under uniform tension (Fig. 21a), with the

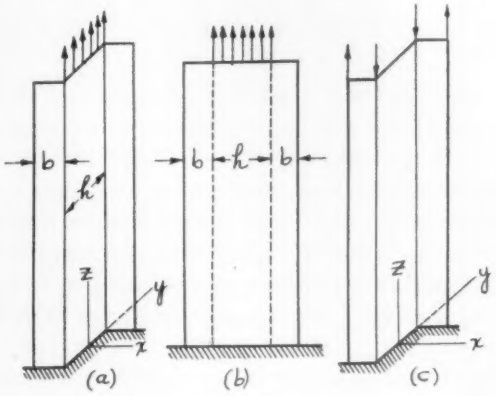

FIG. 21.

flat plate locally loaded, as shown in Fig. 21b, it will be appreciated that the stress distribution in these two cases will be different. In the case of the plate we can assume that the distribution stresses over cross sections rapidly approach uniformity as the distance from the loaded end increases. In the case of the z-section the conditions are more complicated: As a consequence of extension of the web, bending of the flanges and torsion of the z-bar will be produced. The corresponding irregularities in stress distribution do not decrease with increase in the distance from the end as rapidly as in the case of the flat plate. In this example the stresses applied at the end are not in accordance with eq. (33), but it seems reasonable to assume that there will be only a local disturbance in stress distribution and at a short distance from the end a uniform tension combined with stresses given by eq. (33) will be established.* This justifies the application of eq. (44) also in cases similar to that shown in Fig. 21a.

As soon as the law of distribution of normal stresses at the end is given, we substitute the corresponding expression for σ_z into eq. (44) and calculate φ. Knowing φ we can calculate the stresses produced by torsion using eqs. (29), (33) and (35). If there are longitudinal con-

* It seems desirable to verify this statement by experiments.

centrated forces applied at the end, the integration in eq. (44) must be replaced by summation and we obtain

$$\varphi = \frac{1}{C \cosh kl} (\cosh kz - 1) \sum P_s (D - \omega_s). \tag{45}$$

Take, for example, the case shown in Fig. 21*c*. The resultant and the moments M_x, M_y of the four forces P applied at the end vanish. The values of $D - \omega_s$ for a z-section are given in Fig. 17*a*. Using these values we obtain

$$\sum P_s(D - \omega_s) = 2PD + 2P\left(D - \frac{bh}{2}\right) = \frac{bh^2}{h + 2b} P.$$

Substituting in eq. (45) we obtain a formula for the angle of twist. From this discussion we see that longitudinal forces do not produce torsion only if they are applied to the points for which the quantity $D - \omega_s$, defining warping displacements w, vanishes. The positions of such points for the channel and z-sections are shown in Figs. 16 and 17*a*. This conclusion can be obtained also from the reciprocity theorem. If torsion produces warping of the end cross section, i.e. displacements of points at the end in the z-direction, the forces parallel to the z-axis applied at the end must produce torsion. From Fig. 17*a* we conclude that a longitudinal force applied at any point of the web of a z-section produces always the same torsion, while in the case of a channel section the angle of twist will depend on the position of the point of application of the force as can be seen from Fig. 16.

6. **Combined Bending and Torsion.**—Let us consider now the general case of a thin-walled bar under the action of any transverse forces. Each force can be replaced by a parallel force passing through the *axis of shear centers* and a torque. In this manner we obtain the bar loaded along its shear center axis and submitted to the action of torque applied in several cross sections. The transverse forces applied to the shear center axis produce only bending. The corresponding deflections and stresses can be calculated as shown in article 2. In discussing torsion, we use the results of the preceding article. We take the origin of coördinates at the end of the bar and denote by T_o the torque at that end. Then the angle of twist for the portion of the bar between the end and the first transverse load, as obtained from eq. (41), is

$$\varphi = \frac{T_o z}{k^2 C_1} + A + A_1 \sinh kz + A_2 \cosh kz. \tag{46}$$

A similar equation can be written for each portion of the bar between two consecutive transverse forces. It is only necessary to replace T_o by the value of torque at the beginning of that portion. The constants of integration must then be determined from the continuity conditions

at the points of load application. The calculations can be greatly simplified if, instead of constants of integration A, A_1, A_2, we introduce quantities defining the conditions at the end $z = o$ of the bar.* Differentiating eq. (46) and substituting $z = o$, we obtain

$$\varphi_o = A + A_2,$$

$$\varphi_o' = \frac{T_o}{k^2 C_1} + A_1 k,$$

$$\varphi_o'' = A_2 k^2,$$

where the subscript on the left-hand side indicates that the quantities refer to the end $z = o$ of the bar. Solving these equations for the constants A, A_1, A_2 and substituting these values into eq. (46) we obtain

$$\varphi = \varphi_o + \frac{1}{k}\varphi_o' \sinh kz + \frac{1}{k^2}\varphi_o''(\cosh kz - 1) + \frac{T_o}{k^2 C_1}\left(z - \frac{1}{k}\sinh kz\right). \quad (47)$$

Here the angle of twist for any cross-section of the first portion of the bar is expressed by the values φ_o, φ_o', φ_o'', T_o at the end $z = o$. By differentiation of eq. (47) we obtain

$$\left.\begin{aligned} \varphi' &= \varphi_o' \cosh kz + \frac{1}{k}\varphi_o'' \sinh kz + \frac{T_o}{k^2 C_1}(1 - \cosh kz), \\ \varphi'' &= k\varphi_o' \sinh kz + \varphi_o'' \cosh kz - \frac{T_o}{kC_1}\sinh kz. \end{aligned}\right\} \quad (48)$$

Equations (47) and (48) are applicable between $z = o$ and $z = a$, where a defines the position of the first transverse load. In considering now the second portion of the bar and taking $z > a$, we have to take into account the torque applied at the cross section $z = a$. Let T_1 denote that torque. The expression for angle of twist in the second portion of the bar is now obtained by adding the angle of twist produced by T_1 to the previous expression (47). In this manner we obtain, for $z > a$,

$$\varphi = \varphi_o + \frac{1}{k}\varphi_o' \sinh kz + \frac{1}{k^2}\varphi_o''(\cosh kz - 1) + \frac{T_o}{k^2 C_1}\left(z - \frac{1}{k}\sinh kz\right) + \frac{T_1}{k^2 C_1}\left[z - a - \frac{1}{k}\sinh k(z - a)\right]. \quad (49)$$

The last term on the right-hand side represents the angle produced by T_1. It is obtained from the last term of eq. (47) by substituting T_1 for

* This method was developed by A. N. Krilov in connection with a discussion of bending of beams supported by an elastic foundation. See his book: "Calculation of Beams on Elastic Foundation," published by Russian Academy of Sciences, S. Petersburg, 1931.

T_o and $z - a$ instead of z since the distance of T_1 from the cross section under consideration is $z - a$.

In a similar manner we can proceed also with the third portion of the bar and so on, to the last portion. The expressions for φ in all portions of the bar contain the same constants φ_o, φ_o', φ_o'', and T_o. All these constants can now be determined from the conditions at the two ends of the bar.

To illustrate the method let us consider several simple examples. We begin with the case in which the bar is twisted by torque applied at the ends, and at the same time the ends are constrained so that warping is entirely restrained. Since there are no forces applied in the span, eq. (47) can be applied to the entire length of the bar. Assuming that the end $z = o$ is immovable and observing that warping is restrained, we have to put into eq. (47) $\varphi_o = 0$, $\varphi_o' = 0$, which gives

$$\left.\begin{aligned} \varphi &= \frac{1}{k^2}\varphi_o''(\cosh kz - 1) + \frac{T_o}{k^2C_1}\left(z - \frac{1}{k}\sinh kz\right), \\ \varphi' &= \frac{1}{k}\varphi_o'' \sinh kz + \frac{T_o}{k^2C_1}(1 - \cosh kz). \end{aligned}\right\} \tag{50}$$

Since warping on the other end ($z = l$) of the bar is also restrained, we have

$$\varphi_l' = \frac{1}{k}\varphi_o'' \sinh kl + \frac{T_o}{k^2C_1}(1 - \cosh kl) = 0,$$

from which

$$\varphi_o'' = -\frac{T_o}{kC_1} \cdot \frac{1 - \cosh kl}{\sinh kl}.$$

Substituting into the first of eqs. (50), we obtain the angle of twist

$$\varphi = -\frac{T_o}{k^2C_1}\frac{1 - \cosh kl}{\sinh kl}(\cosh kz - 1) + \frac{T_o}{k^2C_1}\left(z - \frac{1}{k}\sinh kz\right).$$

Taking $z = l$, we obtain the rotation of the end, $z = l$, of the bar

$$\varphi_l = \frac{T_o l}{C}\left(1 - \frac{2}{kl}\tanh\frac{kl}{2}\right).$$

The second term in parenthesis gives the effect of the end restraint against warping on the magnitude of the angle of twist.

As a second example let us consider the case shown in Fig. 22. A bar, supported at the ends is eccentrically loaded at a distance a from the left end. Denoting by e the distance of the load from the shear center axis, we reduce the problem to that of simple bending of the bar by a load P combined with torsion produced by the torque Pe applied at the distance a from the left end of the bar. Assume first that the ends of the bar cannot rotate with respect to the z-axis but are free to

warp. In such case

$$\varphi = \varphi'' = o \qquad \text{for} \qquad z = o \qquad \text{and} \qquad z = l.$$

For the portion of the bar from $z = o$ to $z = a$ we use eq. (47). Substituting in this equation $\varphi_o = \varphi_o'' = o$ we obtain

$$\varphi = \frac{1}{k}\varphi_o' \sinh kz + \frac{T_o}{k^2 C_1}\left(z - \frac{1}{k}\sinh kz\right).$$

For the right-hand portion of the bar, $z > a$, we use eq. (49) which, for

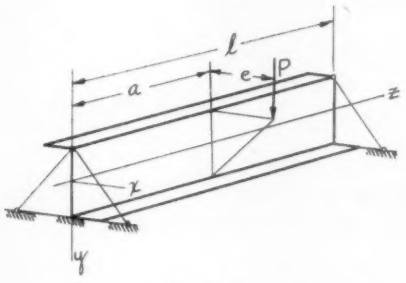

FIG. 22.

$\varphi_o = \varphi_o'' = o$, $T_1 = Pe$, gives

$$\varphi = \frac{1}{k}\varphi_o' \sinh kz + \frac{T_o}{k^2 C_1}\left(z - \frac{1}{k}\sinh kz\right) + \frac{Pe}{k^2 C_1}\left[z - a - \frac{1}{k}\sinh k(z-a)\right],$$

$$\varphi'' = k\varphi_o' \sinh kz - \frac{T_o}{kC_1}\sinh kz - \frac{Pe}{C_1 k}\sinh k(z-a).$$

Observing that at the end $z = l$, $\varphi_l = \varphi_l'' = o$, we obtain the following equations for calculating the constants φ_o' and T_o:

$$\frac{1}{k}\varphi_o' \sinh kl + \frac{T_o}{k^2 C_1}\left(l - \frac{1}{k}\sinh kl\right) = -\frac{Pe}{k^2 C_1}\left[l - a - \frac{1}{k}\sinh k(l-a)\right],$$

$$k\varphi_o' \sinh kl - \frac{T_o}{kC_1}\sinh kl = \frac{Pe}{kC_1}\sinh k(l-a).$$

Solving these equations, we obtain

$$T_o = -Pe\,\frac{l-a}{l},$$

$$\varphi_o' = \frac{Pe}{k^2 C_1 \sinh kl}\left[\sinh k(l-a) - \frac{l-a}{l}\sinh kl\right].$$

Substituting these values into the expressions for φ, we obtain the angles of twist for both portions of the bar. Using them in eqs. (29), (33) and (35) we can calculate the normal and shearing stresses produced by the torque Pe.

If the ends of the bar in Fig. 22 are built-in and cannot warp, the end-conditions are

$$\varphi = \varphi' = o \qquad \text{for} \qquad z = o \qquad \text{and} \qquad z = l.$$

Substituting $\varphi_o = \varphi_o' = o$ into eq. (49) we obtain, for $z > a$,

$$\varphi = \frac{1}{k^2}\varphi_o''(\cosh kz - 1) + \frac{T_o}{k^2 C_1}\left(z - \frac{1}{k}\sinh kz\right) + \frac{Pe}{k^2 C_1}\left[z - a - \frac{1}{k}\sinh k(z-a)\right].$$

Applying this equation at the end $z = l$ we obtain, for calculating the constants φ_o'' and T_o, the following equations:

$$\frac{1}{k^2}\varphi_o''(\cosh kl - 1) + \frac{T_o}{k^2 C_1}\left(l - \frac{1}{k}\sinh kl\right) = -\frac{Pe}{k^2 C_1}\left[l - a - \frac{1}{k}\sinh k(l-a)\right],$$

$$\frac{1}{k}\varphi_o''\sinh kl + \frac{T_o}{k^2 C_1}(1 - \cosh kl) = -\frac{Pe}{k^2 C_1}[1 - \cosh k(l-a)].$$

From these equations the constants φ_o'' and T_o can be calculated in each particular case. Substituting them in the expressions for φ, we again have the complete solution of the problem. Having the solution for one concentrated force, as shown in Fig. 22, we can, by superposition, find the solution for any number of concentrated forces.

The case of distributed load can also be handled without difficulty. As an example, take again the bar shown in Fig. 22 and assume that, instead of a force P, we have the distributed load of constant intensity q applied along the line parallel to z and distance e from the shear center axis. Torque at any cross section then is

$$T = T_o + qez.$$

Substituting this value into eq. (40) and solving it, as before, we obtain

$$\varphi = \varphi_o + \frac{1}{k}\varphi_o'\sinh kz + \frac{1}{k^2}\varphi_o''(\cosh kz - 1) + \frac{T_o}{k^2 C_1}\left(z - \frac{1}{k}\sinh kz\right) + \frac{qez^2}{2k^2 C_1}.$$

Assume that both ends of the bar are built-in so that

$$\varphi = \varphi' = o \qquad \text{for} \qquad z = o \qquad \text{and} \qquad z = l.$$

Then substituting $\varphi_o = \varphi_o' = o$ into the above expression for φ, we obtain

$$\varphi = \frac{1}{k^2}\varphi_o''(\cosh kz - 1) + \frac{T_o}{k^2 C_1}\left(z - \frac{1}{k}\sinh kz\right) + \frac{qez^2}{2k^2C_1}.$$

Applying this equation at the end $z = l$ and observing that, from symmetry, we have

$$T_o = -\frac{qel}{2},$$

the following equation is obtained:

$$\frac{1}{k^2}\varphi_o''(\cosh kl - 1) - \frac{qel}{2k^2C_1}\left(l - \frac{1}{k}\sinh kl\right) + \frac{qel^2}{2k^2C_1} = 0,$$

from which

$$\varphi_o'' = -\frac{qel}{2kC_1}\cdot\frac{\sinh kl}{\cosh kl - 1}.$$

Substituting this value into expression for φ, we obtain

$$\varphi = -\frac{qel}{2k^3C_1}\frac{\sinh kl}{\cosh kl - 1}(\cosh kz - 1) - \frac{qel}{2k^2C_1}\left(z - \frac{1}{k}\sinh kz\right) + \frac{qez^2}{2k^2C_1}.$$

This expression can be simplified and put in the following form:

$$\varphi = \frac{qe}{k^3C_1}\left[\frac{k(z^2 - lz)}{2} + \frac{l}{\sinh\dfrac{kl}{2}}\sinh\frac{kz}{2}\sinh\frac{k(l-z)}{2}\right].$$

It is seen that the solution of eq. (40) in particular cases does not represent any difficulty.

7. **Torsional Buckling under Central Thrust.**—It is known that a thin-walled bar under uniform axial compression may sometimes buckle torsionally while its axis remains straight. Figure 23 shows an example of such buckling in the case of a bar having four identical flanges. The fiber coinciding with the z-axis remains straight during this buckling and the moment M_z of the compressive forces applied at the end vanishes for each cross section of the bar. To determine the torque producing twist as indicated in the figure, the deflection of the flanges during buckling must be considered.

The method to be used in further analysis, we shall first explain by taking the simple case of buckling of a strut, Fig. 24*a*. Initially, the

strut is straight and there acts only centrally applied thrust P. Let us now assume that this force P obtains its critical value and that the strut can have also a slightly deflected form of equilibrium. Due to this deflection some bending stresses will be superposed on the initial uniformly distributed compressive stresses. At the same time the

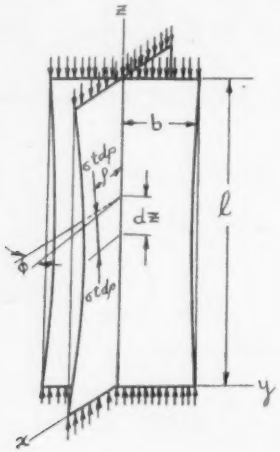

FIG. 23.

initial stresses will act on the slightly rotated cross sections as shown in Fig. 24*b*. Each element of the deflected strut between two adjacent cross sections is in equilibrium and we can state that the bending stresses produced during buckling of the strut are equilibrating the initial compressive stresses acting on the slightly rotated cross sections. Observing

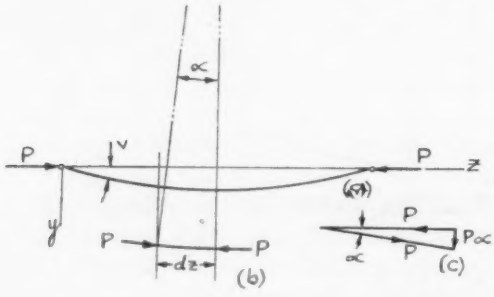

FIG. 24.

that the angle between the two consecutive cross sections after deflection, Fig. 24*b*, is

$$\alpha = -\frac{d^2v}{dz^2}\,dz,$$

we conclude that the action of compressive forces P on the rotated

cross sections is equivalent to the action on each element of the strut of a transverse load, Fig. 24*c*,

$$-P\frac{d^2v}{dz^2}dz.$$

We see that the deflection curve of the strut and the corresponding bending stresses can be found by assuming that the strut is loaded by fictitious load of intensity $-P\,d^2v/dz^2$. The differential equation of the deflection curve (18) in this case is

$$EI_x\frac{d^4v}{dz^4} = -P\frac{d^2v}{dz^2}.$$

From this equation the known critical value of the compressive force P_{cr} can be obtained in the usual way.

Returning now to the problem of torsional buckling, shown in Fig. 23, we can state that under the critical condition, the buckled form of equilibrium is sustained by the longitudinal compressive stresses acting on rotated cross sections of the fibers. Assuming that thickness t of flanges is small and considering a strip of cross section $td\rho$ at a distance ρ from the axis we see that, due to torsional buckling, its deflection is $v = \rho\varphi$. Taking one element of this strip between two consecutive cross sections, distance dz apart, and considering the action of the initial compressive force $\sigma td\rho$ on the slightly rotated cross sections of the strip, Fig. 23, we will obtain the force

$$-(\sigma td\rho)\frac{d^2v}{dz^2}dz = -(\sigma td\rho)\rho\frac{d^2\varphi}{dz^2}dz.$$

The moment of this force with respect to the z-axis is

$$-\sigma\frac{d^2\varphi}{dz^2}dzt\rho^2d\rho.$$

Summing up such moments and extending the summation over the entire cross section, we obtain the torque acting on the element of the buckled bar included between the two consecutive cross sections. Using the notation m_z for torque per unit length of the bar, we obtain

$$m_z = -4\sigma\frac{d^2\varphi}{dz^2}\int_o^b t\rho^2d\rho = -\sigma\frac{d^2\varphi}{dz^2}J_o,$$

where J_o is the polar moment of inertia of the cross section of the bar with respect to the shear-center, coinciding in this case with the centroid of the cross section. To establish now the equation for the buckled bar, we use eq. (40). Differentiating this equation with respect to z and

observing that with our rule of signs

$$m_z = -\frac{dT}{dz},$$

we find

$$C_1\varphi^{IV} - C\varphi'' = m_z. \tag{51}$$

Substituting for m_z the above calculated value, we obtain

$$C_1\varphi^{IV} - (C - \sigma J_o)\varphi'' = 0. \tag{52}$$

From this equation the critical value of compressive stress σ will now be obtained.

In the case shown in Fig. 23, the middle lines of all flanges intersect in one point and the warping rigidity C_1 vanishes; hence

$$(C - \sigma J_o)\varphi'' = 0.$$

This equation is satisfied by assuming that the quantity in parenthesis vanishes, which gives

$$\sigma_{cr} = \frac{C}{J_o} = \tfrac{4}{3}bt^3G/\tfrac{4}{3}tb^3 = G\frac{t^2}{b^2}. \tag{53}$$

We found that the critical value of compressive stress is independent of the length of the bar and of the form of buckling defined by the angle φ. Such a result is obtained because in the derivation of eq. (40) any resistance of the flanges to bending in the direction perpendicular to the flange was neglected. To take it into account we have to consider each flange as a uniformly compressed plate simply supported along three sides and completely free to buckle along the fourth side. This more accurate investigation shows that the critical stress is *

$$\sigma_{cr} = \left(0.456 + \frac{b^2}{l^2}\right)\frac{\pi^2}{6(1-\mu)}\frac{Gt^2}{b^2}.$$

The second term in parenthesis gives the influence on the critical stress of the length of the bar. For bars of considerable length this term can be neglected. Then we obtain

$$\sigma_{cr} = \frac{0.75}{1-\mu}\frac{Gt^2}{b^2}.$$

For $\mu = 0.3$ this value is larger than that calculated above by about 7 per cent.

Equation (52) holds also in the cases when C_1 does not vanish, and for unsymmetrical cross sections if only the axis of the bar remains straight during buckling. This requires, as we will see later, that the

* This solution was obtained by the writer; see *Bull. Polytech. Inst.*, Kiev, 1907, and *Z. für Math. u. Physik*, vol. 58, p. 337, 1910.

shear-center axis coincide with the centroidal axis as in the case of a z-section. In all such cases the critical compressive stress is obtained from the solution of eq. (52). Introducing the notation:

$$k^2 = (\sigma J_o - C)/C_1,$$

we find that this solution is

$$\varphi = A \sin kz + A_1 \cos kz + A_2 z + A_3. \tag{53}$$

If the ends of the compressed bar cannot rotate but are free to warp, we have the following conditions at the ends:

$$\varphi = \varphi'' = o \qquad \text{for} \qquad z = o \qquad \text{and} \qquad z = l,$$

from which follows

$$A_1 + A_3 = 0, \qquad A_1 = 0, \qquad A_2 = 0,$$

$$kl = n\pi.$$

Substituting for k its value, we obtain

$$\sigma J_o - C = \frac{n^2\pi^2}{l^2} C_1.$$

The smallest value of σ satisfying this condition is *

$$\sigma_{cr} = \frac{1}{J_o}\left(C + \frac{\pi^2}{l^2} C_1 \right). \tag{55}$$

If the ends of the bar are built-in and cannot warp, the end conditions are

$$\varphi = \varphi' = o \qquad \text{for} \qquad z = o \qquad \text{and} \qquad z = l.$$

To satisfy these conditions we must take

$$A_1 + A_3 = 0, \qquad A = A_2 = 0,$$

$$kl = 2n\pi.$$

The critical compressive stress in this case is

$$\sigma_{cr} = \frac{1}{J_o}\left(C + \frac{4\pi^2}{l^2} C_1 \right).$$

It should be noted that solution (53) previously obtained for $C_1 = 0$ can also be obtained from eq. (52) for C_1 different from zero if only the ends of the bar are free to rotate with respect to each other so that we can assume that φ' is a constant. In such case we assume, in the general solution (54), that $A = A_1 = A_3 = 0$ and take

$$\varphi = A_2 z.$$

* This solution was obtained by H. Wagner; see Festschrift "Fünfundzwanzig Jhare Technische Hochschule Danzig," p. 329, 1929.

To show the torque sustaining twisting in this case we resolve the external compressive forces $\sigma t ds$ acting on each longitudinal strip and parallel to the z-axis into two components: One in the direction of the inclined fibers and the other parallel to the xy-plane as shown at point N of the upper cross section in Fig. 25. This second component con-

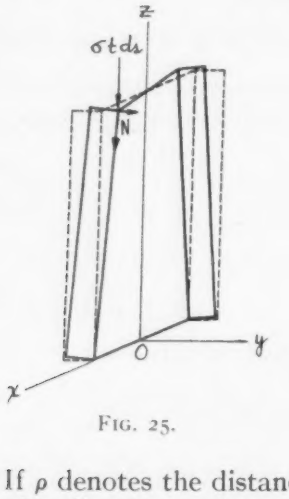

FIG. 25.

tributes to the torque. If ρ denotes the distance of the strip from the axis of rotation, its angle of inclination to the z-axis is $\rho\varphi'$, and the above mentioned horizontal component of compressive force $\sigma t ds$ gives the moment with respect to the z-axis equal to

$$\sigma t ds \cdot \rho^2 \varphi'.$$

Summing up these moments and extending the summation over the entire cross section, we obtain

$$T = \sigma \varphi' J_o.$$

When σ has its critical value (53), we obtain

$$T = C\varphi'.$$

This torque, as we see, is just sufficient to sustain the twisted form of the bar.

(*To be continued in May issue.*)

STUDIES IN THE SENSITIVITY OF PHOTOGRAPHIC MATERIALS.

BY

A. P. H. TRIVELLI.

Communication No. 1020 from the Kodak Research Laboratories.

INTRODUCTION.

This paper deals with the expression of the sensitivity of photographic materials as deduced from the sensitivity of the individual grains. In the general theory of the photographic process, "sensitivity" is a collective term referring to a complex of concepts, which are quantitatively interrelated.

The sensitivity of a grain can be measured by the probability that it becomes developable at a certain exposure, which, for our purposes, can be conveniently measured in ergs rather than in the meter-candle-second units used in practical photography. If, out of N grains, k become developable at a certain exposure, then the probability that these grains have become developable is k/N. When N is constant at different exposures, a $k/\log It$ curve can be constructed from which, at a measured $D_{max.}$, the $D/\log It$ curve of the multigrain layer of the emulsion can be derived by putting $k/N = D/D_{max.}$.

The relation of $D/\log It$ for a definite $D_{max.}$ has been expressed quantitatively by Silberstein [1] in his quantum theory of exposure, to which reference will be made throughout this paper. The theory in its latest form is discussed in a paper by Silberstein and the author [2] under the title "Quantum Theory of Exposure Tested Exclusively on Photographic Emulsions."

THE SHAPE OF THE CHARACTERISTIC CURVE.

A study of the shape of the $D/\log It$ curve requires a fog-correction as suggested by Silberstein.[3] For a definite development time, such a characteristic curve can be regarded as either a single curve with an inflection point or a complex line consisting of a concave toe, a convex shoulder, and a straight-line portion between them. No crucial test has yet been devised which will decide which of these two viewpoints is correct. It is sometimes possible to draw a straight line in the $D/\log It$ relation over a considerable range of exposures between the toe and the

[1] *Phil. Mag.* **44**, 257 (1922); **45**, 1062 (1923); **5**, 464 (1928). *J. Opt. Soc. Amer.* **28**, 441 (1938); **31**, 343 (1941).

[2] To be published in *Journal of Optical Society of America*.

[3] Quoted in A. P. H. Trivelli: "Sensitivity Distribution Among the Grains of Photographic Emulsions," to be published in the JOURNAL OF THE FRANKLIN INSTITUTE.

shoulder regions, but this is not an adequate test. On the other hand, there are characteristic curves which do not show any definite straight-line part, but this also is no criterion for determining which of the viewpoints is correct. There always remains the possibility that a short straight-line portion exists between the toe and the shoulder of the characteristic curve that is not discernible by visual inspection.

There are also considerations of a photochemical nature. If the $D/\log It$ curve consists of a toe, a shoulder, and a straight-line portion between them, it can only be represented mathematically by three separate equations, each holding true only between definite exposure limits. In other words, each photographic emulsion can be divided into three fractions, each having its own specific sensitivity and sensitivity distribution among the different grains. These sensitivities cannot overlap, which is a very improbable picture.

Sensitivity determinations which are restricted to the "straight-line" portion of the characteristic curve, e.g., derived from the position of the inertia point, would refer only to one of the three sensitivities. This would provide a very incomplete picture of the sensitivity of a photographic emulsion.

If the characteristic curve can be held to consist of a single curve with an inflection point, the exposure value of the inflection point would be an essential part of the whole curve from D_{zero} to $D_{\text{max.}}$, and can be used as a measurement of the sensitivity of the photographic emulsion.

THE INERTIA VALUE.

To avoid all complications that arise in determining the location of the inflection point of the characteristic curve, the tangent through this point is used, without requiring a very accurate knowledge of the location of the inflection density, $\bar{D}$. In this way, both the inertia value i, and the gamma, γ, are obtained by a simple manipulation. The physical meaning of the inertia value, however, is then complicated, as will be shown later.

THE SENSITIVITY DERIVED FROM A DETERMINATION OF DENSITY.

A simpler measure of sensitivity is given by the reciprocal value of the exposure necessary to produce at a definite development time a standard density above fog. Such an expression has pragmatic significance in many cases. Its physical meaning is, however, restricted to the standard density only. It is of no general theoretical significance because it is incomplete.

A fixed density may be chosen from any part of the characteristic curve, preferably from the toe. However, as a measure of sensitivity of general significance, difficulties in the choice of such a density may then be encountered, which are quite noticeable when looking at the fog-corrected $D/\log It$ curves of experimental emulsions in Figs. 1 to 5.

having different size-frequency characteristics and grouped into families with the same silver iodide concentrations of 0, 0.77, 2.56, and 6.15 moles per cent., respectively. The film on which these emulsions were coated contains the same amount of silver halide per square centimeter of surface.

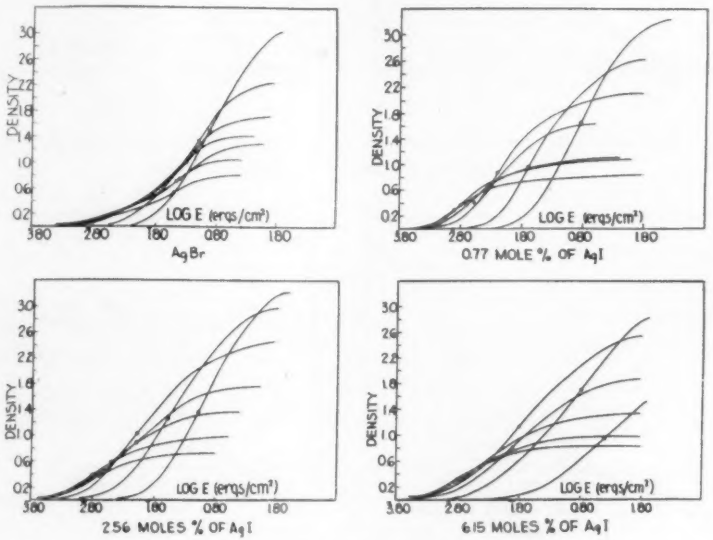

FIG. 1. Characteristic curves of nonconverted precipitation series at 5 minutes' development in DK-50 at 18° C.

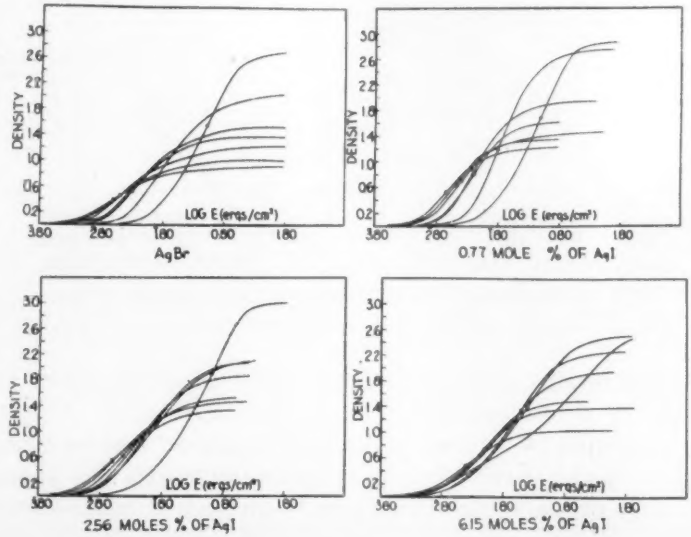

FIG. 2. Characteristic curves of converted precipitation series at 5 minutes' development in DK-50 at 18° C.

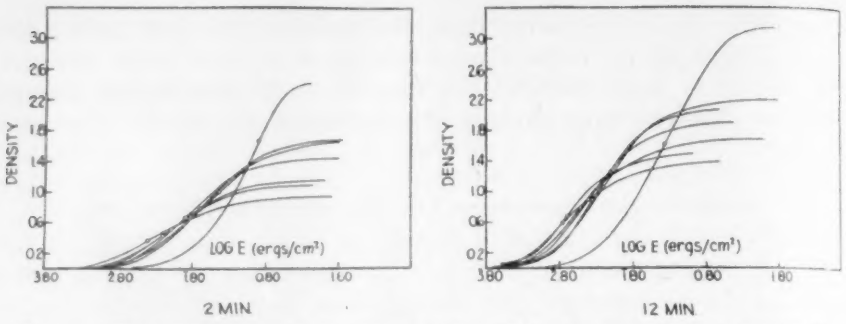

FIG. 3. Characteristic curves of nonconverted precipitation series with 2.56 moles % of silver iodide at different development times.

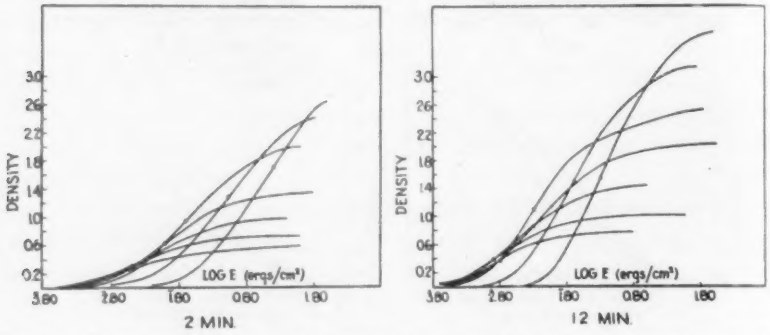

FIG. 4. Characteristic curves of converted precipitation series with 2.56 moles % of silver iodide at different development times.

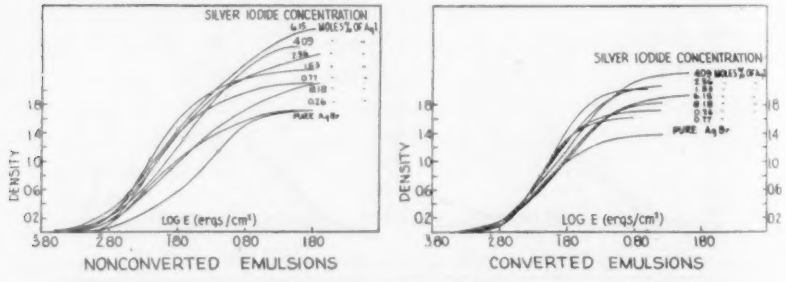

FIG. 5. Characteristic curves of silver iodide concentration series with 10 minutes' precipitation.

The characteristic curves of the nonconverted emulsions obtained with 5 minutes' development in DK-50 developer at 18° C. are shown in Fig. 1, and those of the curves of the converted * emulsions similarly obtained, in Fig. 2. From these graphs it can be seen that these curves intersect each other at different points in such a way that density

* "Converted" emulsions are made by dissolving the silver nitrate with a slight excess of ammonia, a solvent for silver halides.

speeds have no general physical significance for the comparison of the sensitivities of the different photographic materials. Changing the development time does not alter the behavior of these curves. This is seen in Figs. 3 and 4, for two families of nonconverted and converted

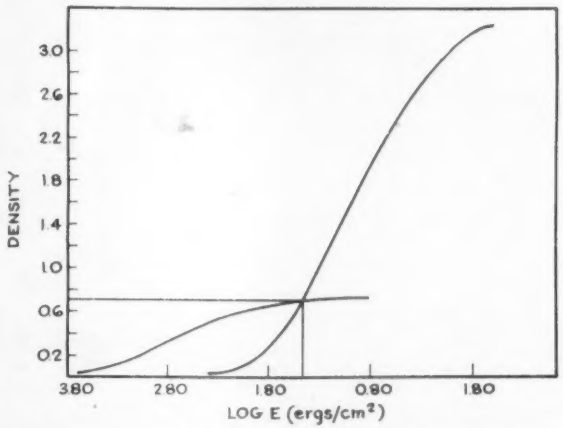

FIG. 6. Characteristic curves of two nonconverted emulsions with 2.56 moles % of Ag I.

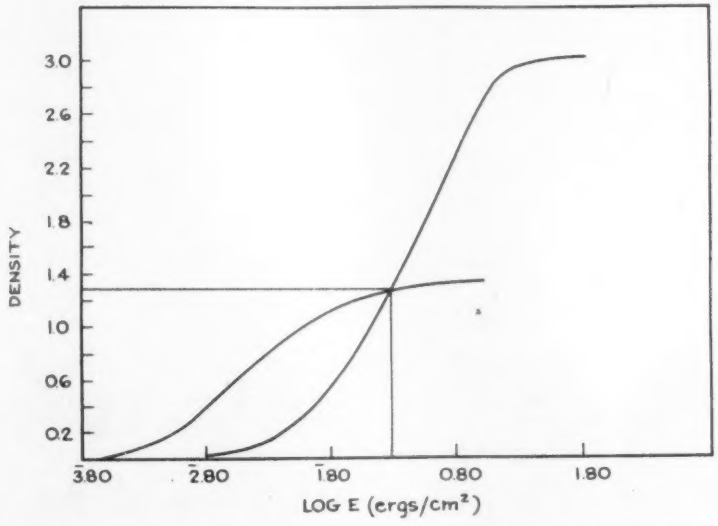

FIG. 7. Characteristic curves of two converted emulsions with 2.56 moles % of Ag I.

emulsions with 2.56 moles per cent. of silver iodide at 2 and 12 minutes' development in DK-50 developer at 18° C. The points of intersection move only with increasing development times towards higher densities. Even varying the silver iodide concentrations from 0 to 6.15 moles per cent. does not remove this difficulty, as can be seen from the curves

of Fig. 5, which were all obtained with 5 minutes' development in DK-50 developer at 18° C. All these curves were obtained with exposures to radiation of $\lambda = 426$ mμ.

These results show that the same density can be obtained repeatedly for two emulsions having different inertia values with the same exposure

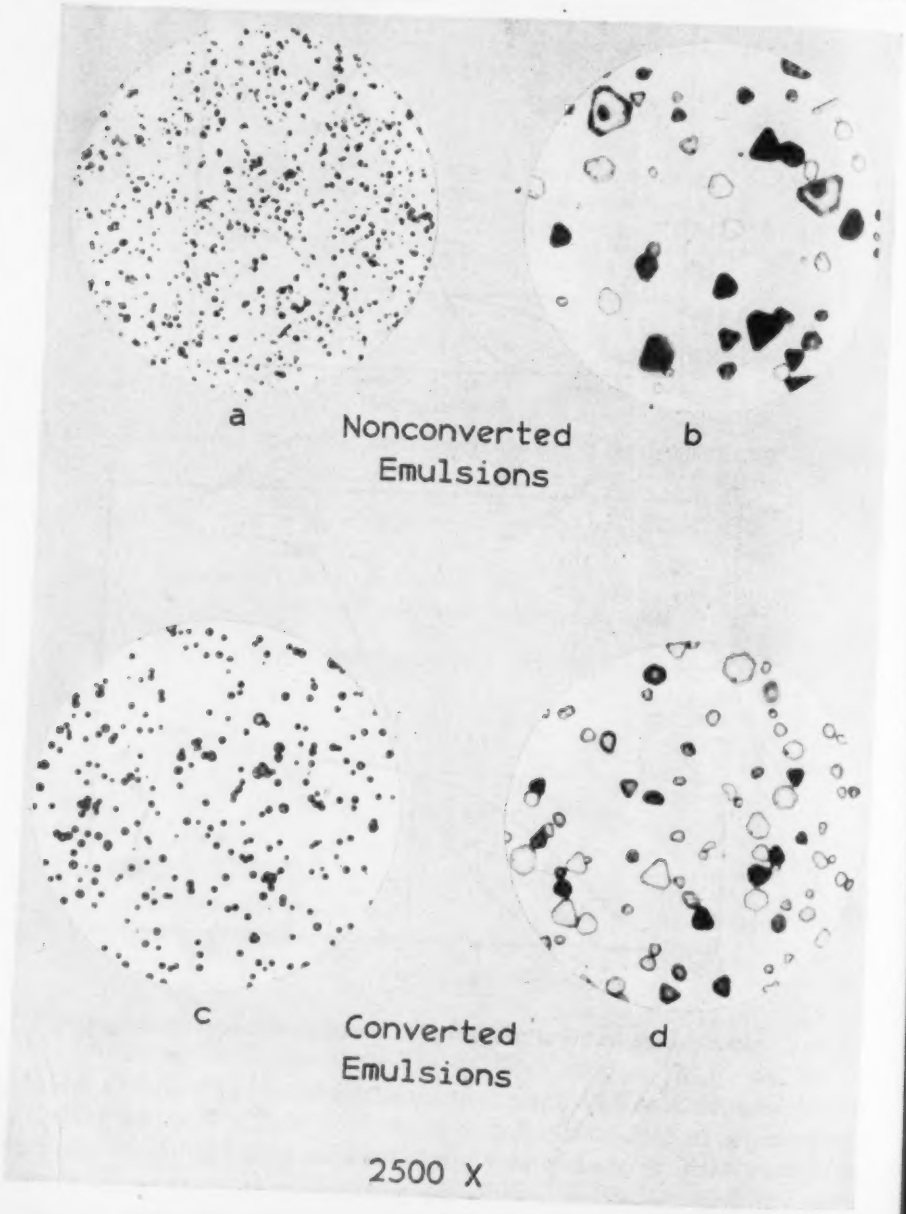

FIG. 8.

time and the same development. In Figs. 6 and 7 are reproduced the characteristic curves of two nonconverted and two converted emulsions, each emulsion containing 2.56 moles per cent. of silver iodide. All four films were developed for 5 minutes in DK-50 at 18° C.

The curves of the nonconverted emulsions shown in Fig. 6 were obtained by precipitating the silver halide for

$$t_p = 0.47 \text{ and } 86.93 \text{ minutes.}$$

They produce a density $D = 0.72$ at the same exposure $E = 30 \times 10^{10}$ quanta per square centimeter of film surface with a wave-length $\lambda = 426$ mμ. This density lies in the toe region of the characteristic curve of one emulsion and in the shoulder region of the corresponding curve of the other emulsion. Photomicrographs of the grains of these emulsions are reproduced at 2500 × magnification, indicated by *a* and *b*, respectively, in Fig. 8.

The different characteristics of the two emulsions at $D = 0.72$ are compared in Table I.

TABLE I.

Characteristics.	t_p = 0.47 Minute.	t_p = 86.93 Minutes.
Number of grains per cm.² of film	7.069×10^9	0.071×10^9
Average grain size	0.14 μ^2	2.61 μ^2
Dispersion of grain sizes	0.07 μ^2	2.65 μ^2
Uniformity of grain sizes	2.00	0.98
Skewness of distribution curve	0.13 μ^2	1.30 μ^2
Average grain volume	0.08×10^{-12} cm.³	15.56×10^{-12} cm.³
Average shape of the grains	0.072	0.031
Absorption coefficient	1655	613
Average absorption per grain	167	499
Covering power of silver	94.73	25.25

The inertia values of these emulsions are:

$$i = 0.646 \text{ and } 0.0141.$$

The curves of the converted emulsions shown in Fig. 7 were obtained by precipitating the silver halide for

$$t_p = 0.73 \text{ and } 86.02 \text{ minutes.}$$

They produce a density $D = 1.27$ at the same exposure $E = 41 \times 10^{10}$ quanta per square centimeter of film surface to radiation of wave-length $\lambda = 426$ mμ. This density lies near the inflection point of the characteristic curve of one emulsion and in the shoulder region of the characteristic curve of the other emulsion.

Photomicrographs of the grains of these emulsions at 2500 × magnification are reproduced in Fig. 8*c* and 8*d*. A comparison of the two emulsions at $D = 1.27$ is given in Table II.

TABLE II.

Characteristics.	t_p = 0.73 Minute.	t_p = 86.02 Minutes.
Number of grains per cm.² of film	1.849×10^9	0.154×10^9
Average grain size	0.20 μ^2	1.72 μ^2
Dispersion of grain sizes	0.12 μ^2	1.20 μ^2
Uniformity of grain sizes	1.67	1.43
Skewness of distribution curve	0.19 μ^2	1.16 μ^2
Average grain volume	0.43×10^{-12} cm.³	7.29×10^{-12} cm.³
Average shape of the grains	0.023	0.035
Absorption coefficient	1638	868
Average absorption per grain	385	302
Covering power of silver	84.58	44.63

The inertia values of these emulsions are:

$$i = 0.455 \text{ and } 0.0229.$$

The size-frequency characteristics listed in Tables I and II were calculated from data obtained according to Loveland's method of measuring the size-frequency distribution.

The dispersion of grain sizes, σ, is given by the standard deviation in μ^2

$$\sigma^2 = \overline{(a - \bar{a})^2},$$

in which a is the grain size measured by its projective area in μ^2 for each class size.

The uniformity of grain sizes is given by the quotient $\bar{a}/\sigma$.

The skewness η in μ^2 represents the deviation from the symmetry of a Gaussian probability curve and is calculated according to the equation

$$\eta^3 = \overline{(a - \bar{a})^3},$$

which expresses the growth of the grains of an emulsion.

The average volume of a grain, $\bar{v}$, in cubic centimeters, is given by the following equation:

$$\bar{v} = \frac{0.057}{N} \text{ cc.}$$

in which 0.057 cc. is the volume of the silver halide and N is the number of grains, both per cubic centimeter of emulsion.

The average shape of the grains is expressed by the ratio between the average thickness of the grains and their diameter. This diameter is calculated by taking twice the radius of a circle which has the same surface as the projective area of a grain.

The average thickness of a grain is calculated from the average volume and from the average size of the grain, the grain being regarded as a disk.

The absorption coefficient, k, is found from the exponent of the equation:

$$I = I_0 e^{-kb},$$

where I_0 is the incident radiation minus that reflected from the surface of the photographic materials; I is the transmitted radiation; b is the thickness of the emulsion layer; and e is the base of the natural logarithm.

The average absorption, K, per grain is obtained from the equation:

$$K = \frac{k}{N \cdot \bar{a}}.$$

The covering power of the silver was determined by Mr. B. Hutchins, of these Laboratories.

These few examples show that sensitivity derived from the exposure required to give a certain density has no definite direct relation to the size-frequency characteristics and radiation absorption of photographic emulsions, but that the density speed is the result of a complex of separate factors which are interchangeable with each other. Moreover, it must be considered that a density does not in itself express the effect of the probability that a grain will become developable at a certain exposure. This is given by the relation between the number of developable grains and the total number of grains. Therefore, $D/D_{max.}$, and not D, can be used with physical meaning in relation to the sensitivity of the emulsion.

THE SENSITIVITY DERIVED FROM THE INFLECTION POINT.

Only a density having a definite relation to the maximum density can be used as a measure of sensitivity for the purpose of this analysis. The simplest one is the density, $\bar{D}$, at the inflection point of the characteristic curve. For rotationally symmetrical curves, $\bar{D} = 1/2 D_{max.}$.

Silberstein [4] used the value of the inflection point of the fog-corrected characteristic curve consistently in his quantum theory of exposure, to express the sensitivity with a physical meaning. On all the curves of Figs. 1, 2, 3, 4, 5, and 6, the inflection points are indicated by open circles. In spite of all the intersections between these curves, nowhere are there two curves having the same density at the inflection point, owing mainly to the fact that no two of the curves that intersect each other have the same $D_{max.}$.

The reciprocal value of the exposure ($1/E$) in ergs required to produce the density at the inflection point gives the sensitivity of the emulsion on the film for a definite time of development. If the average grain size is not known, $1/E$ expresses the sensitivity per grain. Divided by the average grain size, $\bar{a}$, the sensitivity per unit surface of the grain is obtained which is the intrinsic sensitivity, ϵ, of the silver halide of the emulsion. Therefore,

$$\epsilon \bar{a} = \frac{hc}{\lambda E_1} \qquad (1)$$

[4] L. Silberstein: *J. Opt. Soc. Amer.*, **28**: 441–459 (1938).

and

$$\epsilon = \frac{hc}{\lambda E_1 \bar{a}}, \qquad (2)$$

in which h is Planck's constant, equal to 6.547×10^{-27}, and c is the velocity of light, equal to 2.99796×10^{10} cm. per second, giving

$$hc = 19.627 \times 10^{-16} \qquad \text{at} \qquad \lambda = 426 \text{ m}\mu.$$

On simple rotationally asymmetrical characteristic curves, the inflection point is not located at $1/2D_{max.}$. According to the quantum theory, the value of $\bar{D}/D_{max.}$ is determined by the minimum number of quanta necessary to make the grains of the emulsion developable. If r is that number of quanta, then

$$\bar{D}/D_{max.} = \frac{(3r+2)r^r}{(r+2)^{r+1}}. \qquad (3)$$

This gives, for different emulsions with different values of r, the data of Table III.

TABLE III.

r.	$\bar{D}/D_{max.}$
I	0.556
II	0.500
III	0.475
IV	0.461
V	0.452
VI	0.445
VII	0.440
VIII	0.436
IX	0.433
X	0.430
etc.	etc.

The most common curves among medium- and high-speed emulsions are the 2- and 3-quantum characteristic curves. The higher quanta curves appear probably more frequently among the low-speed high-contrast emulsions. Not enough data are available at present to give complete information on this point.

The determination of the location of the inflection point on the characteristic curve does not require the refinements of a mathematical analysis of the $D/\log It$ curve. For most purposes, it is sufficient to obtain the first derivative of the fog-corrected characteristic curve. This curve contains a flat maximum. It is sufficient to determine graphically the middle of this nearly straight-line region of the curve. In this way, the inflection points on the curves of Figs. 1, 2, 3, 4, 5, and 6 were found.

To show the small errors involved in the graphical determination of the values of log It corresponding to the inflection points, a few data are given in Table IV, together with the calculated values, obtained by the quantum analysis of differently shaped curves.

TABLE IV.

γ.	$(\log It)_{obs.}$	$(\log It)_{calcd.}$	$\Delta(\log It)$.
II	0.32	0.34	+ 0.02
III	0.23	0.25	+ 0.02
IV	0.19	0.19	0.00
V	0.18	0.14	− 0.04
IX	0.13	0.08	− 0.05

The majority of the characteristic curves are complex. Their intrinsic sensitivities are not represented by a single value of ϵ, but by two values, ϵ_1 and ϵ_2, belonging to the two components that produce the complex curves. An accurate determination of the sensitivity of these curves requires quantum analysis. More information will be given at the end of this paper.

THE RELATION BETWEEN THE INERTIA AND THE INFLECTION VALUES.

For simple characteristic curves the inertia and inflection points are quantitatively related to each other. Let the fog-corrected $D/\log It$ curve of Fig. 9 be indicated by B, having an inflection density, $\bar{D}$, at

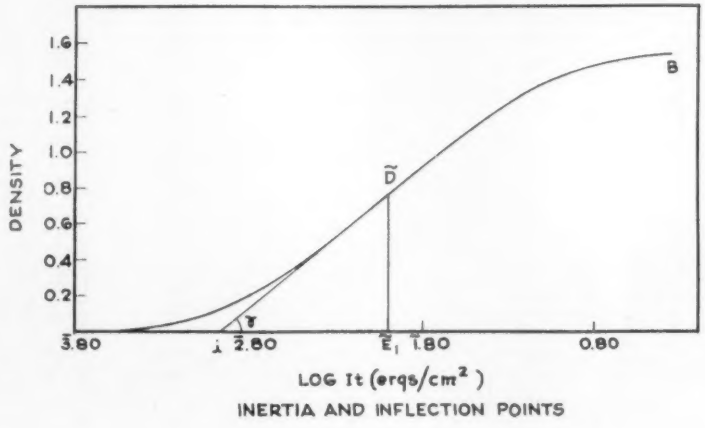

FIG. 9.

the exposure E_1, and let the inertia point at the exposure axis be i. Then, the intrinsic sensitivity of the emulsion is found according to Eq. (2):

$$\epsilon = 1/E_1,$$

at the density

$$\bar{D} = (1/m)D_{max.}.$$

The inertia point is i. Therefore,

$$E_1 - i = \frac{(1/m)D_{max.}}{\gamma} = \frac{D_{max.}}{m\gamma},$$

or

$$i = E_1 - \frac{D_{max.}}{m\gamma}, \qquad (4)$$

in which γ is the maximum slope of the characteristic curve.

This relation between inertia and inflection values can be determined graphically from the curves of Figs. 1 and 2. The observed values are listed in Table V, in which the emulsions are classified in groups having the same silver iodide concentration, in the order of increasing average grain sizes (precipitation series).

TABLE V.

Emulsions.

Development 5 Minutes in DK-50 at 18° C.

AgI in Moles Per Cent.	Nonconverted.		Converted.	
	i.	E_1.	i.	E_1.
0	0.730	100.0	0.588	66.7
	.339	66.7	.136	9.5
	.256	52.6	.078	5.3
	.215	43.5	.056	3.9
	.182	35.7	.040	2.8
	.169	31.3	.028	2.4
	.157	27.0	.022	2.1
0.77	.877	125.0	.543	66.7
	.162	14.1	.160	12.3
	.086	6.5	.100	7.0
	.055	3.8	.072	5.0
	.032	2.0	.047	3.3
	.024	1.5	.037	2.6
	.016	0.9	.028	2.0
2.56	.704	71.4	.400	83.3
	.109	16.7	.096	12.7
	.061	9.4	.060	6.7
	.038	5.6	.044	4.4
	.022	2.8	.033	3.0
	.017	2.0	.029	2.6
	.012	1.2	.026	2.2
6.15	—	—	—	—
	.197	66.7	.139	32.3
	.100	26.3	.122	23.8
	.057	11.2	.101	17.2
	.029	3.7	.068	9.2
	.020	1.8	.052	6.1
	.013	7.6	.035	3.4

From the data were plotted the curves of Figures 10 and 11.

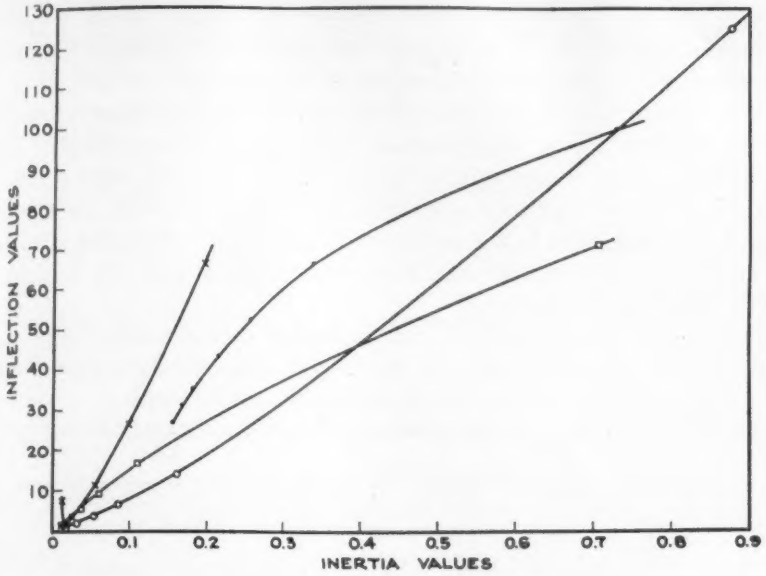

FIG. 10. Moles % of Ag I.

. 0 □ 2.56
o 0.77 × 6.15

Relations between the inflection values and the inertia values of the nonconverted precipitation series. Dev. 5 min. DK-50 at 18° C.

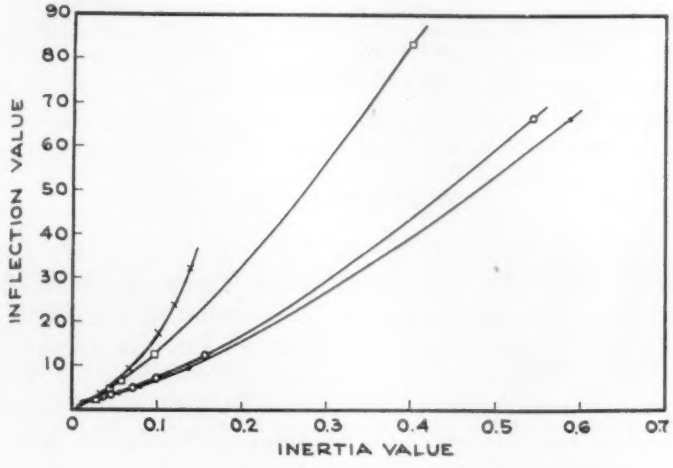

FIG. 11. Moles % of $Ag^{\frac{n}{4}}I$.

. 0 □ 2.56
o 0.77 × 6.15

Relations between the inflection values and the inertia values of the converted precipitation series. Dev. 5 min. DK-50 at 18° C.

COMPLEX CHARACTERISTIC CURVES.

A characteristic curve having a "straight-line" portion cannot be represented by a single mathematical expression. Practical sensitometry has given ample evidence of the existence of seemingly straight-line parts in the $D/\log It$ relation over a wide range of exposures. These straight lines were drawn within the limits of experimental error and if they are to be interpreted as continuous functions must be regarded as tangents through the inflection point of curves, of which the curvature is so small that the deviations from the straight line fall within the limits of experimental error.

The complex characteristic curves which contain inflection points with extremely small curvatures appear as long straight-line parts in the $D/\log It$ relation. This can be shown by an example.

Let curve A in Fig. 12 be a one-quantum characteristic curve with

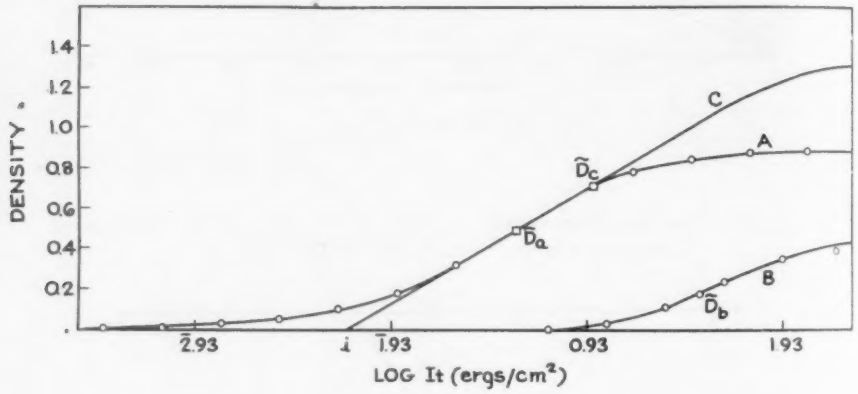

FIG. 12.

the equation:

$$D(y) = 0.88F(y),$$

having a value of $\log E_1 = 0.86$ at the inflection point, $\bar{D}_a$, giving $\epsilon_a = 0.684 \times 10^{-4}$. The first derivative of this curve is shown as curve A in Fig. 13. Its maximum, corresponding to the seemingly straight-line part of the characteristic curve, extends over a region of $\log It = 0.75$.

If the tangent through the inflection point, $\bar{D}_a$, is extended to densities higher than $D = 0.88$, the difference between this straight line and the shoulder of curve A gives the toe of another characteristic curve, curve B. This toe shows, with increasing exposure, an increase of the sixth power of the density, which means that a six-quantum curve can be constructed from this toe. This curve is drawn from the equation

$$D(y) = 0.42F'(y),$$

having a value of $\log E_1 = 1.03$ at the inflection point, $\bar{D}_b$, giving $\epsilon_b = 0.462 \times 10^{-4}$. The first derivative of this curve is shown as curve B in Fig. 13. Its maximum, corresponding to the seemingly straight-line part of the characteristic curve, extends over a region of $\log It = 0.28$.

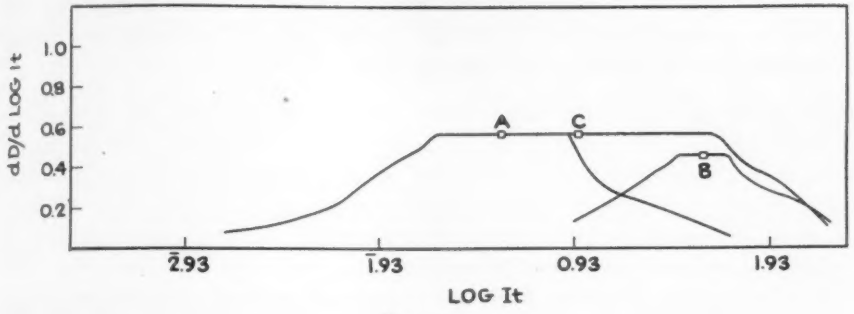

FIG. 13.

The complex characteristic curve C (see Fig. 12), composed of the components A and B, is drawn from the equation

$$D(y) = 0.88F(y) + 0.42F'\left(\frac{y}{m}\right),$$

in which $m = \epsilon_a/\epsilon_b$. The first derivative of this curve is shown as curve C in Fig. 13. Its maximum, again corresponding to the seemingly straight-line part of the characteristic curve, extends over a region of $\log It = 1.51$, which is much longer than that of its components together.

The inertias of the simple curve A and of the complex curve C are the same. In the majority of cases the inertia value does not give any indication about the complexity of the shape of the characteristic curve.

CONCLUSIONS.

Sensitivity derived from the exposure required to produce a given density has no significance in the theoretical determination of the sensitivity of photographic emulsions.

Sensitivity values derived from the inertia have theoretical significance for simple characteristic curves. They are quantitatively related to the exposures at the inflection points.

The exposure at the inflection point has theoretical significance.

SUMMARY.

The sensitivity of photographic emulsions is not measured by the exposure necessary to produce an arbitrarily chosen density. It is measured by a definite value of $D/D_{max.}$, which is given by the inflection point of the characteristic curve.

For simple characteristic curves, the inertia point is quantitatively related to the inflection point.

The most complete measurements of sensitivity are obtainable by a quantic analysis of the shape of the characteristic curve.

ACKNOWLEDGMENT.

We are gratefully indebted to Mr. W. F. Smith for preparing the emulsions analyzed and to Mrs. Ida Tschiderer for carrying out many computations connected with this subject.

ROCHESTER 4, N. Y.,
AUGUST 16, 1944.

MICROWAVE RADIATION FROM THE SUN.

BY

G. C. SOUTHWORTH,

Research Engineer, Bell Telephone Laboratories, New York.

INTRODUCTION.

During the summer months of both 1942 and 1943, the writer and certain of his associates observed a small but measurable amount of microwave radiation coming from the sun. This appeared as random noise in the output of a conventional double-detection radio receiver designed to work at centimeter wave lengths. Other observations made at the time showed that the noise output of such a receiver was sensibly less when it was pointed at open sky than when pointed at nearby objects. A high noise level also prevailed when the receiver was located in a closed room. All of these results are in general accord with ordinary black-body radiation theory. In this connection, it is convenient to regard the room as a black-body enclosure in which the receiver is in thermal equilibrium. When the receiver is pointed at the sun, equilibrium conditions are such that more energy is absorbed than is radiated and when it is pointed at interstellar space, conditions are reversed and more energy is radiated than is absorbed.* In the latter case, the result is almost as though a sensitive pyrometer calibrated to work at high temperatures had been turned suddenly on a block of ice.

NATURE OF THERMAL RADIATION.

Before considering further the experiments and their results it may be well to review briefly certain well-known facts about thermal radiation and follow with an account of some of the more important steps that have led to our present knowledge of the sun's spectrum.

According to the accepted views of radiation, most solids and liquids and also a few of the gases radiate energy when heated. In order to distinguish this form of radiation from that associated with fluorescence and light from ionized gases it is generally known as temperature radiation. The relationship between the energy radiated and temperature is generally rather complicated except for a certain class of surfaces, known as black bodies. The latter are not characterized so much by their apparent color as by their ability to absorb completely a wide range of wave lengths.

* While these simple statements serve a useful purpose as regards orientation of ideas, it is quite possible that they do not apply strictly to the apparatus actually used. We can be certain only that as the apparatus was pointed alternately at the sun and at interstellar space, there was a net differential in favor of energy coming from the sun.

It is almost an axiom that good radiators are also good absorbers. Two similar bodies at the same temperature placed in close proximity receive from each other as much energy as each respectively radiates to the other and the two are said to be in temperature equilibrium. If they are black bodies and are not in temperature equilibrium, the transfer takes place at a rate proportional to the difference of the fourth power of their respective absolute temperatures. The latter relations hold for the *total* energy being emitted on *all* wave lengths. If we are interested in some small part of the total spectrum then the rate of emission is given by the Planck or Rayleigh-Jeans formulas to be discussed later.

Measurements made on hot bodies, as for example the sun, show that the energy is small for the shorter wave lengths, rising to a maximum at some intermediate wave length and diminishing again for long waves more or less as shown in Figs. 1 and 2. As the temperature of a

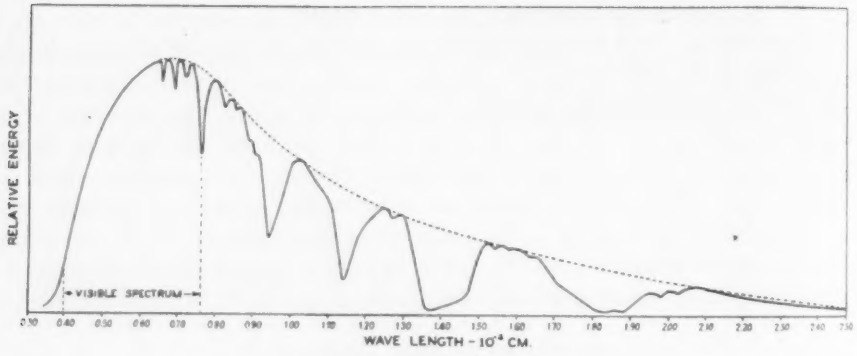

FIG. 1. Tracing of Langley's original graph showing distribution of energy in the solar spectrum.

radiating surface is increased, all of the ordinates of the characteristic increase, and the maximum shifts toward the shorter wave lengths. This shift of the optimum accounts, in part, for the fact that as the temperature of a metallic object is raised, it first appears red, then yellowish, then white and finally blue-white. This shift was first expressed quantitatively by Wien in the formula that follows:

$$\lambda_m T = 0.294 \text{ cm. degree}, \qquad (1)$$

where λ_m is the wave length in centimeters at which the energy E_m is at a maximum and T is the absolute temperature.

Wien also devised a formula for the distribution of energy in a black-body spectrum but it seemed to work well only at the shorter

wave lengths. Lord Rayleigh proceeding along somewhat different lines also arrived at a formula but his formula fitted only at high temperatures and relatively long waves. After some modification by

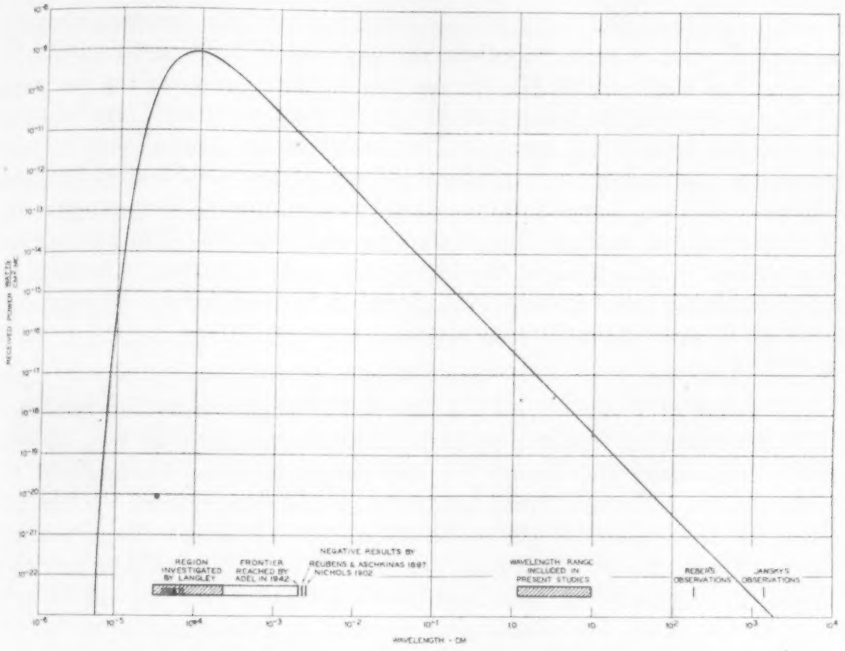
REGION INVESTIGATED BY LANGLEY
FRONTIER REACHED BY ADEL IN 1942
NEGATIVE RESULTS BY RUBENS & ASCHKINASS 1897 NICHOLS 1902
WAVELENGTH RANGE INCLUDED IN PRESENT STUDIES
REBER'S OBSERVATIONS
JANSKY'S OBSERVATIONS
WAVELENGTH - CM

FIG. 2. Calculated energy distribution in the sun's spectrum. Crosses indicate measured points.

Jeans, the latter assumed the form

$$U = \frac{8\pi k T f^2 \delta f}{c^3} \frac{\text{ergs}}{\text{cc. sec.}}, \qquad (2)$$

where f is frequency, c is the velocity of light in free space $\left(\text{i.e., } 3 \times 10^{10} \frac{\text{cm.}}{\text{sec.}}\right)$, T is the absolute temperature and k is the Boltzmann constant $= 1.37 \times 10^{-16}$ ergs per degree. δf is the frequency band under consideration. A more complete formula, derived by Planck from quantum considerations, fits well throughout a large part of the spectrum. It may be put in the form

$$U = \frac{8\pi h f^3 \delta f}{c^3\left(\epsilon^{\frac{hf}{kT}} - 1\right)} \frac{\text{ergs}}{\text{cc. sec.}}, \qquad (3)$$

where h is the Planck constant $= 6.5 \times 10^{-27}$ ergs per second.

At high temperatures and long wave lengths, a condition in which we are particularly interested in the case of radio waves from the sun, the Planck relation reduces to the Rayleigh-Jeans' formula. At short waves it reduces to the Wien formula.

Assuming that the sun's temperature is 6,000° K. and its volume is 1.41×10^{33} cc., we may calculate the power radiated per second over an element of band width δf. From this we may compute the radiation per square centimeter falling on the surface of the earth one hundred fifty million kilometers away. The result is in general accord with experiment throughout a considerable part of the visible and infra-red portions of the sun's spectrum as already mentioned. The experiments to be reported below show that it also fits well in parts of the centimeter-wave region. At first sight the latter may appear rather surprising for we are applying the formula to a range of frequencies far beyond that for which it was originally conceived.

EARLY WORK.

More than fifty years ago Professor S. P. Langley, one-time Secretary of the Smithsonian Institution and pioneer in aviation as well as solar physics, measured the energy in the sun's spectrum throughout the visible region and to a considerable distance either side. After correcting for absorption by the earth's atmosphere his results agreed well with radiation theory assuming the sun to be a black-body having a temperature of 6000° K. and a volume of 1.41×10^{33} cc. His results provided the basis for a new and much more accurate value for the so-called *solar constant*.

Figure 1 attached was traced from one of Langley's composite curves published some time after the experimental work itself had been completed.[1] This shows the distribution of solar power as observed at sea level and also after being corrected for absorption by the earth's atmosphere. Although the graph stops at a wave length of 0.00025 cm. it is said that Langley's observations were carried to a wave length of 0.00054 cm. Beyond this point the available energy presumably became too small for the methods then available. In the years that followed, slow but consistent progress toward the long-wave part of the spectrum was made. By 1917 Fowle,[2] and his colleagues, Abbot and Aldrich, had extended the solar spectrum to 0.0014 cm. and by 1942 a new frontier of 0.0024 cm. had been reached as was reported by Arthur Adel [3] of the Lowell Observatory.

Of the attempts to carry Langley's work to longer waves, mention should be made of a lecture by Sir Oliver Lodge [4] before the Royal Institution in 1894 in which he expressed a hope "to try for long wave radiation from the sun." The author has found no record that such an experiment was actually carried out. In this case, the wave lengths under consideration were presumably a few centimeters and therefore comparable to those of the experiments reported below.

In 1898, Reubens and Aschkinass [5] reported that they were unable to find measurable amounts of power in the sun's spectrum at wave lengths of about 0.0025 cm. It will be noted that this is near the region later investigated by Adel.[3] The failure was attributed to carbon dioxide and water vapor in the earth's atmosphere. In fact, laboratory experiments were performed that seemed to justify these conclusions. In 1907, E. F. Nichols [6] reported similar measurements made at the Mt. Wilson Observatory, elevation 6,000 ft., where the atmosphere is relatively dry and also where the carbon dioxide content is probably low. In this case the wave length was about 0.005 cm. Again nothing was observed. Finally Reber [7] using radio methods, at a wave length of 187 cm., made similar observations in 1940 and also reported negative results. In a paper published in 1942 Reber characterized his results as inconclusive but still more recently (1944) he has reported the actual observation of solar radiation of approximately the same magnitude as that calculated by black-body theory. In passing it may be of interest to note that Jansky [8] in 1931 discovered radiation coming from the vicinity of the Milky Way. This radiation was subsequently known as cosmic noise. His experiments, which were carried out at a wave length of 14.6 meters, were performed in such a way as to detect solar radiation had it been present in any considerable magnitude. He informs the writer that none was found. The relative positions in the spectrum of these various observations are shown in Fig. 2.

A somewhat different approach to the general subject of heat radiation came in 1926 when J. B. Johnson [9] reported a particular kind of noise in the first circuits of high-gain amplifiers. Experiments were performed that enabled him to relate the noise power quantitatively to the resistance and the prevailing temperature as well as to the mean frequency and the width of the band of frequencies under observation. A corresponding formula was established. A short time afterward Nyquist [10] derived the Johnson expression from well-known principles of thermodynamics and statistical mechanics. In the years that followed, observations of the Johnson or resistance noise, as it was sometimes called, were extended from a few hundred cycles to the highest of the radio frequencies where it was found that the formula continued to hold. In the meantime it became increasingly evident that the expression for resistance noise was the one-dimensional equivalent of the Rayleigh-Jeans expression. This equivalence, was pointed out by Burgess [11] in 1941. It was but a step further to speak of the noise associated with the radiation resistance of an antenna and to look for this particular kind of noise when an antenna was pointed at the sun.

Whether one regards solar noise as a form of resistance noise or black-body radiation may be a matter of personal preference. If so,

the writer leans toward the second view. In either case there seems to be a difference, superficially at least, between energy that originates in a local circuit at ordinary temperatures and that from an incandescent mass ninety-three million miles away and conveyed to us solely by electromagnetic waves.* A reader born with an eye for large numbers will probably note that, except possibly for cosmic noise where the length of path is not yet known, this represents a record distance for radio transmission. Presumably, the time of travel from sun to earth is more than eight minutes.

EXPERIMENTAL RESULTS.

The apparatus used in this work consisted of a more-or-less conventional double detection receiver designed to work at wave lengths in the centimeter region. Associated with it was a parabola of fairly high directivity on an improvised altazimuth mounting. Previous calibrations made it possible to measure noise power in terms of second detector plate current in accordance with methods generally used in the past. Observations were carried out at three rather widely spaced wave lengths in the region between one centimeter and ten centimeters. These three frequencies will be referred to below as the high frequency, intermediate frequency, and low frequency, respectively. In each case, the band over which noise was measured was roughly one megacycle. It is expected that further details of the method will be published later.

Measurements of received power made at the longest of the three wave lengths mentioned above agreed well with that calculated by the Rayleigh-Jeans formula. It happened that out of about 125 separate observations made on four different days in August 1943, the mean was about 3 per cent. *below* that calculated. There was no perceptible diurnal variation such as prevails at the shorter wave lengths. At sunrise the received power increased rapidly more or less in proportion to the area of the sun's disc appearing above the horizon until the level prevailing during the day was reached. The variation at sunset was very similar but in reverse order. The maximum deviation of any observation from the mean was about 12 per cent. The mean of all the deviations was about $\pm$ 5 per cent.

Similar measurements of solar radiation were made at the intermediate wave length mentioned above. Of these, perhaps eight hundred were made between June and October 1942, and about a hundred fifty during the summer of 1943. In this case, the mean value was about 12 per cent. *below* that calculated. Again there was no very obvious diurnal variation. The maximum deviation was about 13 per cent. and the mean was about $\pm$ 4 per cent.

* By a somewhat attenuated and possibly specious line of reasoning, it may be said that Johnson's original observations, which were conducted at frequencies as low as 296 cycles, were, in effect, measurements of thermal radiation at wave lengths of the order of a million meters.

Measurements made at the shortest wave length also gave sensibly constant levels during the daylight period, but this time the level was roughly one-ninth of that calculated by the Rayleigh-Jeans formula. Also, it was observed that the transitions incidental to sunrise and sunset extended over a period of roughly an hour instead of two or

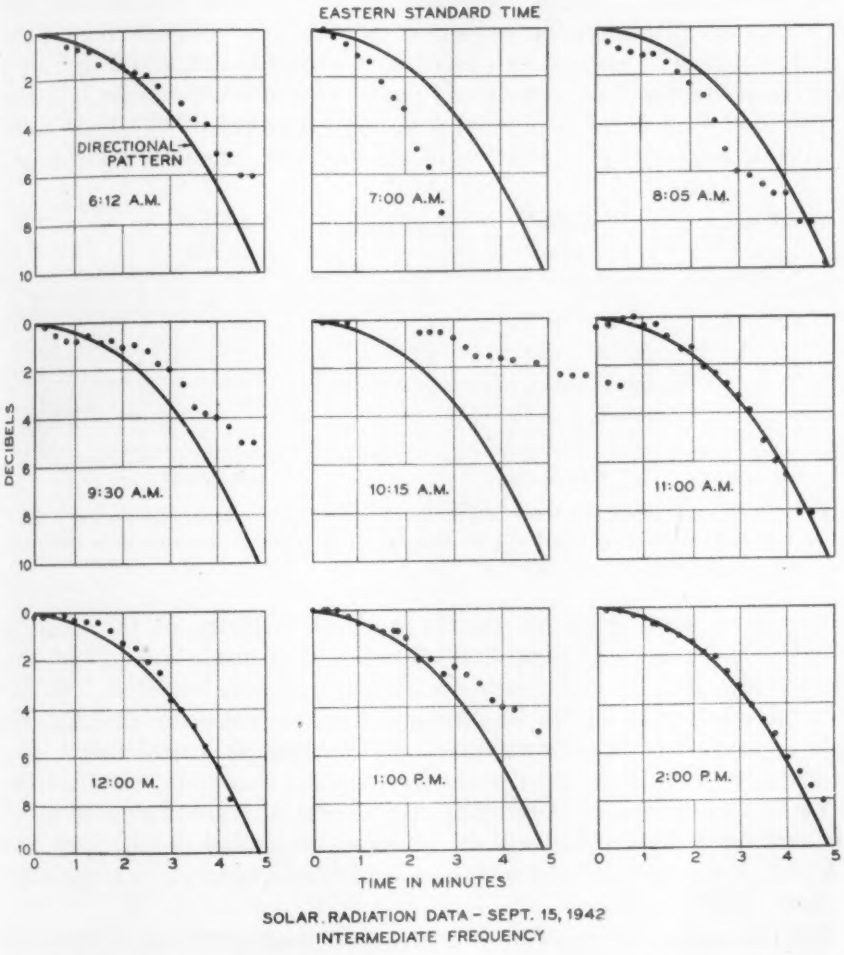

FIG. 3. Representative measurements of the sun's radiation made by centering the receiver on the sun and observing output as the sun passed out of the aperture.

three minutes as in case of the longer waves. The first of these results might, at first sight, suggest attenuation by the earth's atmosphere. However, this is not substantiated by the second result. If the attenuation had been substantial, it might have been expected that, due to increased path lengths through the attenuating medium, the solar signal

in the early morning and late afternoon would have been much less accordingly than that in the middle of the day. Because there was no marked diurnal variation such as prevails at the infra-red wave lengths, one is inclined to look elsewhere for the explanation of the discrepancy noted. This matter is being left for further study.

A particularly interesting part of the work consisted of some directional measurements made by centering the receiver on the sun and observing the output as the sun's disc moved out of the aperture of the receiving mirror. Several representative patterns are given in Fig. 3 along with corresponding patterns made with a local source. It will be observed that there is present a random component of considerable magnitude suggesting a variation in the angle of arrival of solar noise.

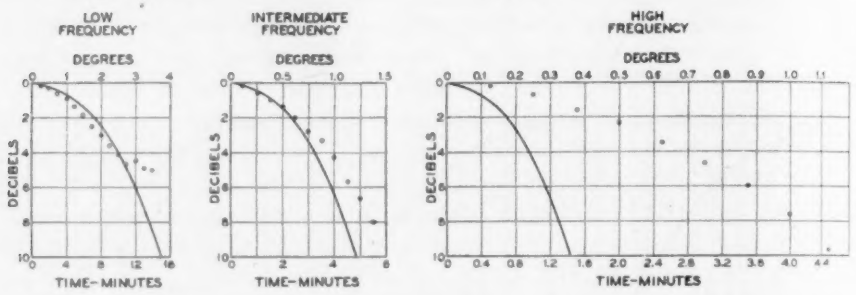

FIG. 4. Measurements like those of Fig. 3 but based on the means of numerous patterns all taken in August 1943 as follows: Low frequency, 16 patterns; Intermediate frequency, 16 patterns; High frequency, 26 patterns.

Attempts were made to obtain a direct measure of the angle of arrival of solar noise hoping that this direction might remain off axis long enough at a time to make such measurements possible. To this end a simple set of sights was arranged on the receiver whereby the angle of arrival of optical waves could be used as a reference. In a few cases, especially during the earlier stages of this work, the direction to the sun as determined optically and electrically seemed to differ by as much as a degree for several minutes at a time. However, this result could not be verified a year later and consequently it was relegated to a position of doubt.

During the period between August 17 and August 28, 1943, numerous directional patterns somewhat more accurate but otherwise similar to those shown in Fig. 3 were taken. For the most part, they showed the same general characteristics observed a year earlier. There seemed to be no very significant difference between patterns taken at various times of the day or on succeeding days so a mean pattern for each wave length was plotted. These are shown in Fig. 4 attached. Each point shown represents the mean of several observations as indicated. Presumably much of the random component has been eliminated by the

averaging process, thereby leaving the features that are characteristic of the system as a whole.

Perhaps the most outstanding feature is the general broadening of the solar pattern as compared with the pattern measured locally. This is particularly noticeable at the highest frequency. It appears also in less definite form at the intermediate frequency. The apparent broadening appearing in the low-frequency pattern may be due largely to errors of measurement for in this case the received levels were very small compared with the set noise.

Some of the broadening noted above is no doubt related to the fact that the sun is an apparent disc and not a point source of waves. In

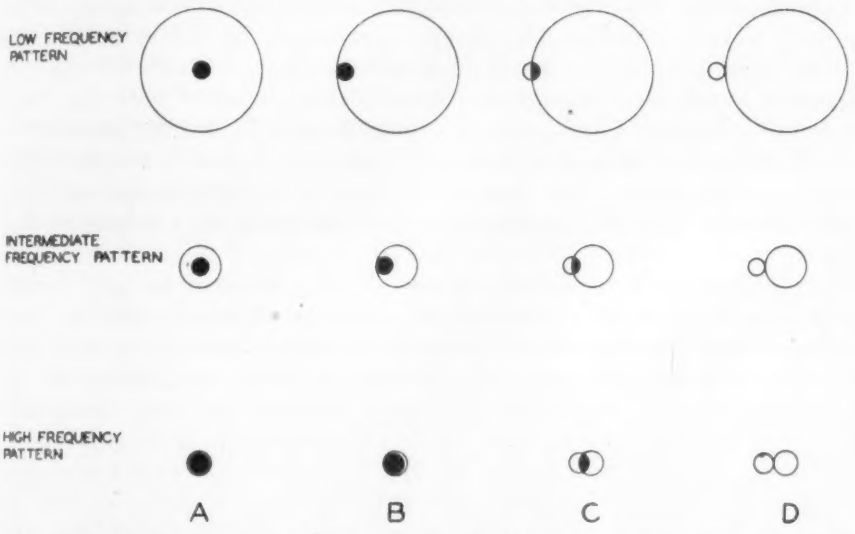

FIG. 5. Relative dimensions of the sun (smaller circle) and the directional pattern of the receiver (larger circle) for each of the three frequencies represented in Fig. 4.

the case of the highest frequency used, the aperture angle of the receiver is comparable with that of the sun. A little reflection will show that as the sun's disc passes the aperture of the receiver, power will continue to be received until the circle corresponding to the aperture angle of the receiver becomes tangent externally to the sun's disc. It may be expected that, to a first degree of approximation, the solar pattern so measured will have a breadth equal to the sum of the aperture angle and the angular diameter of the sun. The relative dimensions involved are made more obvious by Fig. 5 which shows several stages in the transit of the sun across the receiver for each of the three frequencies in question. In each case the larger circle represents the pattern of the receiver while the smaller circle represents the sun. It may be expected that in the transit of the sun, as condition *A* becomes condition *B* the

observed change in output will reflect mainly the directional characteristics of the receiver whereas a change from *B* to *D* will reflect the effect of a progressively smaller area seen by the receiver. At the lowest frequency the change from *A* to *B* occupies a large part of the total transit period while at the highest frequency it is negligible compared with that from *B* to *D*. At the intermediate frequency, conditions are, of course, more or less intermediate between those for high and low frequencies.

Reference to Fig. 4 above will show that, at the highest of the three frequencies, the directional pattern may be even wider than that corresponding to the sum of the aperture angle and the angular diameter of the sun. One reasonable explanation is based on the tentative hypothesis that the angle of arrival of waves from the sun varies rather rapidly over a considerable range. According to this view the sun would appear to the receiver as a shimmering body whose apparent diameter is considerably larger than the true diameter with the result that the pattern is correspondingly broadened. It is quite possible too that this increase in apparent diameter may be due to scattering in the earth's atmosphere. The lack of any very considerable diurnal variation suggests that this scattering may take place in a relatively thin layer.

This increase in apparent diameter may account in part for the discrepancy between measured and calculated energy levels noted above. The comparisons so far made assume that the sun is a point source. This simplification may be warranted in the cases of the two lower frequencies where the directive patterns are only moderately sharp but they may not be warranted in the case of the highest frequency where the angular diameter of the sun is comparable with the angular diameter of the directive pattern. If in addition it turns out that the effective diameter of the sun is perhaps twice that assumed above the error may be very substantial indeed. It is believed that a more accurate calculation should await further measurements of effective diameter.

HORIZON EFFECTS.

While carrying out the above work, it was found that the noise appearing in the output of the receiver was sensibly less when the receiver was pointed at open sky than when pointed at nearby objects or when it was located inside a room. The magnitude of this horizon effect for the longest wave mentioned above was of the order of 10^{-19} watts per sq. cm. per mc. of band width. That for the intermediate frequency was around five times that quantity while that for the highest frequency was barely measurable with the apparatus at hand. More specifically, these figures represent the increase in indicated noise power when the receiver was pointed below the horizon than when pointed above. As might be expected, distant horizons were substantially as

definite as those nearby. The quantitative aspects of this problem will be given further attention.*

In the course of the above work, numerous attempts were made to observe cosmic noise coming from the general region of the Milky Way. As already mentioned, noise of this kind had been reported by Jansky who located also its approximate position in space. His observations were made at a frequency of 20.6 mc. Similar noise in the vicinity of 160 mc. was also reported by Reber [7] in 1940. His observations published in 1944 appear to locate the source more definitely in the region of Cygnus and Sagittarius. It was hoped that cosmic noise might also be found in the microwave range and with the highly directive apparatus at hand, its position might be located still more precisely. So far it has not been found.

Although there was no reason to believe, from general radiation theory, that any appreciable power could be picked up from the moon or from any of the planets or from any particular star, a search for such noise was made. Nothing was found coming from any of the more prominent bodies visible at the time.

It may be of interest to note that a measurable amount of centimeter power was found in fluorescent lights. As is well known, the mercury vapor arc which is an important component of the fluorescent light is one of the common sources of wave power in the far infra-red. Similar noise power was also found in mercury vapor arcs of the so-called Lab-Arc variety.

CONCLUSIONS.

The results reported above establish with little doubt the existence, in the sun's spectrum, of components much longer than have been found generally heretofore. Over a considerable portion of the frequency range, the energy appears to be substantially that predicted by black-body radiation theory. A matter of comparable interest is the fact that temperature differences, of a kind, exist between points on a distant landscape and the sky above. The latter effects are readily explicable, qualitatively at least, from the usual equilibrium considerations of black-body theory.

The above experiments also point rather definitely toward an atmosphere surrounding the earth that is fairly transparent to centimeter waves. However, rapid changes in angle of arrival of the solar signal with a consequent shimmering of the sun's image suggest rapid changes in index of refraction. There is also evidence of small amounts of absorption and perhaps also scattering particularly at the shortest of the three wave lengths at which observations were made. Although

* The possibility of circuit noise being radiated into space by an antenna must certainly have been entertained by many radio engineers and physicists in the past. Reber for one pointed out this possibility in one of the articles cited above.

many of the more important results reported above appear firmly established, it must be recognized that certain details must be regarded as tentative and be contingent upon subsequent verification.

Perhaps the most interesting result of this work, from the radio engineer's point of view, is the establishment experimentally of a much closer relationship between black-body radiation and ordinary radio waves. As already mentioned, such a relationship has existed in a rather attenuated way, since the discovery of the so-called Johnson or first-circuit noise, but the recent appearance of such radiation in a source ninety-three million miles away and conveyed solely by radio means would appear to be a much more direct and tangible result. It may also be of interest that no cosmic radiation of the kind observed by Jansky and Reber has been found at these very high frequencies. This tends to support Reber's 1940 view that cosmic radiation varies inversely as the frequency rather than that of Jansky who was inclined to regard cosmic radiation as a form of black-body radiation.

This paper suggests, perhaps more than anything else, a need for further work preferably carried out with more refined apparatus and with better facilities for calibration. The apparatus needed for the next stage should incorporate the best ideas both of the radio engineer and the designer of astronomical equipment with the hope that additional accuracy will bring out features so far overlooked. Such a program is contemplated. Perhaps there lies ahead a new field of astronomical and terrestrial research comparable in interest and scope with that that has prevailed during the last two decades with respect to the ionosphere. The sun being a localized source of radio waves situated entirely outside the earth's atmosphere provides, for the first time, angles of attack on the structure of the earth's atmosphere not previously possible.

REFERENCES.

(1) S. P. LANGLEY, "The solar constant and its related problems," *Astrophys. Jour.*, Vol. 17, pp. 89–99, 1903.

(2) F. E. FOWLE, Smithsonian Miscellaneous Collection, *68*, No. 8 (1917).

(3) ARTHUR ADEL, "Extension of the prismatic solar spectrum from 14μ to 24μ through a new atmospheric window in the infrared," *Astrophys. Jour.*, Vol. 96, pp. 239–241, September 1942.

(4) Signalling through space without wires—A lecture by Sir Oliver Lodge before the Royal Institution of Great Britain—June 1, 1894, published as a booklet of the Electrician Series.

(5) H. REUBENS AND E. ASHKINASS, "Infra-red absorption," *Wied. Ann.*, Vol. 64, series 3, pp. 584–610, 1898.

(6) E. F. NICHOLS, "Absence of very long waves from sun's spectrum," *Astrophys. Jour.*, Vol. 26, p. 46, 1907.

(7) GROTE REBER, "Cosmic static," *Proc. IRE*, Vol. 30, pp. 367, February 1940.
GROTE REBER, "Cosmic static," *Proc. IRE*, Vol. 30, pp. 367–378, August 1942.
GROTE REBER, "Cosmic static," *Astrophys. Jour.*, Vol. 100, pp. 279–287, November 1944.

(8) K. G. JANSKY, "Directional studies of atmospherics at high frequencies," *Proc. IRE*, Vol. 20, pp. 1920–1932, December 1932.
K. G. JANSKY, "Electrical disturbances of extra terrestrial origin," *Proc. IRE*, Vol. 21, pp. 1387–1938, October 1933.
K. G. JANSKY, "A note on the source of interstellar interference," *Proc. IRE*, Vol. 23, pp. 1158–1163, October 1935.
K. G. JANSKY, "Minimum noise levels obtained on short wave radio receiving stations," *Proc. IRE*, Vol. 25, pp. 1517–1530, December 1937.
(9) J. B. JOHNSON, "Thermal agitation of electricity in conductors," *Physical Review*, Vol. 32, pp. 97–109, July 1928.
(10) H. NYQUIST, "The thermal agitation of electric charge in conductors," *Physical Review*, Vol. 32, pp. 110–113, July 1928.
(11) R. E. BURGESS, "Noise in receiving aerial systems," *Proc. Phys. Soc.*, Vol. 53, pp. 293–304, 1941.

Dam Built to Resist Earthquakes.—(*Compressed Air Magazine*, Vol. 50, No. 1.) Now under construction on the Santa Eulalia River at a point 50 miles east of Lima, Peru, is a dam that will be somewhat unique because it has been designed to withstand earthquake shocks. At the site of the structure, the river flows through a crack in the mountains that was apparently caused by a seismic disturbance. The chasm is approximately 1300 feet long, 500 feet deep, and from 18 to 65 feet wide. There the dam is being reared on a solid concrete plug that extends down to bedrock 55 feet below the bottom of the stream and up between the rock walls to a height of 90 feet. This foundation is roughly quadrangular in cross section.

The Autisha Dam, as it will be known, is being built in the shape of a butterfly, the wing sections being separated by a space 6 inches wide and 10 feet long. The closure of this interstice—the body of the butterfly—is the key point in the design and will, it is expected, permit the two monoliths to move without cracking during an earthquake. On the upstream side, the opening is closed by a length of iron pipe, 10 inches in diameter, filled with concrete. This pipe rests against two vertically disposed I-beams set in the face of the dam and will be forced into the 6-inch space by the pressure of the impounded water. Halfway through the 10-foot-long gap is a shaft, or well, on the down stream side of which is a V-shaped copper expansion joint that closes the space between the two wing sections. This flexible sheath will prevent the passage of any water that may seep past the pipe and the shaft, which will also give access to the interior of the dam.

The project is to be constructed in two stages. At the present time the barrier will rise 256 feet above the river bed and will impound about 396,300,000 gallons of water. Later, when demands justify, it will be heightened by 72 feet so as to create a reservoir with a capacity of 2,377,530,000 gallons. A diversion tunnel nearly 2 miles long will carry the water under a head of 915 feet to the power house in the valley below. When completed, the plant will develop 30,000 kw. The total cost of the undertaking, including connecting highways, is estimated at between $5,000,000 and $6,000,000.

R. H. O.

ECLIPSES OF THE SUN.*

BY

ROY K. MARSHALL, PH.D.,

Associate Director, Astronomy, Photography and Seismology.
Director, Fels Planetarium, The Franklin Institute, Philadelphia.

On August 14, 310 B.C., the Sicilian daredevil Agathocles and his men were blockaded in the harbor of Syracuse by the Carthaginians. This potter-turned-dictator had himself been born a subject of Carthage but as a child he had been brought to Sicily; through his personal charm and the money of his wife he raised an army and, under a guise of help to the city of Syracuse, he took over the city and the rest of Sicily, then a part of Greece. His rise to power was accepted by Carthage as a challenge; Sicily was invaded and Agathocles suffered a severe defeat at Himera, in 310 B.C.

As a counter-attack, Agathocles resolved to invade Africa, and during the night of August 14 his fleet slipped through the blockade and set the course for Carthage. On the next day, according to Diodorus Siculus,

"there was such an eclipse of the Sun that the stars appeared everywhere in the firmament, and the day was turned into night, upon which the soldiers of Agathocles (conceiving that God did foretell their destruction) fell into great perplexities and discontents concerning what was like to befall them.

"The king was at no less pains to satisfy them about this affair than about the war, and therefore he told them that he should have thought this sign an ill presage for them if it had happened before they set out, but having happened afterwards he could not but think it presaged ill to those against whom they sailed."

Certain it is that Agathocles did score great triumphs on Carthaginian soil, although domestic discontent made him hurry back to Sicily in 307 B.C.

Eclipses of the Sun have often figured in historical matters. In eastern Anatolia, the Medes under Cyaxares and the Lydians under Alyattes collided in 585 B.C. This time Herodotus tells us the story:

"As the balance had not inclined in favor of either nation, another engagement took place in the sixth year of the war, in the course of which, just as the battle was growing warm, day was suddenly turned into night. This event had been foretold to the Ionians by Thales of Miletus, who predicted it for the year in which it actually took place.

* The Cuts for Figs. 1–12 have been furnished through the courtesy of the Editors of *Sky and Telescope*, a monthly magazine of popular astronomy, published at the Harvard College Observatory, Cambridge 38, Massachusetts.

"When the Lydians and the Medes observed the change they ceased fighting and were alike anxious to agree upon peace."

And then, "because without some strong bond there is little security to be found in men's covenants," the Median heir-apparent and the princess of Lydia were married, a boundary was decided and it was not violated until almost 40 years had passed.

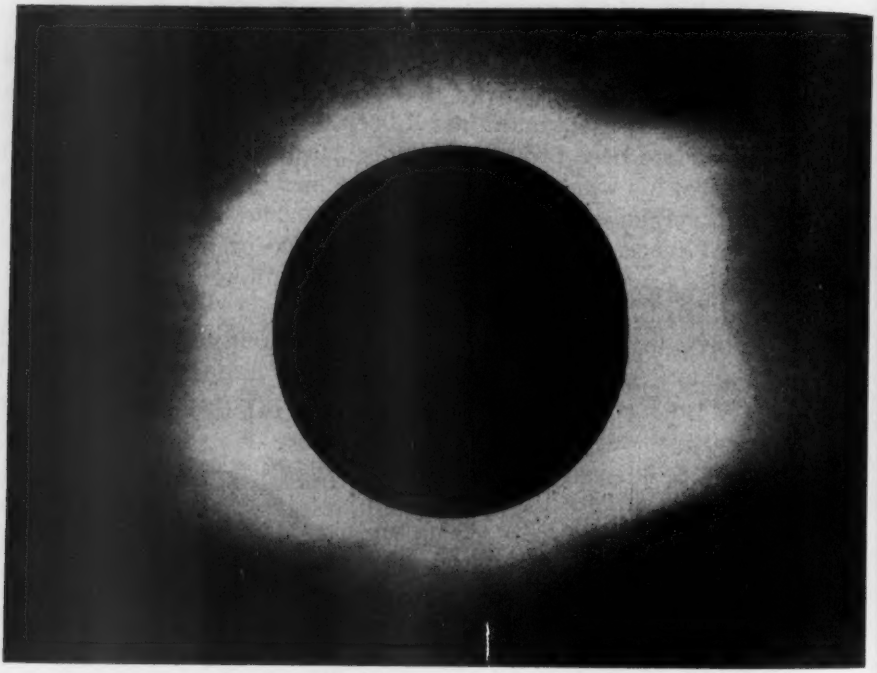

FIG. 1. Eclipse of Jan. 1. 1889, as photographed with the 13-inch Boyden telescope of the Harvard Expedition to Willows, California.

The date of the eclipse was May 28, 585 B.C., which dates the battle for historians. Although Herodotus says that the prediction was only "for the very year," we can be sure that Thales did better than that; he had studied the Babylonian eclipse observations and predictions and surely foretold not only the date but even the probable magnitude of the eclipse.

Concerning this prediction, James H. Breasted, historian and archaeologist, had this to say:

"The prediction of an eclipse, a feat already accomplished by the Babylonians, was not so important as the consequences. . . . Hitherto men had believed that eclipses and all the other strange things that happened in the skies were caused by the momentary angry whim of some god. Now, however, Thales boldly proclaimed that the movements of the heavenly bodies

were in accordance with fixed laws. In the history of human thinking this was probably the most fundamentally important step ever taken. The gods were thus banished from control of the sky-world where the eagle of Zeus had once ruled."

As early as 747 B.C., Babylonian astronomers were observing eclipses and tabulating their results. In 616 B.C., Babylon was conquered by a Persian desert tribe now called the Chaldeans, who effected an alliance with the northern Medes and ended the Assyrian rule. Under Nebuchadnezzar, the Chaldean astronomers continued the work of the Assyrians. About 500 B.C., Nabu-rimannu used the series of observations to derive good values for the length of the year and that of the synodic month—the period of the Moon's phases; less than a century later, his values were improved by another Chaldean, Kidinnu. The work of these two Chaldeans passed to the Greeks and was used in 433 B.C. by the engineer Meton of Athens in the formulation of the *Metonic Cycle*, which states that 19 years are equal to 235 *synodic months;* in other words, after 19 years the phases of the Moon repeat themselves on the same days of the same months.

In order that an eclipse of the Sun may occur, the Moon must be at the new phase, lined up between the Earth and the Sun. If an eclipse occurs at one new moon, it is likely that there will be another on the same date 19 years later; as an example, there are total eclipses of the Sun on June 30 in 1954, 1973 and 1992, on June 20 in 1955 and 1974. Usually four or five eclipses can be traced by using the Metonic Cycle. If 5 leap-years occur between the two dates in question, the next cycle begins on precisely the same date; if only 4 leap-years intervene, the next cycle begins one day later.

But the Chaldeans, and Thales, used another cycle for their eclipse predictions; this is the *Saros*, a cycle which recognizes the fact that 223 *synodic months* are almost equal to 18 years plus 11 days (or 10 days, if 5 leap-days have been inserted in the interval). This cycle can be used to predict more than 70 solar eclipses in a period of about 1300 years, one after the other.

To understand why the *Saros* works so well, it is necessary to consider the motions of the Earth around the Sun and of the Moon around the Earth. The *tropical year*—the year of the seasons—is the one we use; it is the one that the calendar strives to match. The length of the tropical year is 365.2422 days, as nearly as we need it; this is the interval between successive moments when the Sun, apparently traveling eastward and a little northward against the background of the stars, because of the Earth's orbital revolution, stands precisely over the Earth's equator.

As the Moon revolves around the Earth, it stands first in the same direction as the Sun, then by an increasing angular distance farther east until it is opposite the Sun (at full moon), then by diminishing

angular distances to the west of the Sun until once more the new moon occurs when the Moon and Sun are in the same direction. The average interval between successive new moons or successive full moons is the *synodic month*, equal to 29.5306 days.

The Moon's orbit relative to the Earth is an ellipse. The mean distance between the centers of the two bodies is 238,857 miles; the variation of the distance is from 221,463 miles at *perigee* (nearest the Earth) to 252,710 miles at *apogee* (farthest from the Earth). The line joining the *perigee* and *apogee*, the major axis of the orbital ellipse, is not stationary; instead it rotates so that the *perigee* moves eastward, advancing through a complete revolution in 8.85 years. The interval between successive passages of the Moon through *perigee* or through *apogee* is 27.5546 days; this is called the *anomalistic month*.

If the orbit of the Moon were in the same plane as the Earth's orbit around the Sun, the Moon would pass between the Earth and Sun each month and there would be a solar eclipse. Likewise, the Moon each month would pass through the Earth's shadow and itself suffer eclipse. But the plane of the Moon's orbit is inclined to that of the Earth by a little more than 5°; the Moon may pass above or below the Sun by this amount, as a maximum, and this is about ten Moon-diameters, allowing plenty of clearance.

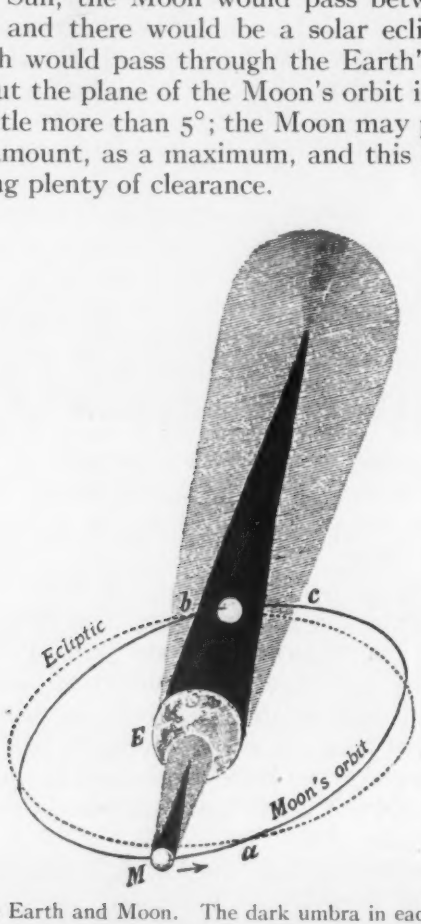

FIG. 2. Shadows of the Earth and Moon. The dark umbra in each instance is surrounded by the much lighter penumbra.

The Moon crosses the plane of the Earth's orbit twice each month; these points where the Moon's orbit intersects the *ecliptic*—the plane of the Earth's orbit around the Sun—are called the *nodes*. These slip westward along the ecliptic at such a rate that a complete circuit is accomplished in 18.6 years. In half this period, or 9.3 years, the *ascending node* (where the Moon crosses the *ecliptic* from south to north) moves around to the place where the *descending node* (Moon crossing from north to south) stood at the beginning of the interval. The time elapsing between two successive passages of the Moon through the same *node* is 27.2122 days; this is known as the *nodical month*.

These interesting behaviors of the orbit of the Moon are produced by the combined attractions of the Earth and the Sun. When the relative distances of the Moon from the Earth and the Sun and the relative masses of the three bodies are put into Newton's gravitational equation, it is found that the Sun pulls the Moon twice as strongly as the Earth does. The Sun tries to draw the Moon's orbit into the plane of the *ecliptic*, the Earth's orbit; the Moon resists because of its motion and the result is the *regression* or westward motion *of the nodes*.

Now we can understand why the *Metonic Cycle* does not continue to predict eclipses, after the first three or four. To produce an eclipse of the Sun, the Moon must be at the new, but it must also be near one of the *nodes* of its orbit, so it will actually pass in front of some part of the Sun as seen from some part of the Earth. Now suppose that at a particular instant of new moon the Sun and Moon are exactly at one of the *nodes*. There will be an eclipse in which, from the center of the Earth, the centers of the Moon and the Sun will be seen to coincide in direction. By the *Metonic Cycle*, on the same date 19 years later there will be a new moon, the 235th one after the first one considered. But the period of regression of the Moon's *nodes* is only 18.6 years, so the node will have revolved westward all the way around the *ecliptic* and a little more; the *node* will now stand almost 8° west of the Sun. The Moon will pass through the *node* before it becomes new, but from some part of the Earth it will still be seen to obscure some part of the Sun. Even after another cycle of 19 years has passed and the *node* is more than 15° west of its original position, such a partial eclipse will occur, but after the next cycle there will be no eclipse; the *node* is too far west of the Sun.

When we consider the *Saros* in the same way, the outcome is very different. This cycle contains 223 synodic months, or a total of 6585.32 days. The remarkable thing is that this is almost equal to 242 nodical months; the total length of this latter period is 6585.36 days, only about one hour longer than 223 synodic months. This means that when the Moon comes around for the 223rd new moon after the first one, the Sun and the Moon are only about one-half a degree away from the *node*.

Another rather startling coincidence is the fact that 239 anomalistic months amount to 6585.54 days, almost the same as the other values given above. This means that if at the first eclipse the Moon is at *perigee*—closest to the Earth, hence appearing its maximum size as we view it—it will be almost exactly at *perigee* again when a *Saros* has passed, and when another passes, and another. Therefore the eclipses that follow the *Saros* pattern differ little from each other in magnitude; if one of them is a long one, the next one will be also long.

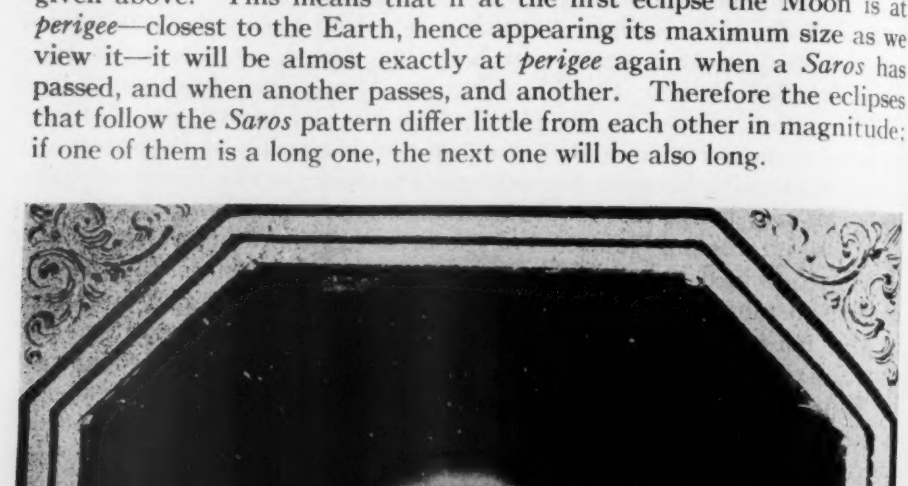

FIG. 3. The First Corona Photograph. This was taken on a daguerreotype plate by Berkowski of Koenigsberg in 1851.

The *Saros* is equal to 18 years plus 10 or 11 days (depending upon the number of leap-days inserted in the interval). There was a total eclipse of the Sun on June 29, 1927; another occurs on July 9, 1945, another on July 20, 1963, another on July 31, 1981, another on August 11, 1999; then follow eight others and the ninth one occurs on November 17, 2161, as the reader may verify for himself as an exercise in eclipse prediction. This is a rather "young" *Saros*, for the first total eclipses of this list are short ones, increasing from one to the next. The maxi-

mum durations of the total phases of the first five of the list are, respectively, 0.7, 1.3, 1.5, 2.2 and 2.6 minutes. The lengths will continue to increase until the maximum of almost $7\frac{1}{2}$ minutes is attained, then, slowly, the maximum durations will diminish until the eclipses of the series are no longer total.

There are other eclipse cycles. One of them is 29 years less almost exactly 20 days (or 21 days, if only 7 leap-days occur in the interval). A series fulfilling this period includes the eclipses of August 30, 1905, August 10, 1934, July 20, 1963, June 30, 1992, and June 10, 2021. If we multiply this cycle by 18, we have a period of 6444 synodic months, equal to 190,295.11 days, and this is very nearly equal to 6993 nodical months or 190,295.05 days. Eclipses should repeat themselves after this interval, which is 521 years, or after multiples of this interval.

Suppose we consider the eclipse of June 10, 2021 as at the end of five of these 521-year cycles. We must proceed cautiously here, for man uses a calendar year that only on the average agrees with the year of the seasons. Indeed, the safest way for us to proceed is to reckon entirely in terms of dates according to the *Julian Calendar*, the one that was abandoned in Catholic Christendom in 1582 and in Britain and the American colonies in 1752. June 10, 2021 A.D., by our *Gregorian Calendar* corresponds to May 28, 2021 in the *Julian Calendar*. Now 521 *Julian years* (of exactly 365.25 days each) amount to 190,295.25 days, and this is almost exactly the cycle we are considering. So we shall count back from May 28, 2021 A.D. (*Julian*) by 5 times 521 *Julian years*, or 2605 years. The result is May 28, 584 B.C., by straight arithmetic, but we have included a year "0," which is not in history; historically, the year 1 B.C. was followed immediately by the year 1 A.D. So our derived date of an eclipse of the Sun becomes May 28, 585 B.C.; it is the one predicted by Thales, and we have predicted it in retrospect, as it were.

One important thing in connection with such cycles as the *Saros* has to do with the fractions of a day left over. The *Saros* includes 223 synodic months, a total of 6585.32 days; 18 *calendar years* plus 11 days total 6585 days, approximately one-third of a day less. Because of this, the successive eclipses of a series fall approximately one-third of the way westward around the Earth. At the same time there is a progression either northward or southward on the Earth, because the *node* is moving past the points where the Sun and Moon stand at the new phase.

Omitting the dates and the months, we find the eclipse of 1945 has its maximum in Greenland; that of 1963 in Alaska; that of 1981 in Central Asia; that of 1999 in Europe; that of 2017 in northwestern United States; that of 2035 in China; that of 2053 in northern Africa; that of 2071 in Mexico; that of 2089 in the China Sea; that of 2107 in Central Africa; that of 2125 in middle South America; that of 2143 in

Borneo; that of 2161 in South Africa. Both tendencies mentioned in the preceding paragraph are obvious in this series; each third eclipse returns to about the same longitude because of the shift of one-third the Earth's circumference westward each cycle, but there is a steady progression southward.

Several *Saros* series of eclipses are in existence at once, some working gradually northward, the others working southward. The series to which the eclipse of July 9, 1945 belongs began as a small partial eclipse visible from the Arctic regions on January 4, 1639; the first total eclipse of the series was on June 17, 1909; the very last eclipse of the series has not yet been computed, but it will occur in the 27th or 28th century, and it will be a small partial eclipse visible only from Antarctica.

These parlor methods of predicting eclipses deal almost exclusively with dates only; exact times and exact locations and circumstances call for much more refined methods. The methods exist with all the degree of perfection necessary for the purposes of astronomers, as will appear in what follows. They are essentially rigorous problems in geometry, elementary in principle, tedious in practice. If we know the ways in which the Earth, the Moon and the parts of the Moon's orbit change with respect to the orbit of the Earth, we should be able to solve the problems involved.

In 1887, Theodor von Oppolzer published at Vienna his *Canon der Finsternisse* (Catalogue of Eclipses), containing the necessary information for good predictions of the circumstances of all eclipses, both solar and lunar, in the interval between November 10, 1207 B.C. and November 17, 2161 A.D. Maps of the approximate tracks of the total eclipses of the Sun are included in the work. There are 8000 solar and 5200 lunar eclipses in the period of 3367 years; only about a quarter of the solar eclipses are total, averaging 66 per century. The information given by Oppolzer is good enough for preliminary predictions, especially with certain corrections to some of his fundamental data, as published in recent years by Schram and Schoch; still greater refinement is possible, however, so each year the various Nautical Almanacs (as the *American Ephemeris and Nautical Almanac* published at the United States Naval Observatory) include the most modern elements for the predictions of eclipses of that year, for any spot on the Earth, with full predictions calculated for the principal cities.

One of the most fortunate accidents in nature has placed the Moon at such a distance from the Earth that its disk is just large enough to cover the disk of the Sun. For no other planet in the Sun's family is such a circumstance true; either a satellite appears much smaller or much larger than the Sun, as seen from the planet. If the Moon's diameter were only 1992 instead of 2160 miles, it would never completely hide the Sun's disk.

If light emanates from a point, the shadow of a body possesses a sharp edge. If light emanates from an area, the shadow of a body on a screen not far behind it will be composed of a dark central portion, called the *umbra*, surrounded by a less dark envelope called the *penumbra*. As seen from the Earth, the Sun possesses an appreciable area, so the shadows of the Earth and Moon (see Fig. 2) are of this two-fold nature.

Because of the variations in distance from the Sun, the shadows of the Earth and Moon can be of several different sizes. The tip of the cone-shaped *umbra* of the Earth's shadow extends to a distance of 870,700 miles from the Earth's center, when we are farthest from the Sun; when we are closest to the Sun, early in January, the length of the *umbra* is 842,000 miles. When the Earth-Sun distance is greatest and the new moon occurs when the Earth-Moon distance is least, the *umbra* of the Moon's shadow is 235,800 miles long, extending 14,300 miles beyond the center of the Earth. When the Earth-Sun distance is least and the new moon occurs when the Earth-Moon distance is greatest, the length of the Moon's *umbra* is only 227,700 miles, falling 25,000 miles short of the Earth's center. On the average, with both the Earth and the Moon at their mean distances, the *umbra* of the Moon's shadow is 232,200 miles long, falling short of the Earth's center by more than 6600 miles, or short of the Earth's surface by more than 2600 miles.

On the average, the *umbra* of the Earth's shadow is so long that its thickness is approximately 5750 miles, at the distance of the Moon's orbit. This is 2.66 times the diameter of the Moon; inasmuch as the Moon appears to move eastward against the background of the stars by approximately its own diameter per hour, a total eclipse of the Moon, when the Moon passes completely into the Earth's *umbra* and out again, can last for approximately 1 hour 40 minutes; for an hour before the beginning of totality, the Moon is entering the *umbra* and after totality an equal period is required for the Moon to emerge from the *umbra*.

The Moon enters the shadow of the Earth from the west side; the *penumbra* is first encountered, about an hour before the Moon begins to enter the *umbra*. Usually, however, it is almost time for the Moon to begin to enter the *umbra* before any darkening can be seen, for there is much light in the *penumbra*. Even during totality, the Moon does not disappear; the surface assumes a dull ruddy brown color, often described as coppery. All along the limb of the Earth, as seen from the Moon, sunlight is refracted or bent as by a spherical lens into the *umbra* of the Earth's shadow, because of the atmosphere. Because most of the blue light is scattered, to form the blue of the sky, what manages to get through to be bent into the shadow is predominantly reddish, so the Moon during eclipse is coppery red in color. The

amount of illumination from this indirect light depends upon the degree of cloudiness in the parts of the Earth's atmosphere where the refraction occurs.

Partial lunar eclipses occur when not all of the Moon enters the *umbra* of the Earth's shadow. In a century, the average number of partial lunar eclipses is 83; in the same interval, there will be 71 total lunar eclipses. The number of lunar eclipses is only 65% as great as that of solar eclipses of all kinds, yet more lunar eclipses are visible wholly or in part to the average individual. Lunar eclipses occur during full moon; at one instant, the full moon can be seen by practically half the area of the Earth. For this reason, then, at least half the Earth can see the Moon in eclipse; but because the eclipse can last for an hour or more, even total lunar eclipses can be seen from more than half the area of the Earth. Solar eclipses, on the other hand, are visible even in the partial phases from limited areas of the Earth.

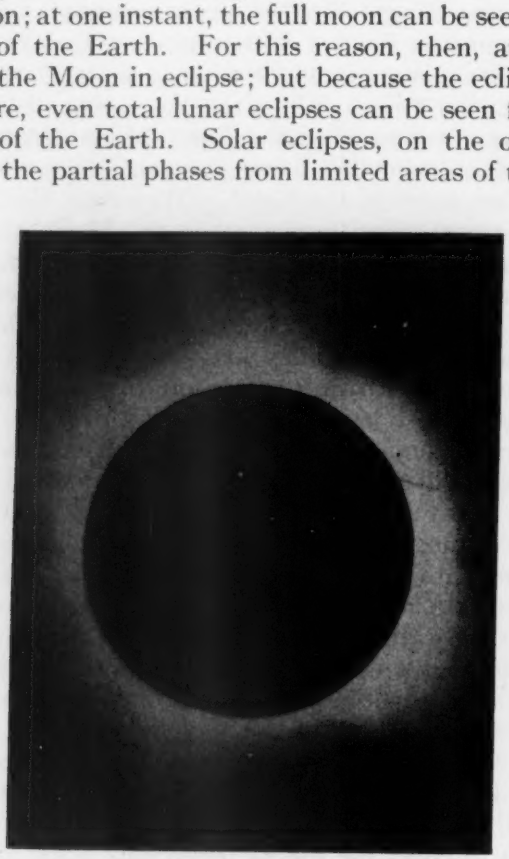

FIG. 4. The Corona in 1936, photographed by the Harvard-M.I.T. Expedition to Ak-Bulak, U.S.S.R.

The average length of the *umbra* of the Moon's shadow is such that it fails to reach the Earth's surface; the Moon then fails to occult all of the Sun. An uneclipsed ring or *annulus* of the Sun's apparent disk surrounds the dark disk of the Moon at such an *annular eclipse*. There are 77 annular eclipses per century.

If the Moon's apparent diameter is equal to or greater than that of the Sun, and if the axis of the *umbra* of the Moon's shadow intersects some part of the Earth's surface, a *total eclipse* of the Sun occurs. Under the most favorable conditions, the diameter of the *umbra* as it is intersected by the nearest portion of the Earth's surface is only 168 miles. Because of the motion of the Moon and the rotation of the Earth, the patch of *umbra* sweeps across the Earth's surface from west to east; the width of the path, never exceeding 168 miles, is usually much narrower than that, and only in that narrow band across the Earth can the *total* eclipse be seen (Fig. 13 shows the track of the umbra for the eclipse of July 9, 1945). If the width of the track is very small, the *umbra* of the Moon's shadow may actually fail to reach as far as the parts of the Earth's surface at the beginning and end of the track; the eclipse will then be *annular* at the ends and *total* in the middle. There are 11 such eclipses per century, and 66 that are seen as total all along the path.

Outside the path of the total eclipse, *partial phases* are observed over the much larger area covered by the *penumbra* of the Moon's shadow; the diameter of the *penumbra* is about 5000 miles, where it is intersected by the Earth's surface, so the partial phases during a total eclipse can be seen over a very large area (see Fig. 13).

Partial eclipses occur also when no part of the *umbra* of the Moon's shadow touches any part of the Earth's surface, while some part of the Earth is immersed in the *penumbra*. There are 84 such eclipses per century.

Partial eclipses, or the partial phases of a total eclipse, are not very impressive. Unless the observer is forewarned, he is not likely to notice that such an eclipse is occurring, unless more than half the Sun's disk is hidden by the Moon. The diminution of the light is so gradual that only a deliberate look at the Sun will reveal what is happening. When the eclipse is almost total, the loss of light, accompanied by a change of character or quality of the illumination, becomes marked. If the season of the year is such that there are leaves on the trees, little crescent images of the Sun will be seen on the pavements, formed by the passage of rays of sunlight through the interstices between the leaves. One way to observe a partial eclipse safely is to pierce an opaque card with a pin-hole, then let the image of the Sun fall on a second card at some distance behind the first one. This works best in the dark of a room where the shades are drawn. The encroachment of the Moon's disk on that of the Sun will be well marked in the image. Another way is to "smoke" a piece of glass over the flame or candle; the glass may be held before the eye as the Sun is observed, or the light of the Sun may be reflected from the glass side of the prepared piece, and viewed safely, although it will be quite bright.

For additions to our knowledge of the Sun and, in smaller degree, of the Moon, total solar eclipses are very valuable. If the Moon's diameter had been a little less, or its distance a little more, we should never have seen a total eclipse and many things that we know today would not be suspected. Several powerful methods of investigation of solar phenomena would never have been developed, for we should not have realized that the investigations were of significance, had there never occurred total eclipses.

As the moment of beginning of totality approaches, the feeling that something of unusual nature is occurring is almost oppressive; the light has grown noticeably faint and has taken on a quality somewhat resembling that of a mercury-vapor lamp, perhaps generously mixed with incandescent lamp light. Atmospheric effects, combined with the thinness of the remaining portion of the Sun's apparent disk, produce the *shadow bands*, weird picket-patterns of dusky bands that move quickly across the ground, as patterns move across the sandy floor of a shallow pool of water while ripples move across the surface. The temperature has noticeably fallen; the humidity has risen. Animals stir restlessly, birds cheep as though settling in their nests for the night; cows meander through the pasture, heading for the barnyard; chickens go to roost.

At the very instant when the last thread of the diminishing crescent of the Sun is obscured by the advancing edge of the Moon, there springs into view a portion of the Sun called the *corona* (Figs. 1, 3, 4), at other times invisible to the unaided eye and only recently partially observable under non-eclipse conditions, following the development of special equipment for the purpose. This irregular halo of light, ranging in total brightness from a half to all of the light of a full moon, according to modern measures, is of spiked and filamentary nature, suggesting the action of powerful forces. The extent of the *corona* varies from one eclipse to another, yet always indicates the presence of solar material and powerful solar forces to distances of more than a million miles from the Sun's apparent surface.

At the base of the *corona* there can be seen rosy flamelike protuberances known as *prominences* (Fig. 5); these are masses of gases rising above the normal apparent surface of the Sun and they have recently been demonstrated to have considerable connection with the *corona*. Sometimes when the duration of the total eclipse is very short, there will be portions of the Sun left shining through depressions of the Moon's limb (Fig. 6); these are called *Baily's Beads*, although it appears that they were noticed by many at several eclipses before the astronomer Baily first called attention to them, at the time of an annular eclipse on May 15, 1836. The serrated edge of the Moon permits sunlight to shine through low places between mountains and craters, either before or after the total phase, or at both instants; sometimes one brilliant

bead of light will show up very strongly, producing what is called the *diamond ring effect.*

The maximum duration of a total eclipse, but seldom in recorded history attained, is $7\frac{1}{2}$ minutes. In mid-Pacific, in 1937, the duration was 7 minutes 4 seconds; eclipses of about the same duration will occur in 1955 and 1973, the first in Ceylon, Thailand and the Philippines, the latter in South America, the South Atlantic and Africa. Eclipses

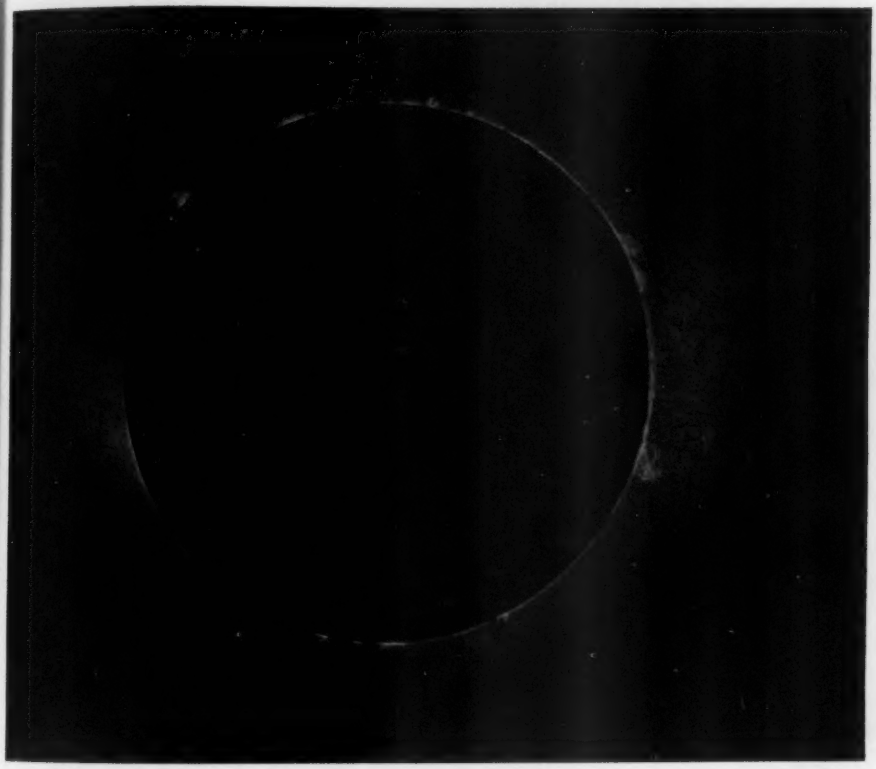

FIG. 5. Inner Corona and Prominences.

of little more than 2 and 3 minutes duration, respectively, occur in the United States and Canada in 1954 and 1970 (Fig. 15); central and southern Europe will see an eclipse of $2\frac{1}{2}$ minutes duration in 1999.

During total eclipse, the illumination of the ground amounts to approximately twenty-five times that of a full moon riding high in a cloudless sky. A little of this comes directly from the *corona* and the *prominences;* almost all of it comes from the sky, illuminated slightly by the *corona* but largely by the sunlight outside the *umbra* of the Moon's shadow. The bright stars and planets come into view but the appearance is far from that of the ordinary moonlit sky because the

intensity of the sky during the eclipse is so much greater. The lack of adaptation of the eye to the diminished light produces a spurious impression of darkness.

With the reappearance of the thinnest crescent of the Sun's disk at the western edge of the Moon, the intensity of the light on the ground leaps at once to what seems almost normal sunlight, after the gloom of the short period of totality; the *corona* disappears, and the *prominences*, and the stars and planets, unless Venus and Jupiter are above the horizon. At times, from the tops of high mountains, the *corona* has been seen for a few seconds after the end of totality, because of the cleanness of the sky.

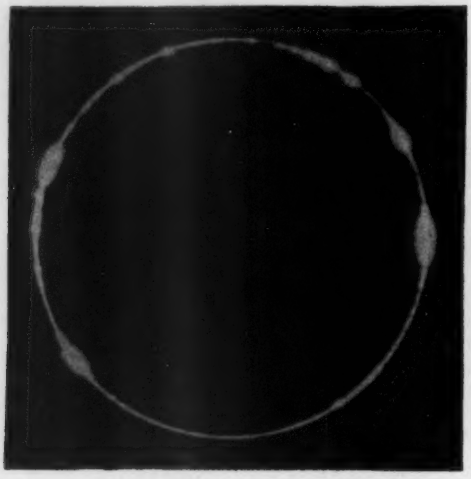

FIG. 6. Baily's Beads. Photographed by the Lick Observatory Expedition to Camptonville, Cal., April 28, 1930. Duration of totality was only one second.

The history of a complete eclipse begins approximately an hour before the scheduled instant of beginning of totality, when the eastern edge of the Moon begins to encroach on the west edge of the Sun; this is the instant of *first contact*. *Second contact* marks the beginning of totality, *third contact* the end of totality. An hour after third contact, the western edge of the Moon uncovers the last bit of the Sun's eastern edge at *fourth contact*. For the astronomer, most of the importance of the eclipse lies between *second* and *third* contacts, a period never exceeding $7\frac{1}{2}$ minutes and usually only 2 or 3 minutes.

Astronomers travel to the antipodes to observe total eclipses of the Sun; during those few minutes when the Moon's bulk blacks out the direct light of the Sun from a thin swipe across the Earth's surface, observations can be made that are not possible at other times. Allowing 3 minutes for an average eclipse and perhaps an eclipse in an accessible part of the world each three years, one astronomer is fortunate if he

has as much as half an hour of eclipse observation in his professional lifetime. A few astronomers have attended as many as ten or eleven eclipses; no man has seen that many, for one of the heart-breaking possibilities is that there will be clouds at the time of totality. After having transported an expedition of several observers and several tons of equipment to some insect-infested or ice-clad part of the world, it requires a peculiar brand of stolidity to grin in the gloom beneath the clouds and say, "Well, we had the trip, anyway." Cloudy or not, however, the strict program of observations is followed; if there should come a sudden break in the clouds, after the eclipse has begun, something would be salvaged.

The precious interval of totality must be budgeted carefully, in order to use it to good advantage. One aim of every eclipse expedition is to make a few photographs of the *corona*, so its shape, extent and structure may be compared with its appearances at other eclipses. One or two instruments to take care of this part of the program and nothing else will have their own observers who may be so busy changing plate-holders and making the exposures that they have scarcely a moment to glance toward the sky to see the *corona*. If the eclipse is a very short one, perhaps one instrument will make only one photograph, after having been dismantled at its home observatory, carefully crated, shipped several thousand miles across the world, then set up in a temporary station, on piers that have required several days to construct. A long exposure on the *corona* is necessary to show its great extent; short exposures are necessary to reveal the structural details close to the edge of the Moon. This *inner corona* is now known to be closely connected with the *prominences;* photographs that reveal it clearly will also show the prominences (Fig. 5).

Some of the light of the *corona* is sunlight, reflected and scattered by the particles of the extensive envelope. Some of the light is truly *coronal*, consisting of specific radiations in all regions of the spectrum from infra-red to ultra-violet. These are relatively few in number, however; hardly more than a score of these emission lines are known in the observable region of the spectrum. It was at the total eclipse of August 7, 1869 (for the observation of which The Franklin Institute organized an expedition; see JOURNAL, Vols. 88, 89), Professors Young and Harkness first saw a strong green emission line in the spectrum of the *corona*. Since that time, observations of the coronal spectrum have been among the major aims of expeditions. Other lines have been discovered and increased accuracy of measurement of the wavelengths has been accomplished.

The failure to identify the emission lines at once as originating in the vapors of any known materials led to the coining of the name "coronium" for the material responsible for them; while at first it may have been believed that this might represent a new element, as yet

unknown terrestrially, latterly it was tacitly agreed that "coronium" must be familiar materials under such unfamiliar conditions that its identity is obscured.

In 1941, the solution of the riddle was forthcoming when Edlen, a Swedish astrophysicist who has made many other outstanding contributions in the field of high-excitation spectra, gave identifications for all of the strong coronal lines. His work is highly theoretical but it consists of an extrapolation from observational material derived by him in his own laboratory. There is little doubt that his explanations are valid, although our present laboratory methods are incapable of permitting direct observational tests of the identifications he has given.

The elements responsible for the emission lines in the spectrum of the *corona*, according to Edlen, are calcium, nickel, iron and argon; we would never recognize them, however, for the calcium atoms have 11, 12 and 14 electrons removed, the nickel atoms have 11, 12, 14 and 15 electrons removed, the iron atoms have 9, 10, 12, 13 and 14 electrons removed, and the argon atoms have 9 and 13 electrons removed. Even if we could accomplish these high degrees of *ionization*—removal of electrons from the atoms—in our laboratories, the observed spectral lines would not be produced, for they are "forbidden" lines that can occur only when conditions are very un-terrestrial—unearthly.

While Edlen has solved the obvious part of the problem—the origins of the radiations of the *corona*—he has posed other problems of even greater fundamental importance. To remove 12 electrons from an iron atom by pure thermal excitation requires a temperature of approximately 100,000° C.; the removal of 12 electrons from a calcium atom demands a temperature of the order of 1,000,000° C.! Surely temperatures as great as this cannot exist hundreds of thousands of miles from the main body of the Sun, when the temperature of the radiating surface, the *photosphere*, is only about 6000°. Yet the degree of excitation must exist, although it is not due to temperature. The lines of the spectrum of the *corona* have been found to be broader than we should expect from such a rare medium as the *corona;* the reason for this is that the excitation produces high speed particles and such particles emit wavelengths a little longer or a little shorter than those of stationary particles, so the lines are all widened. Something else is explained, as well; there is a portion of the coronal spectrum that is neither ordinary scattered sunlight nor coronal emission. This is like ordinary sunlight except that the absorption lines that reveal the composition of the Sun's atmospheric layers beneath the *corona* are missing. This must be due to sunlight scattered from the extremely high-speed electrons that have been torn from the atoms whose emissions are found in the coronal spectrum discussed above.

Whatever the source of the excitation—strange electro-magnetic forces or strange utilization of the large amounts of energy in the Sun's

far ultra-violet spectrum—the absence of such plentiful materials as hydrogen in the *corona* is now easily explained. The excitation is so high that the components of the hydrogen atoms—one proton and one electron to each one—are kept apart, except in the very lowest layers; there they are permitted to unite and hydrogen "condenses" out of the *corona*, to pour down onto the ordinary body of the Sun. This precipitation of hydrogen from levels high above the *photosphere* has been found to be very common, in continuous motion-picture registration of solar phenomena taken at the McMath-Hulbert Observatory of the University of Michigan.

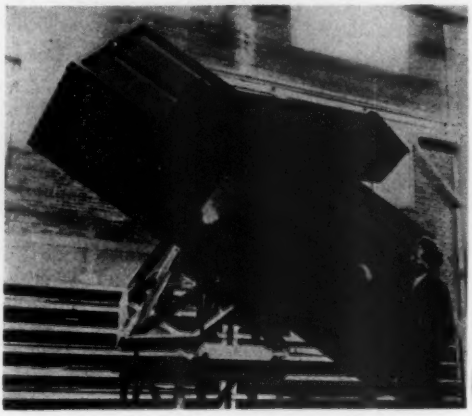

FIG. 7. Four Plane-grating and One U.V. Prism Spectrographs used by the Harvard-M.I.T. Expedition to Ak-Bulak, U.S.S.R., 1936.

Until 1931, no one had succeeded in photographing the *corona* or its spectrum at any time other than that of total eclipse, when the Moon removed most of the scattered sunlight from the sky. But the Moon itself can be seen in daylight, when it stands above the horizon, and the *corona* is comparable in brightness with the full moon; it should therefore be possible to see the *corona* by day, in a clear atmosphere. Many astronomers had tried it, from the tops of lofty mountains; some of them thought they had succeeded but careful study of their photographs revealed that they were photographing only instrumental defects. A French astronomer, Lyot, came to the conclusion that the source of failure in these previous efforts to detect the *corona* outside eclipse was "parasitic light" emanating from the foreign particles of the atmosphere and imperfections in the telescopes. A scratch or bubble or striation in a lens will scatter light; as soon as a perfect lens is made, the scattering should be practically eliminated. Lyot realized such lenses and, atop a high mountain in the French Alps, he succeeded in photographing the *corona* and its spectrum. To his instrument he

gave the name *coronagraph;* other instruments have been made, following his original pattern, and are in operation in Switzerland and in Colorado (the Climax Station of the Harvard College Observatory). But there appear to remain decided limitations to the powers of these instruments; only the bright *inner corona* can be photographed and the long fantastic extensions of the Sun's great envelope remain unattainable except during total eclipse—at least until we can establish observatories outside our atmosphere!

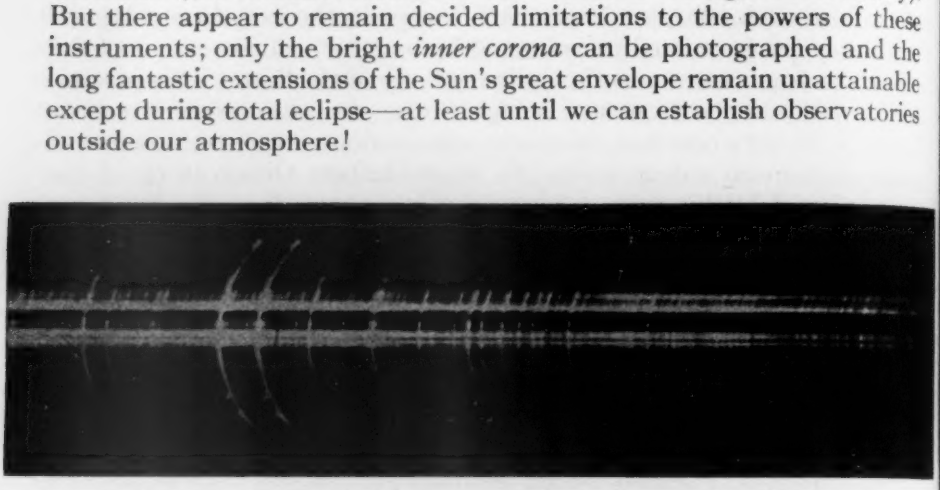

FIG. 8. The Flash Spectrum. The two longest arcs are due to atoms of ionized calcium; other arcs are due to hydrogen, helium and metal vapors.

Much of the need for photographs of the *inner corona* and *prominences* (Fig. 5) during total eclipse has now been removed. The *coronagraph* and other instruments can operate on any clear day to give us those pictures. Evidence of material in elevated masses at the limb of the Sun was first obtained at total eclipses, about 1700, and rosy-red "flames" were observed at the eclipse of July 8, 1842. It was not until the Spanish eclipse of 1860 that these appendages were demonstrated to belong to the Sun; the proof consisted of the observation that the Moon covered up these rosy *prominences*, as it moved across the limb of the Sun. Surrounding the inky-black disk of the Moon, a thin crimson ring, named by Lockyer the *chromosphere* ("color-sphere"), contrasts sharply with the creamy-white *corona* stretching out beyond it. The *prominences* are elevated masses of the *chromosphere.* In 1866, Lockyer proposed a way in which they might be observed at any time; no one seems to have tried it until 1868. At the total eclipse of August 18 of that year, Janssen from Paris observed at Guntoor, India; he was so struck by the brilliance of the *prominences* that he tried to see them on the day after the eclipse. He set the slit of his spectroscope on the image of the limb of the Sun and a thin slice of the *chromosphere* was at once visible in the eyepiece. By turning the instrument around, keeping the slit tangent to the Sun's limb, he could see the whole *chromosphere;* by moving the slit outward a little, a section through a *prominence* could be seen.

Janssen sent off a description of his observations; before his manuscript arrived at the Academie des Sciences, Lockyer in England had accomplished the same result on October 20; the two manuscripts were read at the same meeting and the two men shared the honor of the discovery.

It was at this same eclipse in 1868 that observers first noted a strong yellow line in the spectrum of the *chromosphere*, not present in the spectrum of ordinary sunlight. Lockyer gave the name *helium* to the material giving rise to this strong yellow line, because the material existed in the Sun (*helios*, in the Greek). Not until 1896 was this new element isolated terrestrially; it is now known to be very abundant, cosmically, and very important as the end-product of the destruction of hydrogen in the process of energy-generation in the stars.

At the eclipse of December 22, 1870, in Spain, Professor Young of Princeton set the slit of his spectroscope perpendicular to the direction of the Moon's motion across the Sun's face, and tangential to the limb of the Sun at the middle of the fast-diminishing crescent. An instant before the light faded out, there was a bright flash, in which Young saw the ordinary absorption lines of the solar spectrum become emission lines—change from dark to bright. This *flash spectrum* is obtained by almost all eclipse expeditions by the simple expedient of placing a prism over the objective of a telescope and exposing the photographic plate at a carefully-computed instant. The exceedingly slim crescent remaining an instant before second contact or appearing an instant after third contact acts as the narrow source to produce sharp lines in the spectrum; these lines are curved, of course, because they are monochromatic images of the curved limb of the Sun (Fig. 8). The highest materials of the Sun's atmosphere will give rise to the longest arcs; by extension of this idea, the distribution of the various atoms and ions in the solar envelope can be studied. Hydrogen and calcium occur at high levels; helium seems not to occur so far from the photosphere; the heavier atoms, as iron, nickel, titanium, chromium, etc., produce the very short arcs of the *flash spectrum*.

The thickness of the layer responsible for this appearance is very small; the duration is very short. By timing very accurately the instant of appearance of the *flash spectrum*, a very accurate knowledge of the time of beginning or ending of the total phase can be derived. This method, only recently suggested, will be used at future eclipses to perfect our knowledge of the dimensions and motions in the solar system.

Fortunately we are not dependent today on observations only at the limb of the Sun for our knowledge of the distribution of various materials in the Sun. By extension of the method suggested by Lockyer and Janssen in 1868, the American Hale and the French Deslandres in 1893 showed how it is possible on an clear day to photograph only the

hydrogen in the Sun, or the calcium, or some other material. The *spectroheliograph* and variations of it have proved very fruitful in our search for knowledge of the composition and structure of the Sun (Figs. 9 and 10). Without total eclipse observations to suggest a need for such studies, it is extremely doubtful if any of these methods would have been developed.

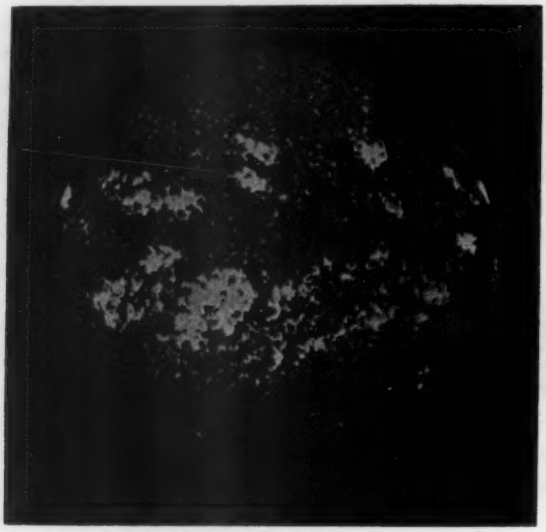

FIG. 9. Calcium Spectroheliogram. The distribution of ionized calcium over the Sun.

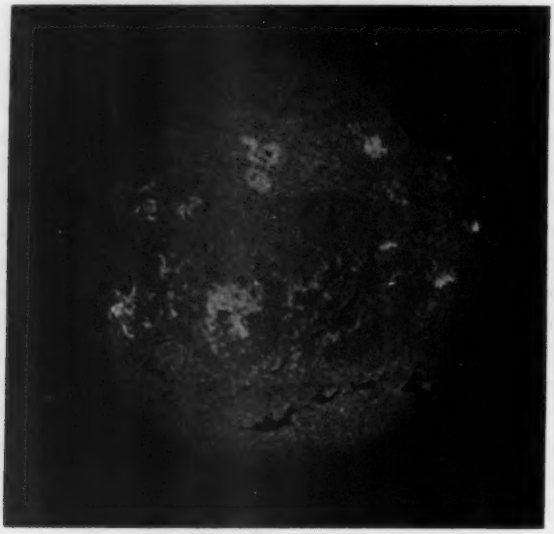

FIG. 10. Hydrogen Spectroheliogram. Taken at the same time as Fig. 9, showing the hydrogen distribution.

FIG. 11. Curves of Sun-Spot Numbers (below) and Magnetic Activity of the Earth (above). High magnetic activity means that the compass needle vibrates and is otherwise disturbed.

When the Sun is observed visually or photographed, there often appear on its apparently smooth face dark blemishes called *sun spots*. We know today that they are vortical disturbances in the *photosphere*, dark only because the material rising from below and expanding at the surface is at a temperature of about 4500° C., at least 1500° cooler than the rest of the solar surface. *Sun spots* vary in size, number and degree

FIG. 12. The Northern Lights, Sept. 18, 1941. Photographed at Cambridge, Mass., by R. Newton Mayall.

of activity in a period averaging a trifle more than 11 years (Fig. 11). A maximum in 1938 was followed by an irregular decline to a minimum in 1943; another maximum should occur in 1948 or 1949. At times of maximum, no day passes without many *sun spots* and *sun-spot groups;* at times of minimum, sometimes many weeks will pass without the appearance of a single spot. *Prominence* activity is strongly marked over *sun spots;* the longest extension of the streamers of the *corona* are above the zones where *sun spots* are found. Bright *eruptions* or *flares* occur in and near active *sun spots*, as high-temperature masses of gases, chiefly hydrogen, burst out above the surrounding levels of the *photo-*

sphere. When sun-spot minimum is at hand, the equatorial extension of the *corona* is greatest (as in Fig. 1); at time of maximum, the *corona* seems not to extend so far (Fig. 4). In the opinion of S. A. Mitchell, the best maximum-type *corona* occurs perhaps two years after sun-spot maximum and the most typical minimum-type *corona* occurs two years after sun-spot minimum.

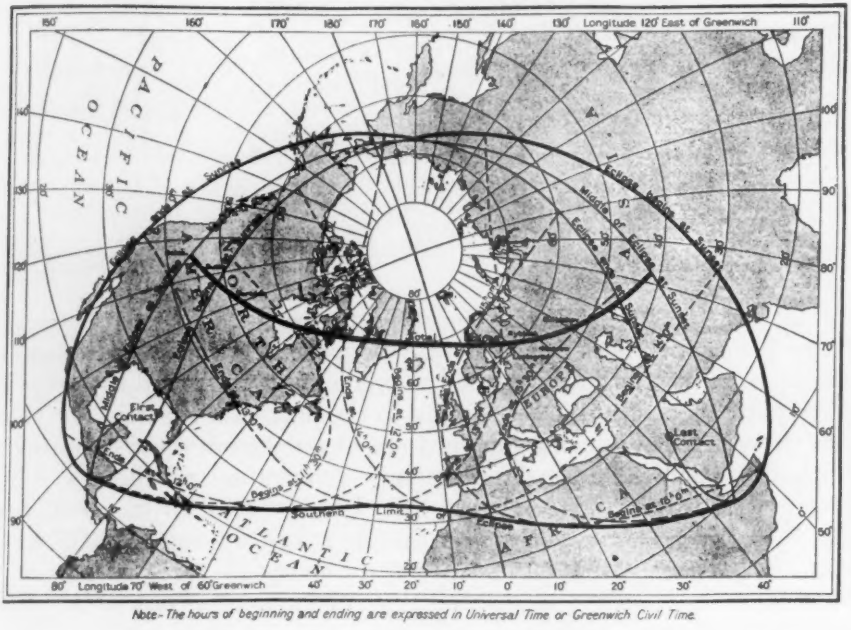

FIG. 13. Area of Visibility of Total Solar Eclipse of July 9, 1945. The path of totality extends from Boise, Idaho, through Hudson Bay, Greenland, Scandinavia and U.S.S.R., along the heavy line through the middle of the area marked out. Throughout the remainder of the area, various amounts of partial eclipse will be observable, ranging from 100% at the path of totality to 0% at the bottom and top limits.—From *American Ephemeris*, 1945, U. S. Naval Observatory.

Other phenomena, chiefly terrestrial, vary along with *sun spots*. Activity of the Earth's magnetic field parallels the behavior of *sun spots* (Fig. 11) in such a way that no room for doubt exists that they are intimately connected with each other. Displays of the *polar aurora*—Northern Lights and Southern Lights—as well as the strength of the *permanent aurora* and other night-sky radiations are linked with the degree of sun-spot activity at the moment; the maximum number of auroral displays seems to follow the maximum of *sun spots*. Terrestrial temperature-departures from the mean values, precipitation and phenomena (as thickness of tree rings) dependent upon precipitation—

these and many other variable quantities here on Earth are linked with solar activity.

It is very probable that the *sun spots* themselves are not responsible for the variations in these other observable phenomena; rather, the spots are easily observed manifestations of something far more funda-

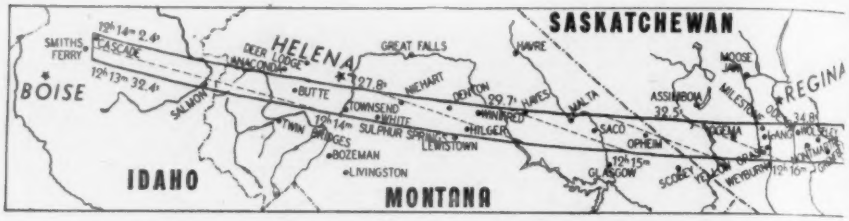

FIG. 14. The Beginning of the Path of the Total Solar Eclipse of July 9, 1945. At intervals along the bottom of the path, the Greenwich Civil Times of mid-totality are given. (12^h0^m Greenwich Civil Time is 8 a.m., E.W.T., 7 a.m., C.W.T., 6 a.m., M.W.T.) At corre-

(See page 323.)

mental that is happening at least in the surface layers of the Sun. There are many unestablished links between the various phenomena; eclipse observations have revealed so much and have urged the necessity of so many methods of investigation in the past that it seems inevitable that there is much information yet to be gleaned from these few precious minutes of time when the Moon stands between us and the Sun. It is not very likely that astronomers will ever say that all has been done that ever can be done; yet should that ever be said, many of them will continue to schedule their vacations for times of total eclipse, for a sight of one of nature's most impressive phenomena is not to be missed for lack of scientific utility.

Thre eare not many total solar eclipses visible from any part of the United States between now and the end of this century (see Fig. 15). The best one is that of 1970; in southern Georgia the duration is about 200 seconds and the Sun stands high when it is eclipsed. The runner-up is that of 1979; in mid-afternoon, in northeastern Montana, the duration is 160 seconds. In 1963, in Maine, the time is late afternoon; the duration is 70 seconds.

On July 9, 1945, the maximum duration of approximately $75\frac{1}{2}$ seconds occurs as the Sun stands less than 42° high, at noon near Scoresby Sound in East Greenland (Fig. 13); in southeastern Saskatchewan, not far from Regina, the Sun stands only 12° high, early in the morning, and the duration is 35 seconds. Near Boise, Idaho, the beginning of the path of totality is only 28 miles wide; in Saskatchewan it is about 38 miles; in Greenland, almost 60 miles, the maximum for this eclipse.

An examination of the path of totality through the meager portions

of the United States and populated southern Canada (Fig. 14) reveals that a great many communities lie near the center of the path. The durations of the total phase for points on the central line of the path are given along the top edge of the path; the instants of mid-totality for the points along the dashed lines crossing the path diagonally are

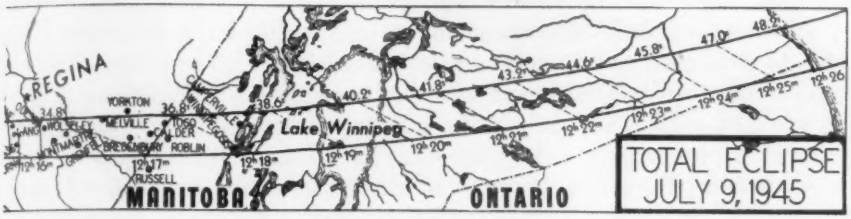

sponding intervals along the top of the path, durations of totality are given, in seconds. A dashed line connects the corresponding times and durations, but the latter apply only to points on the center line of the path.—Adapted from *Supplement* to the *American Ephemeris*, 1945, U. S. Naval Observatory.

given, in terms of Greenwich Civil Time, along the bottom edge of the path. From the central line outward to the edges of the path of totality, the duration diminishes from the value marked at the top of

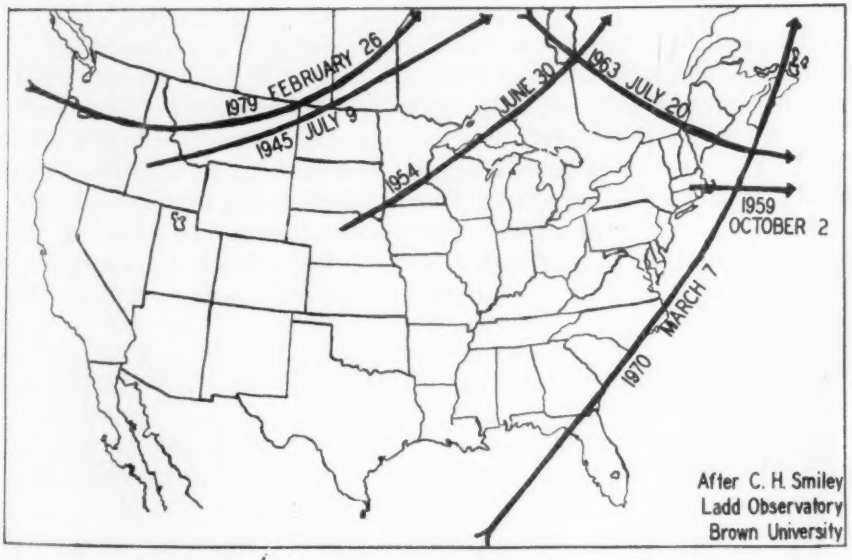

FIG. 15. Central Lines of Total Solar Eclipses Visible in the United States from 1933 to 2000 A.D.

the path to zero. For six or eight miles on either side of the central line, the duration is less than that at the middle by only two or three seconds, over most of the path, so any of the communities in south-

eastern Saskatchewan would seem to be suitable stations for eclipse expeditions. Many of them are very small, but most of them (as Montmartre, Wolseley and Bredenbury) have 115-volt, 60 cycle electrical supply for those who might wish to employ electrically driven instruments; many of them are on railroads, thus facilitating the shipment and erection of equipment. Six railroad lines cross the path of totality between Lang and Camperville, a distance less than 240 miles.

The chances for clear weather in this part of the country at this time of year are very good. The low altitude of the Sun (12° near Bredenbury) makes it imperative that a clear eastern horizon exist for the station. The Sun is totally eclipsed only about an hour and 20 minutes after it rises. On photographs of the eclipse, the image will be noticeably flattened because of the differential refraction between the top and bottom of the image of the Sun.

As Fig. 13 shows, the partial eclipse can be seen over all of North America except Lower California, all of Europe and a large portion of Asia. On a line running from Salt Lake City through James Bay and Iceland, about 90 per cent. of the Sun's diameter will be obscured; on a line from Pueblo, Colorado, through Sault Ste. Marie, Labrador and the tip of Greenland, 80 per cent. of the Sun's diameter will be covered by the Moon; on a line from San Antonio through mid-Pennsylvania, Boston and Prince Edward Island, the eclipse is 60 per cent.; at Havana, Cuba, 25 per cent. of the Sun's diameter will be obscured.

Eclipses of the Sun have contributed greatly to our knowledge of the behavior of matter and have stimulated many lines of investigation of the nature of the Sun and other stars. For the non-scientific observer, perhaps the greatest interest lies in the fact that the motions in the universe are so well understood that eclipses can be predicted to the second, and the conditions of their visibility can be foretold long in advance. As the Moon's dark disk moves inexorably over the bright face of the Sun, there is at least some small comfort in the thought that while man cannot stop the eclipse, the eclipse cannot avoid occurring as astronomers say it will occur.

NOTES FROM THE NATIONAL BUREAU OF STANDARDS.*

NEW RESISTANCE THERMOMETER.

Dr. Peter G. Strelkov of the Institute for Physical Problems of the Russian Academy of Sciences, U.S.S.R., is visiting the Bureau. He brought with him five precision resistance thermometers of a new and ingenious design developed by himself in Moscow after examining the types in use in the United States and other countries. The new thermometers are enclosed in quartz and the resistance coil is supported on a quartz helix in a novel manner that should simplify construction. These thermometers will not carry quite so much measuring current as those designed here and their response to temperature changes is somewhat slower, but in quality of platinum used and in apparent constancy, they are the equal of any that have been built here or have come to the Bureau's attention. These thermometers are being given a full National Bureau of Standards certification for the entire range of temperatures for which such thermometers are adapted.

THERMAL PROPERTIES OF WATER.

There is nothing new about steam tables; mechanical engineers have used them in engine design and operation for nearly 100 years, but the preparation of tables covering adequately the pressure and temperature ranges that are now common is a comparatively recent development. In 1923 the American Society of Mechanical Engineers sponsored researches on water and steam at several laboratories, and requested the Bureau to determine the specific heat of liquid water and its heat of vaporization. In his address as retiring president of the Philosophical Society of Washington on January 6, Dr. H. F. Stimson reviewed the Bureau's part in this project. He pointed out that the late N. S. Osborne, in taking up the Bureau's assignment, first studied the theory of "calorimetry of saturated fluids" and then proceeded to use this theory for the measurement of the enthalpy (formerly called total heat or heat content) of saturated liquid water and water vapor from 0° C. to the critical temperature at 374.15° C. The precision of his results was such that it is hoped they will meet every requirement of engineering practice for years to come. The vapor pressure of water was also determined from 100° C. to 374° C.

The vapor pressure of water between 0° and 100° has not been carefully determined since 1909 but a precision manometer has been

* Communicated by the Director.

developed with which Dr. Stimson plans to make measurements at pressures below two atmospheres. The vapor pressure of water can be measured, with this manometer, to a higher relative precision than the precision to which the corresponding temperature can be measured with platinum resistance thermometers calibrated at the steam and ice points by routine methods. The calibration of thermometers at 100° C. can be done with this precision manometer to an accuracy of .0001°. In order to obtain this same accuracy for calibrations near the ice point, the triple point of pure water was used. Special triple-point cells have been made and a technique developed which is suitable for precision calibration of thermometers. The temperature of the triple point was determined to be .0100° C.

SPECIFIC HEATS OF CHEMICAL COMPOUNDS USED IN SYNTHETIC RUBBER MANUFACTURE.

For research on synthetic rubber it is important to have as much information as possible concerning the properties of the chemical compounds used. A program for obtaining such information has been in progress at the Bureau for several years. Recently, Russell B. Scott and Jane W. Mellors have determined the specific heats of the vapors of four compounds, 1,3-butadiene, isobutene, styrene, and ethylbenzene. (*Journal of Research* for March, RP1640.) Butadiene and styrene are the principal ingredients of GR–S (Government rubber-styrene type). Isobutene is co-polymerized with isoprene in the manufacture of butyl rubber. Ethylbenzene is converted into styrene by dehydrogenation, this process supplying most of the styrene used.

The specific heat of a substance is the amount of heat required to raise the temperature of unit mass of the material one degree. Specific heats of solids, liquids, and vapors are of value in calculating the amounts of heat involved in plant processes, but the specific heat of a vapor has a more fundamental significance, because of its simpler relationship to the internal motions of the atoms within the molecule. In the case of some compounds, it is possible to calculate the specific heat of the vapor by using spectroscopic data only. With more complicated molecules, such as those dealt with in the present study, the spectroscopic data alone do not permit the complete solution; calorimetric data extending to very low temperatures must also be utilized. In addition, certain assumptions must be made before values of specific heat can be calculated. It is in these cases that the experimental values of specific heat are very useful. If the calculated values agree with the experimental, the accuracy of the assumptions is demonstrated, and it is possible to calculate specific heats at high temperatures where the experimental method would be unsatisfactory. The calculations are not limited to specific heats. Other thermodynamic

properties, which enable the chemist to predict reactions and compute changes of heats of reaction with temperature, can also be obtained. The measured specific heats of the vapor provide one of the best checks of the accuracy of these calculations.

HEATS OF COMBUSTION AND FORMATION OF THE PARAFFIN HYDROCARBONS.

In a report (RP1642) by Edward J. Prosen and Frederick D. Rossini, which will appear in the March number of the *Journal of Research*, selected "best" values are given for the heats of combustion (in oxygen to form gaseous carbon dioxide and liquid water) and the heats of formation (from the elements solid carbon, graphite, and gaseous hydrogen) for methane and ethane in the gaseous state, and for all the paraffin hydrocarbons from propane through the octanes and all the higher normal paraffins through C_{20}, in both the liquid (except for one octane which is solid) and gaseous states, all at 25° C. Values for the normal paraffins above C_{20} are given in the form of equations. A new and more accurate value for the increment per CH_2 group, for both the liquid and gaseous states, is given for the heat of combustion and correspondingly for the heat of formation.

FREE ENERGIES AND EQUILIBRIA OF ISOMERIZATION OF THE 18 OCTANES.

A joint report of the Bureau's Thermochemical Laboratory and the American Petroleum Institute Research Project 44, prepared by Edward J. Prosen, Kenneth S. Pitzer, and Frederick D. Rossini, appearing in the March number of the *Journal of Research* (RP1641), presents in tabular and graphical form, for the 18 octanes, in the ideal gaseous state (range 298° to 1000° K.), values of the following thermodynamic properties: (a) the standard free energy of isomerization divided by the absolute temperature, $\Delta F°/T$; and (b) the relative amounts of the several isomers present at equilibrium with each other.

The values presented in this report for the octanes follow substantially the general conclusions previously drawn from the butanes, pentanes, hexanes, and heptanes, as regards thermodynamic stability in the gaseous state:

(1) At 25° C., the normal isomer is among the isomers of lesser stability. Relative to the other isomers, the normal isomer increases in stability with increase in temperature, and at 1000° K. is among the most stable of the isomers.

(2) At 25° C., 2,2-dimethylhexane is among the most stable of the isomers, but it rapidly becomes less stable with increasing temperature and at 1000° K. is among the least stable of the isomers.

(3) The more highly branched isomers are among the least stable at the higher temperatures.

PURITY OF SAMPLES OF ORGANIC SOLVENTS.

Studies of the uniformity of different samples of organic solvents by ultraviolet spectrophotometry are described in a paper (RP1643) by Marion E. Maclean, Priscilla J. Jencks, and S. F. Acree in the March number of the *Journal of Research*. The procedure used is applicable to the detection of impurities originally present or formed by deterioration, and to the study of the effectiveness of purification procedures.

Absorption curves are given for *n*-heptane, 2,2,4-trimethylpentane, cyclohexane, methylcyclohexane, decahydronaphthalene, benzene, carbon tetrachloride, methyl alcohol, ethyl alcohol, ethyl acetate, and dioxane, in two or more grades of purity. The absorption curves of tetrahydronaphthalene, toluene, xylene, chlorobenzene, ethylene dichloride, trichloroethylene, acetone, dimethyldioxane, and carbon bisulfide are discussed briefly. The effect of filtration through silica gel on the ultraviolet absorption of several commercial solvents is shown.

REDUCING SUGAR ANALYSIS.

In the determination of reducing sugars, copper solutions containing carbonates and bicarbonates have in general proved to be less reliable, as regards reproducibility of results, than copper solutions containing caustic alkali. However, since the carbonate solutions are less destructive to sucrose, Richard F. Jackson and Emma J. McDonald have made a careful study of the macro method proposed by Shaffer and Hartmann for dextrose analysis. This method has been applied to dextrose, levulose, invert sugar, and invert sugar-sucrose mixtures. The copper-sugar ratios have been determined in each case.

As pointed out in the March *Journal of Research* (RP1638), even under carefully controlled conditions, the Shaffer and Hartmann method proved to be inferior to Munson and Walker's and to Lane and Eynon's methods in which caustic alkali is a constituent of the copper reagent. However, because of its convenience it is valuable for rapid work where a precision not greater than 0.5 per cent. is required.

MACHINE FOR SPLITTING MICA.

D. W. Kessler of the Bureau has been working on the problem of a feasible means of removing mica films, in thicknesses between one and three mils, from commercial mica blocks. This is to be substituted for hand splitting—the method which has always been employed. It requires three or four months to train a hand-splitter, and the average rate of splitting is between 15 and 20 films per minute.

When this project was undertaken, various chemicals were tried to determine if the cementing material holding the sheets together could be dissolved. Several physical means, such as high voltage electricity,

heat, sudden release of air pressure in the container, flexing, steaming, sudden changes of temperature, etc., were tried. Most of these methods gave no promise whatever, and those that showed some tendency to separate the films produced other effects that were undesirable. Efforts were then started to develop a machine that would remove films one by one.

Two devices for splitting mica have been constructed at theBureau. The first consists of a single suction chuckplate which holds the mica blocks while it slides back and forth on a track. The gage which starts the split is stationary except for a slight rotation in a vertical plane. When a film is started and bent upwards, it is caught by two claws actuated by suction, and pressed on a small drum. As the drum rolls back, the film is stripped and carried to a suction belt which deposits it in a tray at some distance from the machine. This device produces about 30 films per minute, the slow rate being caused mainly by the fact that the operation has to be stopped while new blocks are being placed on the chuck. The method of stripping is also believed to be too severe since the bending of films caused more scales and defective sheets than hand splitting.

The second device consists of a disc carrying six chuckplates, a starter gage similar to the first, two stripper blades, and a suction belt for removing the films from the machine. With this device little time is lost in changing blocks, since one chuck is loaded by the operator while another block is being split. When the first block is finished, the operator turns the disc until the chuck comes into position which requires only about one second for the change. With this device there is very little bending of the films, and the results are more satisfactory. It has been demonstrated to representatives of the War Production Board who have shown keen interest and expressed their belief that it will be of value to the industry.

Great Bell of Moscow.—(*Compressed Air Magazine*, Vol. 50, No. 1.) The casting of bronze bells was an art that commanded the interest of foundrymen down through the ages, starting in pre-Christian times. The earlier bells were small, but gradually their size was increased, especially after the eleventh century, A.D., when a bell weighing 2600 pounds was considered remarkable. This trend continued until it was climaxed by the casting, at the Royal Russian Gun Factory, of the 220-ton great bell of Moscow, a work that required three years to complete. The initial pouring took place in November, 1734, with four reverberatory furnaces being used to melt the bronze. On the 26th, 100 tons of metal was charged into them, and this was followed the next day by additional charges of 90 and 36 tons. Two of the furnaces failed under the weight, and the molten metal went through their bottoms. More metal was obtained, including 74 tons of copper coins, and charged into the two remaining furnaces. On the 29th these also failed, and the building caught fire from the molten metal and was destroyed. John Motorin, the foundry foreman, died from worry over this chain of unfortunate events, but his son took up the unfinished work and succeeded in casting the bell on November 23, 1735. However, while preparations were in progress for removing the bell from its pit, a fire swept through Moscow and the building was destroyed. The heat cracked the bell in eight places; and one section, weighing ten tons, fell out. The bell was $19\frac{3}{4}$ feet high, $60\frac{3}{4}$ feet around the bottom, and had walls ranging from 6 inches to 2 feet in thickness. The cost of making the mold alone was nearly $48,000.

R. H. O.

THE FRANKLIN INSTITUTE.

STATED MONTHLY MEETING, WEDNESDAY, MARCH 21, 1945.

The regular monthly meeting of The Franklin Institute was called to order by Mr. Charles S. Redding, President. The National Anthem was played.

Upon motion, duly seconded and carried, the minutes of the January meeting, as printed in the February JOURNAL, were approved.

Mr. Redding called upon Dr. Henry Butler Allen, Secretary of the Institute. Dr. Allen reported the following increase in membership since last month:

Active	55
Associate	22
Student	35
Total	112
Total Membership as of February 28, 1945	5,510

He then spoke about Medal Day Exercises which this year will be held on Wednesday, April 18th, in Franklin Hall. He pointed out that due to the ruling of the Office of Defense Transportation restricting travel, announcements only would be sent to members and friends of the Institute outside the commuting area of Philadelphia. He then cordially invited all members to attend the dinner and the exercises following when the award of Medals would be made. It was announced that the Hostess Committee would give a reception preceding the dinner.

The Chairman then introduced the speaker of the evening, Dr. W. F. G. Swann, Director of the Bartol Research Foundation of The Franklin Institute. Mr. Redding explained that Dr. Swann and his staff are devoting practically all of their time to war work which could not be reported upon at this time. He then stated that Dr. Swann had prepared an interesting lecture on "Certain Matters Pertaining to the Production of Tone in Bowed Musical Instruments," and turned the meeting over to the speaker.

Dr. Swann gave an interesting talk dealing with certain characteristics of the motion of the string of a violin or 'cello when bowed, with particular relation to those elements concerned in the production of acoustical intensity. The lecture was illustrated by experiments and demonstrations.

The meeting was dismissed with a rising vote of thanks to the lecturer for a very instructive and entertaining evening.

HENRY BUTLER ALLEN,
Secretary.

March 21, 1945.

LIBRARY NOTES.

The Committee on Library desires to add to the collections any technical works that members would wish to contribute. Contributions will be gratefully acknowledged and placed in the library. Duplicates received will be transferred to other libraries as gifts of the donor.

Photostat Service. Photostat prints of any material in the collections can be supplied on request. Orders received in the morning are filled the same day. The average cost for a print 9 × 14 inches is thirty-five cents.

The library and reading room are open on Mondays, Tuesdays, Fridays and Saturdays from nine o'clock A.M. until five o'clock P.M., Wednesdays and Thursdays from two until ten o'clock P.M.

RECENT ADDITIONS.

AERONAUTICS.

FREDERICK, JOHN H. Commercial Air Transportation. 1943.
SMITH, HENRY LADD. Airways. 1944.

AGRICULTURE.

GRAY, A. N. Phosphates and Superphosphates. 1944.

ARCHITECTURE AND BUILDING.

GAY, CHARLES MERRICK, AND CHARLES DEVAN FAWCETT. Mechanical and Electrical Equipment for Buildings. Second Edition. 1945.
National District Heating Association. Official Proceedings Thirty-Fifth Annual Meeting. 1944.
VANDERWALKER, F. N. Wood Finishing. 1944.

BIOLOGY.

GERSHENFELD, LOUIS. Bacteriology and Allied Subjects. 1945.

CHEMISTRY AND CHEMICAL TECHNOLOGY.

Institution of the Rubber Industry. Annual Report on the Progress of Rubber Technology. Volume 7. 1943.
Society of Chemical Industry. Chemical Engineering Group. Proceedings. Volume 23. 1941.

DIRECTORIES, ALMANACS, ETC.

Raymond Rich Associates. American Foundations and their Fields. 1942.
World Almanac and Book of Facts for 1945.

EDUCATION.

STOCKFORD, CLARK C. Move Up in Your Job. 1943.

ELECTRICITY.

STILL, ALFRED. Soul of Amber. 1944.

ENGINEERING.

CREAGER, WILLIAM P., JOEL D. JUSTIN AND JULIAN HINDS. Engineering for Dams. Three Volumes. 1945.

FOUNDING.

American Foundrymen's Association. Alloy Cast Irons. Second Edition. 1944.
American Foundrymen's Association. Foundry Sand Testing Handbook. Fifth Edition. 1944.
American Foundrymen's Association. Recommended Practices for the Sand Casting of Non-Ferrous Alloys. 1944.
American Foundrymen's Association. Symposium on Centrifugal Casting. No Date.
American Foundrymen's Association. Symposium on Gating and Heading Malleable Iron Castings. No Date.

MANUFACTURES.

DEARLE, D. A. Plastic Molding and Plant Management. 1944.
HAGEN, VICTOR WOLFGANG VON. The Aztec and Maya Papermakers. 1944.

MATHEMATICS.

HÂDAMARD, JACQUES. An Essay on the Psychology of Invention in the Mathematical Field. 1945.

MINING AND METALLURGY.

American Institute of Mining and Metallurgical Engineers. Transactions. Reduction and Refining of Nonferrous Metals. 1944.

HAYWOOD, F. W., AND A. A. R. WOOD. Metallurgical Analysis by Means of the Spekker Photo-Electric Absorptiometer. 1944.

TAGGART, ARTHUR F. Handbook of Mineral Dressing. 1945.

PHOTOGRAPHY.

MORGAN, WILLARD D., HENRY M. LESTER, and Others. Graphic Graflex Photography. 1944.

PHYSICS.

AUGER, PIERRE. What Are Cosmic Rays? 1945.

HAWLEY, GESSNER G. Seeing the Invisible: the Story of the Electron Microscope. 1945.

SHIPBUILDING.

HANSEN, EMIL M. Ship Outfitter's Handbook. 1943.

NOTES FROM THE BIOCHEMICAL RESEARCH FOUNDATION.

A Chlorometric Method for the Determination of Some Organic Sulfides: A Preliminary Report.—JAMES L. LEITCH. The determination of sulfur in organic compounds usually involves either the Pregl catalytic combustion method or the Parr Bomb method. In the synthesis of organic compounds containing sulfur and particularly when its radioactive isotope is used, a more rapid procedure than the two mentioned above is required so that the course of the reactions can be followed. Since many organic sulfides can be fairly readily oxidized to the sulfoxide (R_2SO) and even to the sulfone (R_2SO_2), it was thought that this property could be used as a basis for their quantitative determination.

Goldstone and Jacobs (*Industrial and Engineering Chemistry, Analytical Edition*, **16**: 206, 1944) have recently shown that trivalent arsenic and antimony could be quantitatively oxidized in acid solution to the pentavalent state using a standard sodium hypochlorite solution (prepared by them from Chlorox) as oxidant and methyl orange as indicator. Kolthoff and Stenger (*ibid.*, **7**: 79, 1935) had studied the use and stability of calcium hypochlorite solutions as a volumetric oxidizing agent in connection with the determination of ammonia. They prepared the standard hypochlorite solutions from H.T.H., a high-test, stabilized, calcium hypochlorite manufactured by Mathieson Alkali Works, Inc., New York City. Both of these investigations showed that either sodium or calcium hypochlorite solutions were sufficiently stable to be used as volumetric oxidizing agents in acid or in slightly alkaline solutions.

EXPERIMENTAL.

Preparation and Standardization of Sodium Hypochlorite Solutions. In the work herein reported, the standard sodium hypochlorite solutions were prepared from Zonite (manufactured by the Zonite Products Corp., New Brunswick, N. J.) which is a stabilized solution of this hypochlorite having a concentration equivalent to approximately one per cent. available chlorine. The stock Zonite solutions are quite stable in the original containers and relatively constant in composition. An approximately 0.01 N hypochlorite solution was prepared by diluting 35 ml. of the stock Zonite solution to 1000 ml. with distilled water containing 1 or 2 grams of C.P., sodium hydroxide. Such a solution was stored in an amber bottle with a synthetic, screw-cap closure and used in an automatic 5 ml. burette, the reservoir of which was also of amber glass.

These solutions were standardized either against arsenous oxide solutions as described by Goldstone and Jacobs or by the use of potassium iodide and standard sodium thiosulfate solution as recommended by Kolthoff and Stenger. Both procedures were used initially in this work but the arsenous oxide method has become the preferred one because it required only one additional reagent and was more rapid.

Stability of Sodium Hypochlorite Solutions. The stability of two sodium hypochlorite solutions prepared from Zonite has been studied over a period of 7 months during which time the solutions have been used continuously. The change in normality of these two solutions is given in Table I.

TABLE I.

Stability of 0.01 N Sodium Hypochlorite Solutions.

Age in Days	Solution A (1), Normality	Solution B (1), Normality
0	0.009852	0.01075
1	0.009794	—
5	0.009579	—
6	0.009560	—
9	0.009497	—
12	0.009346	—
15	—	0.01069
20	0.009166	—
72	—	0.01058
94	0.009355 (2)	—
7 mon.	—	0.01029

(1) Solution A contained 1 gram of sodium hydroxide per liter while Solution B contained 2 grams.

(2) This sample of Solution A was removed from the stock solution on the day of preparation and stored, unopened, in a screw-cap, amber bottle.

From Table I it is seen that the stability of these solutions depends in part on the amount of sodium hydroxide used which is in agreement with the work of Chapin (*Journal of the American Chemical Society*, **56**: 2211, 1934) who found in a study of the decomposition of hypohalites that potassium hypochlorite solution had its maximum stability at pH 13.1. In view of the above results, work has already been initiated to study the stability of sodium hypochlorite solutions prepared in 0.1 N sodium hydroxide solutions.

Indicators, Indicator Blank and Corrections. The present work has involved the use of only methyl orange solution as the indicator. Kolthoff and Stenger have shown that other indicators can be used although varying pH conditions are required with different indicators.* A 0.05 per cent. aqueous methyl orange solution was found most

* Preliminary tests indicate that a 0.05 per cent. aqueous neutral red solution can be used in place of the methyl orange in acid solution. A 0.01 per cent. aqueous basic fuchsin solution can be used providing the titration is carried out in the presence of excess sodium bicarbonate.

suitable for the work providing the solution to be titrated was made acid to this indicator by the addition of concentrated hydrochloric acid.

Since a certain definite amount of the sodium hypochlorite solution is used up in the titration for the bleaching of the methyl orange, the volume of indicator used must be carefully controlled. It was found that one drop of this indicator required 0.015 ml. of 0.01 N sodium hypochlorite solution to completely bleach it. This value will vary slightly with changes in the normality of the hypochlorite solution so that indicator blanks should be determined at frequent intervals. This can be readily done by titrating 2 drops (0.01 ml.) of the indicator in 2 ml. of distilled water.

Over and above the correction for the amount of indicator used, it was found that at the end of the titration a slight excess of the hypochlorite solution was present as indicated by the standard *o*-tolidine test for free chlorine. This correction was dependent primarily upon the volume of the solution titrated and was found to be equivalent to the following:

Volume	Correction
1– 5 ml.	0.010 ml. 0.01 N hypochlorite
10–50 ml.	0.020 ml.
100 ml.	0.025 ml.

Analysis of Some Organic Sulfides. The sodium hypochlorite solutions previously discussed were used for the determination of the amount of chlorine required to completely oxidize one milligram of the sulfide under investigation.

For this purpose not more than 10 mg. of the compound were accurately weighed into a 5 or 10 ml. volumetric flask and dissolved in distilled water to the mark. An aliquot of this solution was placed in a 25 ml. Erlenmeyer flask. One drop (0.05 ml.) of a 0.05 per cent. methyl orange solution was added and the sample adjusted with normal hydrochloric acid until it was just acid to the indicator. After the addition of 1 ml. of concentrated hydrochloric acid, the sample was titrated dropwise† with the standard sodium hypochlorite solution until the methyl orange had been decolorized. An additional drop of indicator was then added and the sample titrated again until colorless. Duplicate samples were analyzed concurrently with distilled water blanks. Whether or not the end-point has been exceeded can be determined by the addition of a third drop of the methyl orange indicator. If a permanent red color appears, the correct end-point was reached, but if the sample remains colorless the end-point has been passed. In the latter case, the solution can be back-titrated with the methyl orange indicator until the sample becomes red and the end-point

† A dropwise titration of the sample is essential, otherwise the indicator will be bleached before the actual end-point has been reached and low results will be obtained.

again obtained by titration with the hypochlorite solution. In this procedure, because the end-point of the back-titration does not correspond to that of the hypochlorite titration, giving slightly low results, it is not practical to simply back-titrate with the indicator as was done by Teorell (*Biochemische Zeitschrift*, **248**: 246, 1932) who used naphthyl red for determining excess hypobromite.

Since this analytical method was used primarily for the determination of the amount of chlorine required for complete oxidation of the sample, the results were calculated in terms of a "Chlorine Factor" which represented the milligrams of chlorine per milligram of compound as follows:

$$\frac{(\text{ml. hypochlorite used} - B) \times N \times 35.46}{\text{mg. compound in sample}} = \text{Chlorine Factor}$$

where N represents the normality of the sodium hypochlorite solution and B the blank correction for the indicator and volume of the sample. For semiquantitative work with 0.01 N hypochlorite solutions, the value for B may be taken as equivalent to 0.025 ml. although for accurate results it should be determined concurrently with the experimental samples. Some representative results are given in Table II.

TABLE II.

Representative Results of the Determination of the "Chlorine Factor" for Two Organic Sulfides.

Compound	"Chlorine Factor" (mg. chlorine per mg. of compound)	
	Theoretical	Observed
Redistilled 2,2'-thiodiethanol (B.P. 167–9 at 15 mm.)	1.161	1.163
Redistilled bis-(2-chloroethyl)sulfide (B.P. 135 at 50 mm.)	0.892	0.891
Crude bis-(2-chloroethyl)sulfide	—	0.902

DISCUSSION.

Zonite has been found to be a very satisfactory source for the preparation of dilute sodium hypochlorite solutions for use in chlorometry. The stability of the 0.01 N solutions containing only one or two grams of sodium hydroxide is not quite as good as that of the solutions prepared by Kolthoff and Stenger from H.T.H. However, since standardization of these solutions can be carried out relatively rapidly using standard arsenous oxide solutions, the somewhat lower stability of these solutions is a factor that can be readily overcome. It is possible that Zonite diluted with tenth-normal sodium hydroxide will give solutions whose stability will approach more closely that found by Kolthoff and Stenger.

Up to the present time, the procedure described above has been applied only to the analysis of aqueous solutions of (1) pure 2,2′-thiodiethanol, (2) pure bis-(2-chloroethyl)sulfide and (3) mixtures of these two compounds. As can be seen from Table II, the theoretical and observed values for the "Chlorine Factor" for the two pure compounds agree quite closely. The synthetic sample of the dichloro-compound was impure and contained some of original hydroxy-compound. By microgravimetric determination of the chlorine content of this sample, it was found to consist of 96.1 per cent. of the bis-(2-chloroethyl)sulfide.‡ The purity of the dichloro-compound can be calculated from the data given in Table II, as follows:

$$100\,\frac{A - B}{A - X} = \text{per cent. of dichloro-compound}$$

where A equals the "Chlorine Factor' for the pure dihydroxy-compounds, B that for the pure dichloro-compound and X that of the unknown mixture. This relationship holds since the "Chlorine Factor" increases linearly from that of the dichloro-compound to that of the pure dihydroxy-compound as the proportion of the latter is increased in the mixture. From the above equation and the data in Table II, the crude sample of bis-(2-chloroethyl)sulfide is found to have a purity of 96.6 per cent. which agrees closely with the value found from the chlorine determination.

Although the chlorometric determination of organic sulfides has only been applied so far to the two previously mentioned compounds, preliminary tests indicate that it is applicable to many other organic sulfides. Complete data will be published at a later date.

In the analysis of water supplies for both civilian and military personnel, the degree of contamination with certain war gases has been determined by Buswell *et al* (*Journal of the American Water Works Association*, **35**: 1303, 1943) using the chlorine demand of the water as a criterion. In this procedure, water was treated with an excess of Chloramine-T, H.T.H. or other source of available chlorine, and the residual chlorine determined after a definite period of contact using *o*-tolidine. Similar data can be obtained by the use of the chlorometric procedure described in this paper.

‡ This analysis was carried out by the Microchemical Laboratory of the Biochemical Research Foundation.

BOOK REVIEWS.

SOUL OF AMBER, THE BACKGROUND OF ELECTRICAL SCIENCE, by Alfred Still. 274 pages. 14 × 21 cms. New York, Murray Hill Books, Inc., 1944. Price $2.50.

From ancient times to the present electricity and its phenomena have made men ponder upon its true nature. This book recounts the various hypotheses and experiments which have proven to be milestones in our growing knowledge of electrical facts. Beginning with the earliest speculations of the ancients on the properties of attraction of rubbed amber, the story moves rapidly until the emergence of electricity as a science after the dark ages of medievalism. For it was in 1600 that William Gilbert published his *De Magnete* which gained for him the title, "Father of Electrical Science."

Then pass in review such landmarks as the frictional electrical machine, the Leyden jar, the electrophorus, the kite experiments of Franklin, galvanism, laws of the electric circuit and the electromagnet. The author concludes his narrative with the development of the dynamo by Faraday and does not consider subsequent progress in the field of electronics. As an interlude he offers an interesting chapter on electrical theories concerning earthquakes, meteors and the aurora borealis.

Nor is this a bare record of facts and dates, but rather an account intended for ready perusal by the informed layman. To further that end it is filled with numerous unfamiliar facts about the men whose achievements laid the foundation for our modern electrical world. Considerable attention has also been paid to the effect of contemporary philosophy, religion, art and politics upon the state of science. To Mr. Still's qualifications as an electrical engineer he has added an aptitude for writing to produce an entertaining and informative story of electricity.

GEORGE E. PETTENGILL.

TELESCOPES AND ACCESSORIES, by George Z. Dimitroff and James G. Baker (one of the Harvard Books on Astronomy). The Blakiston Co., Philadelphia, 1945. 309 pages, 150 illustrations. $2.50.

This is the seventh of the series of Harvard Books on Astronomy to appear and, like its predecessors, this one is written by those who know what they are writing about. Dr. Dimitroff is the Superintendent of the Oak Ridge Station of Harvard College Observatory and has in his charge instruments ranging from 1-inch cameras to a 61-inch reflector; Dr. Baker has established a considerable reputation for himself in the design and construction of instruments of the most advanced type, chiefly modifications of the extremely fast Schmidt-type cameras.

From the first chapter—*Light as a Tool*—to the last Appendix, in which are included a great number of diffraction patterns resulting from various apertures, the book is filled with accurate information for the amateur and professional alike, presented in a style that leads one from topic to topic with practically no pain. There are no significant omissions, despite the complexity of types and uses of the specialized instruments of astronomy. In Chapters 4 and 5, *Photographic Telescopes* and *Sifting Light—Spectroscopy*, the book is particularly complete and explicit. Many optimum cameras, from the old astrographic lens to the most rapid Schmidt- and Wright-type, are completely described, with the optical specifications given for their manufacture; sources of error, both in direct photography and in spectrography, are fully discussed, without the pedantry of equations. Indeed, there is hardly an equation in the book, so the rational meanings are clear even to those who abhor thinking in terms of mathematical symbols.

Every professional astronomer can learn something about his instruments and the uses to which they had best be put, from the many comparisons given; every amateur who has a telescope or who wants to buy or make one had better read this book first.

ROY K. MARSHALL.

THE PHYSICS OF FLIGHT, by Alfred Lande. 122 pages, illustrations, drawings and diagrams, 15 × 23 cms. New York, Reinhold Publishing Corporation, 1945. Price $2.50.

This is an elementary text designed to fit into a course of training just after the first year of college physics and algebra. As such its coverage and method of presentation are of special importance. With regard to the former, there must not be too much stress on derivations and other more or less complex side-issues or relatively unimportant contributions to the subject or too wide a scope; and with reference to the latter the method must be direct, easy-to-read, logical, and must make an impression. Otherwise, students would become discouraged at the beginning of a course without its being given a fair trial.

The book is not a large one—only 103 pages of text. It opens with a discussion of general principles which include Bernoulli's Theorem, Reynolds' Law of Similarity and its use in determining the transition from laminar and turbulent flow. This opening section is indicative of the simpleness of explanation used throughout the book. Photos, illustrations, drawings and diagrams, supplement the test and definitions and functions are given in a clear, concise manner. Mathematics are paired down to within the prerequisites and keep within these bounds. Examples as illustrations are given with full solutions. With this as a background, the description of an airplane is then given by first covering its principle parts and their functions. Following is a chapter on the planform of the wing which includes the vortex theory of induced drag. This section is quite technical but is not long enough to become fatiguing. Biplanes are then taken up, reasons being given for more than one wing, and the load distribution. Brief but intensive is the section devoted to stability and control. The material so far collected is then used as a basis for the discussion of the factors determining the performance of an airplane in flight, which is followed by a treatment on the propeller. The latter part of the work is devoted to unconventional types of aircraft such as jet propulsion, the helicopter, the autogiro, and automatic pilot, and finally instruments of navigation.

The treatment is compact, well within the grasp of those for whom it is intended and interestingly presented.

R. H. OPPERMANN.

AERODYNAMICS, by Leslie R. Parkinson. 112 pages, illustrations, 15 × 22 cms. New York, The Macmillan Company, 1944. Price $2.25.

Today there are workers in the aircraft industry who are doing work more or less thrust upon them by the emergency, and who need a knowledge of terminology, basic facts, and modern theories of aerodynamics. The intent of this little book is to satisfy this need. The treatment is mainly descriptive and only where wording is involved, is resort made to mathematics using algebra and trigonometry of high school grade. It starts with a discussion on the physical properties of the atmosphere, then progresses through the phenomena of air in motion, and the Reynolds Number and the Bernoulli Theorem. Subsequently lift and drag, airfoils, and lift-increasing devices are taken up in order. There is a section on performance and stability, followed by a treatment on propellers, and finally wind tunnels. The 107 pages of this book is a serious but simplified review of the essentials of aerodynamics. Stress is laid on the practical sides of the subject.

R. H. OPPERMANN.

PUBLICATIONS RECEIVED.

Telescopes and Accessories, by George Z. Dimitroff and James G. Baker. 309 pages, drawings and illustrations, 15 × 23 cms. Philadelphia, The Blakiston Company, 1945. Price $2.50.

Mechanical and Electrical Equipment for Buildings, by Charles M. Gay and Charles De Van Fawcett. (Second Edition.) 453 pages, tables, diagrams and illustrations, 14 × 22 cms. New York; John Wiley & Sons, Inc., London; Chapman & Hall, Ltd., 1945. Price $5.00.

CURRENT TOPICS.

ARMY AND NAVY NOTES.

Production of Tiny Radio Waves.—Efficient production of radio waves many times the frequency of the shortest "short waves" used a few years ago, has been one of the most important electronic developments of the war, said William C. White, head of the electronics section of the General Electric Research Laboratory, before the Philadelphia Section of the American Institute of Electrical Engineers.

"During the past few years, the war years, the outstanding electron-tube developments have been in connection with the generation, control, and utilization of ever higher frequencies," he said. "Extraordinary progress has been made. Many of the techniques that the radio engineer has used in broadcasting and communication have been extended more than ten-fold upward along the spectrum of electromagnetic radiations. This has not only given engineers many additional frequency channels to utilize for radio and its by-products but made practical new elements such, for instance, as sharply directed beams with relatively small antenna structures."

Discussing the trend of electronics in the future, Mr. White declared that "one may be sure that just as soon as manpower and material restrictions are relaxed, the promotion of frequency modulation broadcasting and television will become very active. There always have been more individuals or groups desirous of going into the business of broadcasting than there have been suitable available frequency channels. Broadcasting by FM meets this demand and there is every reason to believe that hundreds of such stations will be put into operation as soon as they can be manufactured. As for television, there have already been enough applications filed for licenses for transmitting stations to indicate that most big city areas will have regular evening programs; in fact, several to choose from in some areas."

He pointed out that of the many new and ingenious industrial uses of electronics which have been widely publicized, "most are technically possible but some are economically unsound for most applications." He cited electronic heating, "which is heat in one of its most expensive forms. For simply removing moisture from bulk, low-cost material, such as paper or clay, it cannot be justified. If, however, the product is of high unit value, if time is an all-important factor and if the selective heating property of high frequency electronic methods are involved, the story may be quite different."

The same is true, he warned, in connection with electronic devices for the home. "Take for example," he said, "the garage door opener. You drive up to your closed garage door and, by a certain sequence of flashing of your headlights, radio impulses or blowing of your horn, the garage door opens. There is no stepping out in the cold, rain or snow. The same method is used on leaving the garage. Now this device is entirely practical technically, but would you seriously consider paying, say $250 for it? This is one of the chief problems to be faced in most new devices."

R. H. O.

Irradiation Causes Mold Mutation.—Ultraviolet irradiation of a mold, useful in industrial fermentations, to make it do its work better were successful enough so that the experimenters now face the job of repeating the irradiation on a superior mold, hoping to make the new strain still more productive. The details of the work are related in a technical report of results that are significant both scientifically and practically, according to the Agricultural Research Administration of the U. S. Department of Agriculture.

The Fermentation Division of the Northern Regional Research Laboratory discovered recently how to ferment corn sugar to produce itaconic acid—used in plastics—for a selling price of 50 cents a pound instead of the $10 a pound it had been costing. The mold that did the work was *Aspergillus terreus*, and Strain 1960 from the laboratory collection is the best mold to be had for the work. It produces the most acid from a given quantity of sugar.

Ultraviolet irradiation can kill many microscopic organisms. But quick treatments may modify them without killing them, and may cause inheritable changes. With the cooperation of Dr. Alexander Hollaender of the National Institute of Health at Bethesda, Md., the Peoria scientists irradiated Strain 265, a good itaconic acid producer used earlier in the work. They then tested hundreds of the irradiated organisms. Most of them made no more acid and many made much less than Strain 265, but a few produced more—up to 20 per cent. more. This was the practical angle of the research.

Many of the irradiated organisms were unchanged, most were killed, a few reproduced for a few generations and then went back to the Strain 265 form. Most of the modified molds or "mutants" continued to breed true in the modified form, including two of the most productive new strains—those that were 20 per cent. better than the old Strain 265. This was scientifically significant. If Strain 265 can be changed and improved in this way, there is hope to work similarly with other organisms—perhaps even with the one that manufactures life-saving penicillin.

But these new mutants of Strain 265 are not likely to be put to work. While this research was under way, Drs. Lewis B. Lockwood and Kenneth B. Raper, two of the experimenters, also were testing hundreds of "wild molds," new strains of the same species collected from nature. Of these new strains, several are better acid producers than the best of the irradiated mutants. The new job now is to irradiate the better wild molds, and perhaps change them to still better producers.

R. H. O.